Pontificia Universidad Católica de Chile
Facultad de Ciencias Biológicas
Programa de Doctorado en Ciencias Biológicas
Mención Biología Celular y Molecular

TESIS DOCTORAL:

"EFECTOS DE LA VÍA DE SEÑALIZACIÓN WNT SOBRE LA PERMEABILIDAD MITOCONDRIAL INDUCIDA POR OLIGÓMEROS DEL PÉPTIDO β-AMILOIDE"

Por

MACARENA SOLEDAD ARRÁZOLA TELLO

Septiembre 2014

Pontificia Universidad Católica de Chile
Facultad de Ciencias Biológicas
Programa de Doctorado en Ciencias Biológicas
Mención Biología Celular y Molecular

TESIS DOCTORAL:

"EFECTOS DE LA VÍA DE SEÑALIZACIÓN WNT SOBRE LA PERMEABILIDAD MITOCONDRIAL INDUCIDA POR OLIGÓMEROS DEL PÉPTIDO β-AMILOIDE"

Tesis entregada a la Pontificia Universidad Católica de Chile en cumplimiento parcial de los requisitos para optar al grado de Doctor en Ciencias Biológicas Mención en Biología Celular y Molecular

Por

MACARENA SOLEDAD ARRÁZOLA TELLO

Director de tesis: Dr. Nibaldo Inestrosa C.
Comisión de tesis: Dra. Alejandra Álvarez R.
Dr. Claudio Hetz F.

Septiembre 2014

Dedico este trabajo a toda mi familia…
en especial a mi marido Musa Majluf por ser mi soporte constante, mi confidente y amante,
a mi hija Belén que llegó a entregarme la luz, energía y motivación que necesitaba,
a mis padres Raúl Arrázola y Yorka Tello por darme la vida y amarme incondicionalmente,
y finalmente a mis queridos hermanos que son parte de mi ser y mi complemento.

Quisiera además dedicar especialmente esta Tesis a mi querida abueli Amini quien esperó con ansias la culminación de este proceso y que por cosas del destino tuvo que presenciarlo desde el cielo…te quiero

AGRADECIMIENTOS

En primer lugar quisiera agradecer al Dr. Nibaldo Inestrosa por haberme recibido desde mis inicios en su laboratorio y formarme desde aquel entonces para ser el científico que actualmente soy. Además por creer en mí y permitirme explorar en un área de trabajo nueva en la cual éramos todos inexpertos, dándome la opción al desafío que aquello significaba y a desarrollar esta Tesis libremente.

Quisiera dar gracias además a todos las personas que conforman el Laboratorio de Neurobiología Molecular, comenzando con Eliseo Campos quien fue indispensable a lo largo de todo este proceso, simplemente por confiar en mis capacidades, por guiarme y apoyarme constantemente. Gracias también a Daniela Ordenes por ser mi "otro yo" durante esta Tesis, por apoyarme codo a codo y por el compromiso que adquirió mientras trabajamos sacando adelante este lindo proyecto. Agradezco también a mi compañero de puesto y amigazo Juan Francisco Codocedo por las largas conversaciones, a veces muy serias y otras no tan científicas, que nos desviaban simplemente a hablar de las nuevas habilidades de nuestras niñas, gracias por eso y por el apoyo. Imposible dejar de agradecer a mi gran amiga Cheril Tapia, con la cual discutimos muchos experimentos, intentamos arreglar el mundo y manejar el laboratorio a la perfección, cosa que aún no logramos…simplemente gracias por tu linda y sincera amistad. Quiero agradecer también a Gloria Méndez, más que por su trabajo excepcional en la preparación de los cultivos primarios y que fue esencial para esta Tesis, por ser paciente, transparente y amiga…gracias Glorita por el cariño. No puedo dejar de agradecer a todos y cada uno de los integrantes del laboratorio por apoyar cada una de mis presentaciones, concursos y ensayos que se me ocurrió hacer...sin sus críticas y consejos nada hubiese sido igual.

Quisiera agradecer también a todo el equipo de microscopía de la Facultad de Ciencias Biológicas, a Alejandro, Jorge y Ximena, donde pase largos días de trabajo y a partir de lo cual se generó gran parte de mi trabajo.

Finalmente quisiera dar gracias a la Comisión Nacional de Investigación Científica y Tecnológica (CONICYT) por promover la investigación científica y por financiar esta Tesis Doctoral tanto con la Beca para Estudiantes de Doctorado en Chile, como con la Beca de Apoyo para la Realización de Tesis Doctoral.

INDEX

FIGURES INDEX

TABLES INDEX

ABBREVIATIONS

ABAD: Aβ-binding alcohol dehydrogenase

AD: Alzheimer's disease

ANT: adenine nucleotide translocase

APC: adenomatous polyposis coli

APP: amyloid precursor protein

ATP: adenosine triphosphate

Aβo: amyloid-β oligomers

Ca^{2+}: calcium

CNS: central nervous system

CsA: cyclosporin A

CypD: cyclophilin D

DAG: diacyl-glycerol

DKK1: Dickkopf-1

Dvl: Dishevelled

ER: endoplasmic reticulum

ETC: electron transport chain

Fz: Frizzled

GSK-3β: glycogen synthase kinase-3β

HKII: hexokinase II

IMM: inner mitochondrial membrane

IP3R: inositol triphosphate receptor

JNK: Jun N-terminal kinase

LRP 5/6: lipoprotein receptor-related protein 5/6

LTD: long-term depression

LTP: long-term potentiation

mΔΨ: mitochondrial membrane potential

MM: mitochondrial matrix

mPTP: mitochondrial PTP

NMDA: N-Methyl-D-aspartate

OMM: outer mitochondrial membrane

PCP: planar cell polarity

PLC: phospholipase C

PS1: presenilin1

PSD-95: postsynaptic density-95 protein

PTP: permeability transition pore

ROS: reactive oxygen superoxide

Ru360: Ruthenium 360

RyR: ryanodine receptor

TCF/LEF: T cell factor/lymphoid enhancer factor

Tg: transgenic

TOM: translocase of the OM

VDAC: voltage-dependent anion channel

RESUMEN

La enfermedad de Alzheimer (EA) es una enfermedad neurodegenerativa caracterizada por la pérdida progresiva de memoria y daño cognitivo. Las placas seniles presentes en los cerebros de pacientes con EA están formadas por el péptido β-amiloide (Aβ), que en su forma soluble, conocida como oligómeros de Aβ (Aβo), es la principal causa de neurotoxicidad en la EA, ya que presenta diversos blancos dentro de la neurona, como la mitocondria. La mitocondria es un organelo indispensable para la respiración celular y el abastecimiento energético y también participa en la regulación de los niveles de calcio neuronal. La sobrecarga de calcio en la mitocondria puede producir la apertura del poro de permeabilidad transitoria (mPTP), el cual es un poro no selectivo que se forma de manera dependiente a la concentración de calcio dentro de la matriz mitocondrial, generando la permeabilización de la membrana interna de la mitocondria e induciendo la muerte neuronal. Sin embargo, los Aβo también afectan a la mitocondria de manera directa, interactuando con diversas proteínas que son importantes para la mantención de su estructura y su funcionamiento. Una de estas proteínas es Ciclofilina D, la cual participa en la apertura del mPTP y por tanto regula la permeabilidad y función de la mitocondria. La apertura del mPTP por períodos largos, potenciada por estímulos apoptóticos como el Aβ, produce diversos cambios estructurales y funcionales en la mitocondria, que incluyen aumentos de volumen, disipación del potencial de

membrana mitocondrial, disrupción de las membranas y liberación descontrolada de calcio y factores pro-apoptóticos. En consecuencia, el bloqueo de la acción de Aβ en la mitocondria o la inhibición directa de la apertura del mPTP generada por Aβ, son potenciales estrategias terapéuticas para la EA.

Estudios previos de nuestro laboratorio han demostrado que la activación de la vía Wnt canónica o vía Wnt/β-catenina protege a las neuronas frente a la toxicidad del Aβ, previniendo la muerte neuronal, sin embargo, el mecanismo por el cual esta protección ocurre no es claro y aun no se ha explorado si la vía Wnt podría ejercer su papel neuroprotector a través de preservar la estructura y función mitocondrial.

En esta tesis se estudiaron los eventos celulares involucrados en la neurotoxicidad de Aβ y si la activación de la vía Wnt canónica, a través del ligando Wnt3a, previene estos eventos patológicos relacionados con la disfunción mitocondrial, la permeabilización de las membranas mitocondriales y la muerte neuronal en la EA. Para abordar esta interrogante, hemos propuesto estudiar los efectos de la activación de la vía Wnt en la permeabilidad mitocondrial inducida por Aβo en neuronas hipocampales. Para llevar a cabo este objetivo, desarrollamos ensayos en células vivas para medir los niveles de calcio mitocondrial y la inducción del mPTP en respuesta a Aβo. En esta tesis se describe que la pre-activación de la vía Wnt previene el aumento de calcio mitocondrial y la apertura del mPTP en neuronas expuestas a Aβo. De acuerdo a estas observaciones, también mostramos por microscopía electrónica que los cambios morfológicos y estructurales que sufre la mitocondria fueron completamente prevenidos por Wnt3a, sugiriendo que la inhibición del mPTP por la activación de la vía Wnt contribuye a preservar la estructura de la mitocondria, favoreciendo su buen funcionamiento y la viabilidad de la neurona.

ABSTRACT

Alzheimer's disease (AD) is a neurodegenerative disorder characterized by progressive memory loss and cognitive decline. Senile plaques present in AD brains are formed by the amyloid-β peptide (Aβ), which on its soluble form, known as Aβ oligomers (Aβo), is the main cause of neurotoxicity in AD, since presents several targets inside a neuron, such as the mitochondria. Mitochondrion is an essential organelle for cellular respiration and energy supply, and also participates in the regulation of neuronal calcium. The mitochondrial calcium overload can lead to the opening of the permeability transition pore (mPTP), which is a non-selective pore that is formed in a calcium concentration-dependent manner inside the mitochondrial matrix, producing the permeabilization of the inner mitochondrial membrane and inducing neuronal death. However, Aβo oligomers also directly affect mitochondria, interacting with several proteins that are important for the maintenance of its structure and function. One of these proteins is Cyclophilin D, which participates in the opening of the mPTP and therefore regulates the permeability and function of the mitochondria. The opening of the mPTP for long periods, potentiated by apoptotic stimuli such as Aβ, induces several structural and functional changes on mitochondria, including a volume increase, dissipation of the mitochondrial membrane potential, disruption of the membranes and an uncontrolled release of calcium and pro-apoptotic factors. Thus, blocking the effect of Aβ on mitochondria

or directly inhibiting Aβ-dependent mPTP stimulation, are potential therapeutic strategies for AD.

Previous studies from our laboratory demonstrated that the activation of the canonical Wnt signaling pathway or Wnt/β-catenin protects neurons against Aβ toxicity, preventing the neuronal death, however, the mechanism by which this protection occurs is not clear and neither has it been explored whether Wnt signaling could exert its neuroprotective role through the preservation of the mitochondrial structure and function.

In this thesis we studied the cellular steps involved in the Aβ neurotoxicity and whether the canonical Wnt signaling activation, through the Wnt3a ligand, prevents these pathological events related to mitochondrial dysfunction and mitochondrial membrane permeabilization and the neuronal death in AD. To address this question we proposed to study the effects of Wnt signaling activation in the mitochondrial permeability induced by Aβ oligomers in hippocampal neurons. To accomplish this aim, we performed live cell imaging assays to mainly measure mitochondrial calcium and the induction of mPTP in response to Aβ oligomers. We described in this thesis that the pre-activation of the Wnt signaling pathway prevents the mitochondrial calcium overload and the mPTP opening in neurons exposed to Aβo. According to these observations, we also showed by electron microscopy, that the morphological and structural changes that mitochondria undergo were completely prevented by Wnt3a, suggesting that the inhibition of the mPTP by Wnt signaling activation contributes to the preservation of mitochondrial structure, favoring its precise function and the viability of neurons.

1. INTRODUCTION

1.1. Alzheimer's Disease

Alzheimer's disease (AD) is one of the most common neurodegenerative disorders, characterized by a progressive loss of memory and cognitive decline, because mainly affects brain regions related to these functions (Hardy and Selkoe, 2002). At the neuropathological level, brains of AD patients are characterized by the presence of different protein aggregates: senile plaques and neurofibrillary tangles (Serrano-Pozo et al., 2011). Senile plaques are extracellular depositions of amyloid-β peptide (Aβ) aggregates (Mattson, 2004), whereas neurofibrillary tangles are intracellular aggregates of hyperphosphorylated Tau protein (Wang et al., 2013). Although it is not clearly known which is the molecular triggering factor of the disease in most of the AD patients, there are several studies suggesting that the Aβ peptide play a key pathogenic role in the early stages of the disease (Bates et al., 2009; Hardy and Selkoe, 2002). Aβ peptide is generated by the proteolytic processing of the amyloid precursor protein (APP) by β- and γ- secretases to form a peptide of 40 or 42 aminoacid long (Chow et al., 2010). Once Aβ has been produced on its monomeric form, it can aggregate to form soluble species known as Aβ oligomers (Aβo) and insoluble aggregates called amyloid fibrils, which are the result of a higher state of aggregation (Morgan et al., 2004; Ross and Poirier, 2005). Both aggregates form the senile plaques on AD brains (Sakono and Zako, 2010). Since Aβ fibrils are neurotoxic both, *in vivo* and *in vitro* (Alvarez et al., 2004; Dinamarca et al.,

2006), for several years it was thought that these insoluble aggregates were the main cause of the neurodegeneration observed in AD (Hardy and Higgins, 1992), however, currently there is consensus that Aβo are the main cause of neurotoxicity in AD, since they are the most neurotoxic species responsible for the synaptic dysfunction observed in this pathology (Cerpa et al., 2008; Li et al., 2009; Walsh et al., 2002)

1.2. Aβ oligomers and neurotoxicity

Recent studies have shown a strong correlation between Aβo levels and the severity of the synaptic and cognitive damage (Ferreira et al., 2007; Haass and Selkoe, 2007; McLean et al., 1999), suggesting that Aβo are the main effectors of the synaptic loss and neuronal degeneration in AD (Cerpa et al., 2008; Cleary et al., 2005; Lambert et al., 1998). Studies in AD animal models, in which APP is overexpressed, have demonstrated that high levels of Aβ induces a significant reduction in the presynaptic protein synaptophysin (Mucke et al., 2000), an observation that has also been made in AD patients, in which the levels of this protein is decreased from the early stages of the disease (Masliah et al., 2001). On the other hand, studies from our laboratory show that Aβo also affect the postsynaptic terminal, inducing the reduction of the levels of the postsynaptic density-95 protein (PSD-95) and the NMDA receptor (Dinamarca et al., 2008; Farías et al., 2009). Furthermore, functional studies have shown that Aβo are able to block the long-term potentiation (LTP) in the hippocampus, which is an electrophysiological correlates of learning and memory processes (Shankar et al., 2008; Wang et al., 2002). In the same way, different sources of Aβo electrically facilitates the long-term depression (LTD) evoked in the CA1 region of the hippocampus, disrupting the synaptic plasticity, to promote synapse depression (Li et al., 2009). The evidences presented so far

point to Aβ peptide as the major constituent of senile plaques and to its soluble oligomeric forms as the highest neurotoxic agents responsible for the early synaptic dysfunction, which is the initial step for neuronal degeneration observed in AD (Selkoe, 2002).

1.3. Intracellular calcium dysregulation in AD

Besides synapses, Aβ presents several molecular and cellular targets inside neurons, contributing to the neuronal damage that this peptide generates in AD. One of these targets is calcium (Ca^{2+}), which is a fundamental ion in the physiology of neurons and homeostasis, since modulates many neuronal processes, including membrane excitability, neurotransmitter release, genes expression, neuronal growth, and viability (Bezprozvanny and Mattson, 2008; LaFerla, 2002). Neuronal Ca^{2+} signaling is regulated by the balance between influx and release of the ion. Ca^{2+} influx across the plasma membrane occurs through voltage-gated Ca^{2+} channels, NMDA receptors and transient receptor potential channels (Alford et al., 1993; Berridge, 1998). Ca^{2+} release from intracellular Ca^{2+} stores occurs via inositol triphosphate receptor (IP3R) and ryanodine receptor (RyR) channels in the endoplasmic reticulum (ER) (Marks, 1997). Moreover, mitochondria also participate in the regulation of neuronal Ca^{2+} levels through the uptake of this ion, stimulating mitochondrial metabolism and energy production (Babcock et al., 1997). However, excessive calcium uptake into mitochondria can lead to opening of the permeability transition pore (PTP) and apoptosis (Spät et al., 2008).

During the slow progression of AD, the early phase of memory loss is exacerbated by the onset of neuronal cell death, which may also be driven by an increased dysregulation of Ca^{2+} homeostasis (Berridge, 2011; Demuro et al., 2010). It has been proposed that Aβ interaction with the plasma membrane results in elevated intracellular Ca^{2+} concentrations and increased

vulnerability of neurons to excitotoxicity (Mattson et al., 1992). The oligomeric forms of Aβ may increase Ca^{2+} entry by either functioning as channels or by activating channels in the plasma membrane such as the NMDA receptor (Berridge, 2011; Dinamarca et al., 2010). Moreover, mitochondrial dysfunction and ER stress are two central pathways leading to the apoptosis observed in AD (Takuma et al., 2005). The evidence suggests that the ER is under stress in neurons affected in AD and might contribute to perturbed cellular Ca^{2+} homeostasis (Lindholm et al., 2006). Neurons from mice expressing the presenilin1 mutation (PS1), which is part of the γ-secretase complex responsible for APP processing, present a large increase in the amount of Ca^{2+} release by IP3R (Cheung et al., 2008). RyR also contributes to Ca^{2+} disruption in AD by an enhanced recruitment of active RyRs in the ER in AD mice from different stages (Stutzmann et al., 2007) and through the increase in the expression and function of these receptors (Paula-Lima et al., 2011; Supnet et al., 2006). On the other hand, the increase in cytosolic Ca^{2+} directly affects mitochondria, disrupting its critical function as a Ca^{2+} buffering organelle (Celsi et al., 2009), which disturbs ATP generation and therefore neuronal viability. For this reason, mitochondrial dysfunction appears an obligatory downstream step in the pathogenesis of AD (see below).

1.4. Mitochondrial dysfunction in AD.

Mitochondrial dysfunction is an early feature of AD since several abnormalities have been described in brains from different models of AD (Moreira et al., 2007; Supnet and Bezprozvanny, 2010; Swerdlow et al., 2010). The activity of respiratory chain enzymes associated with the mitochondrial complex III (cytochrome-c reductase) and IV (cytochrome-c oxidase) is significantly decreased in mitochondria from transgenic (Tg) APP mice (Caspersen

et al., 2005; Manczak et al., 2006) and in isolated mitochondria exposed to Aβ *in vitro* (Canevari et al., 1999). Generation of ROS is also deregulated in AD and an enhanced production of free radicals and oxidative damage is a feature of the progression of the disease (Reddy, 2006). In addition, metabolic properties, such as ATP levels and glucose uptake are also decreased in AD brains from Tg APP mice (Chen and Yan, 2010; Yao et al., 2009). All of these mitochondrial alterations produced by Aβ create a negative environment for the maintenance of an appropriate function of the mitochondria, since directly affect the electrochemical gradient that is generated along the electron transport chain (ETC), favoring the leakage of electrons from the ETC and therefore the production of superoxide species, the loss of mitochondrial membrane potential (mΔΨ), permeability and structure (Reddy, 2009). It has been clearly demonstrated that Aβ accumulates progressively within AD brains, Tg mice models and cells overexpressing APP (Devi et al., 2006; Du et al., 2008; Lustbader et al., 2004). Aβ produced at the extracellular space, through APP processing, enters the neuron by the endocytic pathway (Yu et al., 2010) and it has been proposed that its oligomerization begins intracellularly to produce the neurotoxicity and cell death (Walsh et al., 2000). But once Aβo are localized inside neurons, how can these oligomers directly affect mitochondria? Mitochondrial accumulation of Aβ could explain why Aβ interferes with the function and structure of this organelle to finally affect neuronal viability.

1.5. Mitochondrial accumulation of Aβ

The accumulation of Aβ in mitochondria occurs early in brains of Tg APP mice, between 4 to 5 months, and increases with aging, even before the massive extracellular deposition occurs (Caspersen et al., 2005), an observation that is in agreement with previous findings

which indicate that intracellular accumulation of Aβ occurs previously to amyloid plaques formation (Wirths et al., 2001). The first study that described the presence of Aβ in mitochondria was performed by Lustbader et al., in 2004. They demonstrated by immunofluorescence assay and electron microscopy that Aβ colocalized with Aβ-binding alcochol dehydrogenase (ABAD) inside mitochondria from human AD brain, and that the interaction between Aβ and ABAD promotes leakage of ROS, mitochondrial dysfunction and cell death (Lustbader et al., 2004). Moreover, mitochondrial Aβ accumulation appears to strongly favor deposition of oligomeric $A\beta_{1-42}$ than $A\beta_{1-40}$. In the same way, Tg animals at 12 months of age present $A\beta_{1-42}$ aggregates about six-fold greater than those of $A\beta_{1-40}$ (Caspersen et al., 2005). This increased $A\beta_{1-42}/A\beta_{1-40}$ ratio is correlated with the high toxicity described for $A\beta_{1-42}$ rather than $A\beta_{1-40}$ in AD brain, probably due to $A\beta_{1-42}$ aggregates much more quickly than $A\beta_{1-40}$, providing seeds for further Aβ deposition (Bates et al., 2009). However, how does Aβ gain access to mitochondria? It has been proposed that APP could be located at the outer mitochondrial membrane (OMM) where can be processed by the mitochondrial γ-secretase (Devi and Anandatheerthavarada, 2010), however this particular event has not been directly demonstrated and, despite the presence of mitochondrial APP, the evidences suggest that Aβ is not likely to be produced locally in mitochondria, and instead, that it is imported from the cytoplasm into the organelle (Chen and Yan, 2010). It has been demonstrated that the import of Aβ into mitochondria occurs through the protein transport machinery of mitochondria, specifically via the translocase of the OM (TOM), to localize it at the cristae of mitochondria. The mitochondrial Aβ import has been observed both *in vivo* and *in vitro* and even when Aβ is extracellularly applied (Hansson Petersen et al., 2008). Therefore, mitochondrial Aβ accumulation is a key process, which leads to the understanding of how Aβ

can damage neurons so effectively in AD. Once inside mitochondria, Aβ can interact with several proteins that are important for the correct function of this organelle and/or for the maintenance of its structure. Regarding this idea, one of the proteins that regulates mitochondrial structure and that interacts with Aβ is cyclophilin D (CypD), which participates in the opening of the mitochondrial PTP (mPTP) and therefore regulates the permeability and function of the mitochondria, affecting both its energetic and calcium buffer functions (Du and Yan, 2010a).

1.6. Mitochondrial permeability transition pore and Aβ-CypD interaction

The mPTP is a non-selective pore that is formed and remains open for periods that are highly dependent on calcium concentration inside the mitochondrial matrix. The opening of the mPTP for short time periods induces a rapid and regulated calcium release from the mitochondrial matrix, however, if the pore remains open for long periods, potentiated by an apoptotic stimulus, such as Aβ, or by elevated calcium concentrations, which can also be produced by Aβ, occurs an uncontrolled release of this ion from the mitochondria (Muirhead et al., 2010; Rao et al., 2013). The permeabilization of the inner mitochondrial membrane (IMM) induces morphological changes in the mitochondria, including an increased volume, a phenomenon known as *swelling*, and the dissipation of the mΔΨ, disruption of the membrane and uncontrolled release of calcium and pro-apoptotic factors, such as cytochrome-c, into the cytoplasm, activating neuronal death cascades (Petronilli et al., 2001) (Figure 1). The detailed structure of the mPTP is not well established (Celsi et al., 2009), but it is known to be at least formed by the voltage-dependent anion channel (VDAC) at the OMM, the adenine nucleotide translocase (ANT) at the IMM, and cyclophilin D (CypD) in the mitochondrial matrix

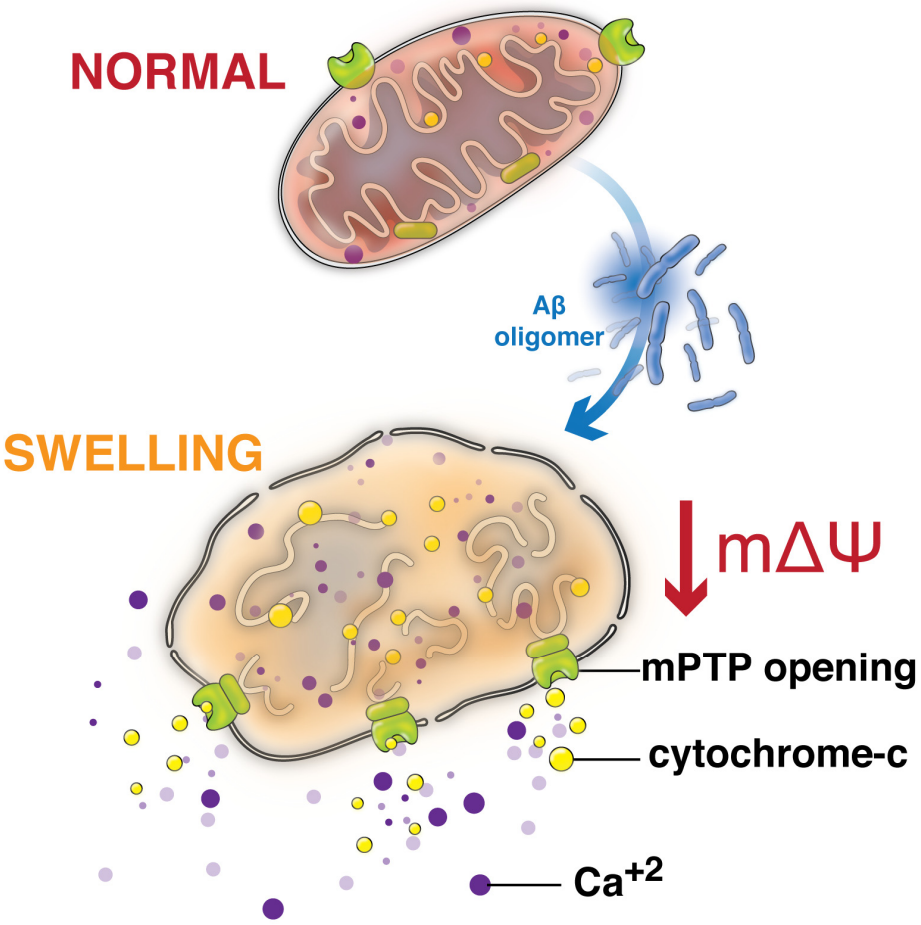

Figure 1. Morphological changes of mitochondria during membrane permeability transition in AD. Mitochondria are structured organelles which in normal or healthy conditions present a conserved structure of both, the inner mitochondrial membrane (IMM) and the outer mitochondrial membrane (OMM). This organization allows the formation of the mitochondrial cristae, which are important since therein resides the electron transport chain (ETC) to support cellular respiration. Under AD conditions, in the presence of Aβo, mitochondria undergo structural changes as a result of Aβ-induced mitochondrial membrane permeability. This phenomenon is triggered by the opening of the mitochondrial permeability transition pore (mPTP), which produces water and solutes entry into the mitochondria, inducing increase volume and the loss of the mitochondrial structure, to promote mitochondrial membrane potential (mΔΨ) dissipation and the release of pro-apoptotic factors and calcium to the cytoplasm. These morphological changes that mitochondria undergo during membrane permeability are known as mitochondrial swelling, which finally generates the loss of mitochondrial function to activate neuronal death processes.

(Figure 2A) (Baines et al., 2005; Halestrap, 2009; Schinzel et al., 2005). CypD, is a peptidyl prolyl cis-trans isomerase found in the mitochondrial matrix that has been described as a key positive regulator of the mPTP, since translocates to the IMM during the opening of the pore in oxidative stress conditions (Connern and Halestrap, 1994). CypD association with ANT on the IMM contributes to the formation and opening of the mPTP. Regarding the mechanisms proposed for the action of Aβ peptides at the level of mitochondrial membrane permeability, it has been postulated that Aβ directly interacts with CypD to induce mPTP opening (Figure 2B). Despite it has been proposed that CypD is the main component required for the mPTP formation, it has been demonstrated that the pore can be form and open in the absence of CypD, suggesting that this event may depend on multiple factors (Basso et al., 2005). In agreement with this idea, studies of protein-protein interaction have shown that Aβ also binds ANT and that this interaction is stronger than Aβ-CypD interaction, possibly affecting the normal physiological function of ANT and the formation of the mPTP (Singh et al., 2009). Despite this evidences it is very clear that CypD is a key component of the mPTP since modulates the mPTP sentitivity to Ca^{2+} and the cell susceptibility to apoptotic stimuli (Baines et al., 2005; Schinzel et al., 2005). On the other hand, and related to AD, it has been demonstrated that the deficiency of CypD, in an AD transgenic mice background, attenuates the cellular death induced by Aβ and improves memory and synaptic function (Du and Yan, 2010a; Du et al., 2008). Thus, blocking Aβ entry to mitochondria or inhibiting CypD-dependent mPTP stimulated by Aβ, are potential therapeutic strategies for AD. For this reason, the study of molecules that could be able to prevent the mitochondrial permeability induced by Aβ is crucial for the development of tools for the early treatment of neurodegenerative diseases in which mitochondria are involved.

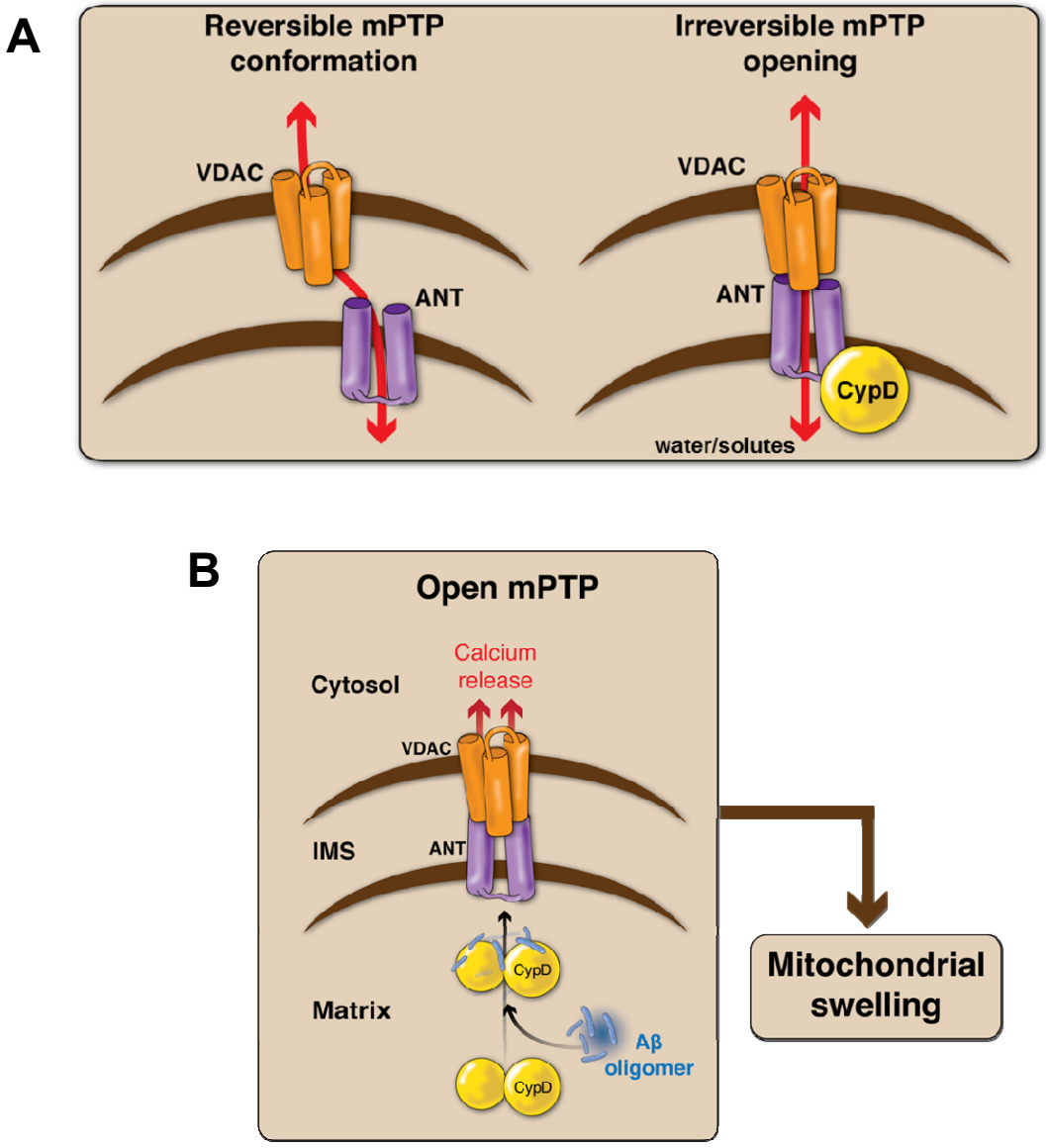

Figure 2. Mitochondrial permeability transition pore conformation. A) mPTP is mainly formed by the voltage-dependent calcium channel (VDAC, in orange), the adenine nucleotide translozase (ANT, in purple) and Cyclophilin D (CypD, in yellow). Under physiological conditions mPTP presents a reversible conformation and CypD is not part of the protein complex and mainly resides into the mitochondrial matrix (MM). The interaction between all of the components, mediated by an apoptotic stimulus, produces the formation and opening of the mPTP, which generates an irreversible response, leading to water and solutes entry into the MM. **B)** In an AD context, Aβ oligomers induce the translocation of CypD from the MM to the IMM to facilitate their interaction with ANT, and therefore the formation and opening of the mPTP. This final step induces uncontrolled release of calcium and mitochondrial swelling.

1.7. Wnt signaling and its neuroprotective role in AD

Previous studies from our laboratory demonstrated that the activation of the canonical *Wnt* signaling pathway protects neurons against Aβ toxicity *in vitro* and *in vivo* (Alvarez et al., 2004; Toledo and Inestrosa, 2010; Vargas et al., 2014). *Wnt* ligands are secreted proteins that mainly activate two *Wnt* pathways: the canonical, or β-catenin-dependent, signaling pathway (the *Wnt*/β-catenin pathway); and the non-canonical signaling pathways (the *Wnt*/PCP and *Wnt*/Ca^{2+} pathways) (Figure 3) (Inestrosa and Varela-Nallar, 2014; Willert and Nusse, 2012). The Wnt/PCP pathway is activated by the interaction of a Wnt ligand with its Frizzled (Fz) receptor. This binding produces the activation of Dishevelled (Dvl), which in turn activates the small GTPases Rho and Rac, to finally activate the Jun N-terminal kinase (JNK), regulating the cytoskeleton reorganization (Rosso et al., 2005). On the other hand, in Wnt/Ca^{2+} pathway, the binding between Wnt ligand and the Fz receptor activates the trimeric G proteins, which induces the activation of phospholipase C (PLC) and the production of diacyl-glycerol (DAG) and inositol triphosphate (IP3), generating an increase in the intracellular Ca^{2+} levels and the subsequent activation of Ca^{2+}-dependent proteins (Inestrosa and Arenas, 2010). By contrast, the Wnt/β-catenin pathway is activated by the binding of a Wnt ligand to its Fz receptor and to the co-receptor LRP5/6. This interaction activates Dvl, which causes the dissociation of the destruction complex to inhibit glycogen synthase kinase-3β (GSK-3β) and prevent β-catenin degradation through the proteasome, therefore inducing its accumulation into the cytoplasm, to finally translocate to the nucleus to trigger the expression of Wnt target genes (Arrázola et al., 2009; Clevers and Nusse, 2012). About Wnt signaling functions, it has been implicated in the development and maintenance of the nervous

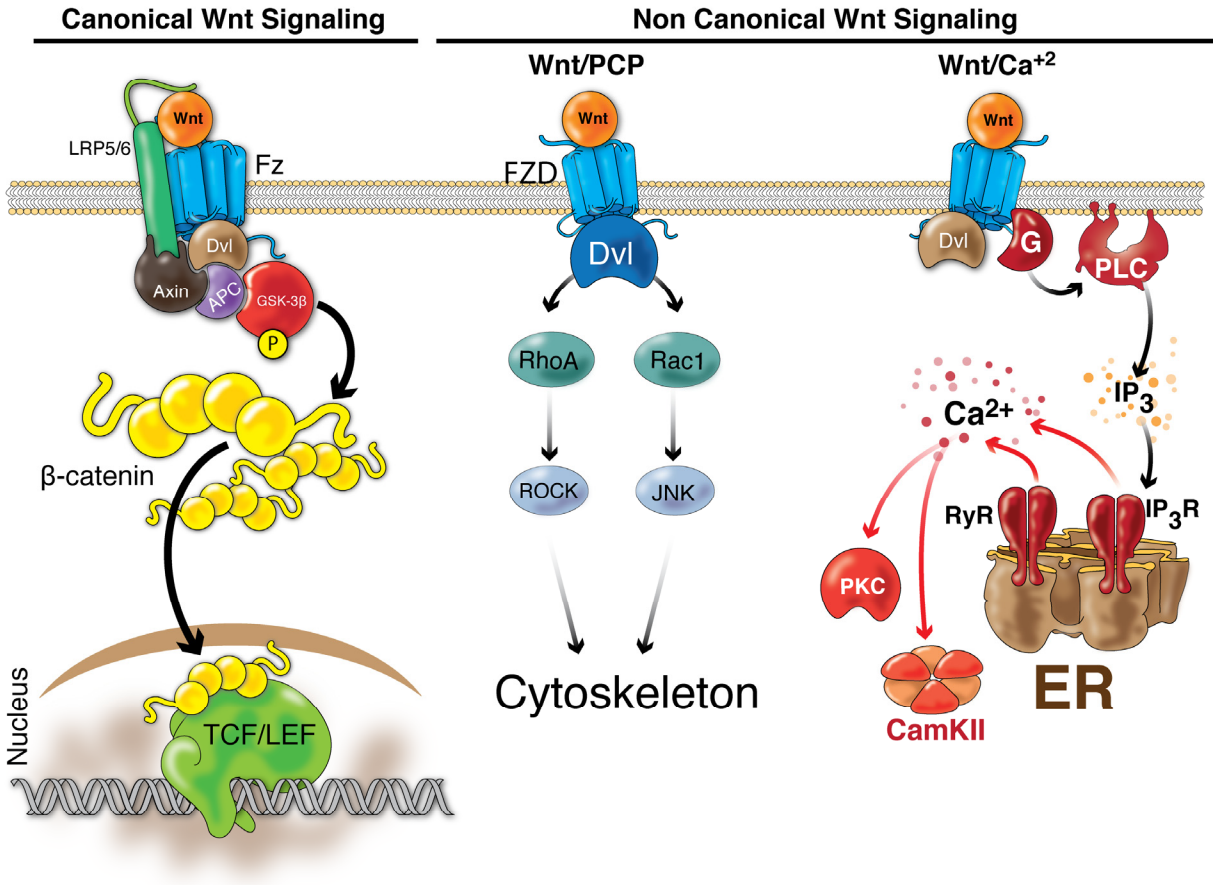

Figure 3. Canonical and non-canonical Wnt signaling pathways. ***Left:*** The activation of Wnt/β-catenin signaling begins with the binding of Wnt ligand to a Frizzled (Fzd) receptor and the low density lipoprotein receptor-related protein 5/6 (LRP 5/6), producing the recruitment of Dishevelled (Dvl) and the subsequent inhibition of the "β-catenin destruction complex" mainly formed by Axin, adenomatous polyposis coli (APC) and glycogen synthase kinase-3β (GSK-3β). The phosphorylation and inhibition of GSK-3β the accumulation of β-catenin, which is no longer phosphorylated and then translocate to the nucleus to activate the transcription of Wnt target genes mediated by the TCF/LEF factors. ***Middle:*** In the Wnt/PCP pathway, Wnt-Fzd interaction promotes the activation of Dvl to induce the activation of Rho and Rac small GTPases. Activation of Rho signals through the Rho-associated kinase (ROCK) and the activation of Rac signals to the c-Jun N-terminal kinase (JNK), modulating the actin cytoskeleton. ***Right:*** In the Wnt/Ca^{2+} pathway, the binding of *Wnt* to Fzd activates heterotrimeric G-proteins which in turns signal through phospholipase-C (PLC) and inositol-1,4,5-thriphosphate (IP3) to induce the release of intracellular Ca^{2+} and the activation of both protein kinase C (PKC) and Ca^{2+}/calmodulin-dependent protein kinase type-II (CaMKII).

system (Inestrosa and Arenas, 2010) because it regulates synaptogenesis (Rosso and Inestrosa, 2013; Salinas and Zou, 2008) and participates in the adult neurogenesis of the hippocampus (Lie et al., 2005; Varela-Nallar and Inestrosa, 2013). Related to the AD, the canonical Wnt signaling has been involved in the neuroprotection against Aβ-induced neuronal damage (Cerpa et al., 2009) because its activation protects hippocampal neurons from Aβ-induced cell death (Alvarez et al., 2004) and also prevents the intracellular calcium increase generated by Aβ in neurons, which directly affects mitochondrial calcium levels (Dinamarca et al., 2010; Quintanilla et al., 2005). However, the mechanism by which this protection occurs is unknown and neither has it been explored whether Wnt signaling could exert its neuroprotective role against Aβ-induced toxicity through the protection of the mitochondria.

Studies from our laboratory have shown that the activation of the canonical Wnt signaling pathway regulates the expression of the mitochondrial anti-apoptotic protein Bcl-2 (Fuentealba et al., 2004) and that the up-regulation of this protein protects hippocampal neurons from Aβ-induced mitochondrial damage (Fuenzalida et al., 2007). Moreover, Bcl-2 has also been involved in the inhibition of the mPTP through its capability to interact with CypD (Eliseev et al., 2009). On the other hand, a key component of the canonical Wnt signaling, glycogen synthase kinase-3β (GSK-3β), has been involved in cardioprotection models with the inhibition of the mPTP through its interaction with several components of the pore inside mitochondria, including ANT and CypD (Nishihara et al., 2007; Zorov et al., 2009). These evidences suggest an appealing role for Wnt signaling in neuroprotection through the regulation of mitochondrial-dependent cell death cascades, especially through the inhibition of mitochondrial membrane permeability, to favor the maintenance of the structure and therefore the function of the mitochondria.

In this thesis we studied the mitochondrial events involved in the neurotoxicity induced by Aβ and whether the canonical Wnt signaling activation, through the Wnt3a ligand, prevents these pathological events in particular related to mitochondrial dysfunction and mitochondrial membrane permeabilization, which are the earliest events, that will trigger the neuronal death process in AD brain. The data presented here suggests that Wnt3a protects neurons against Aβo-induced neuronal cell death through the inhibition of mPTP opening, preventing the disruption of the mitochondrial integrity and its loss of function.

1.8. Hypothesis and Objectives

1.8.1. Hypothesis

The activation of the Wnt/β-catenin signaling pathway prevents the mitochondrial membrane permeability induced by Aβ oligomers in hippocampal neurons.

1.8.2. Objectives

Aim:

To study the role of Wnt/β-catenin signaling on mitochondrial dysfunction in hippocampal neurons exposed to Aβ oligomers.

Research Objectives:

1. To evaluate the effect of the canonical Wnt signaling activation on mitochondrial calcium overload caused by Aβ oligomers in hippocampal neurons.

2. To study the role of Wnt in the formation and opening of the mitochondrial permeability transition pore in Aβo-exposed neurons.

2. CHAPTER I

The next section presents the results obtained in order to accomplish the Research Objectives N° 1 and 2. This work was submitted to The Journal of Neuroscience on April 30th, 2014 (Manuscript ID: JN-RM-1750-14).

As is shown below, this manuscript describes the protective effects of the canonical Wnt signaling activation on mitochondrial membrane permeability induced by Aβ. Live cell imaging assays indicated that Wnt3a ligand prevents the mitochondrial calcium overload generated by Aβ exposure on hippocampal neurons, which was also accompanied by a protection at the mitochondrial membrane potential level and with the inhibition of the mPTP opening. To directly study the permeability of mitochondrial membranes and cristae disruption, electron microscopy analysis was performed. The results indicated that the mitochondrial structure was protected from the Aβo damage that is generated in brain mitochondria of AD when Wnt signaling was previously activated. These results were also consistent with a prevention of the morphological changes that mitochondria undergo during the swelling process, such as increase volume and sphericity, which were evaluated from 3D reconstructions of the mitochondrial network. Thus, the results indicated that the activation of the canonical Wnt signaling inhibits the mPTP opening to finally, protect neurons against Aβo-induced cell death.

Wnt Signaling Prevents Mitochondrial Permeability Transition Pore Opening Induced by Aβ Oligomers in Hippocampal Neurons

Abbreviated title: Wnt3a prevents Aβ-mediated mPTP opening

Macarena S. Arrázola[1], Daniela Ordenes[1] and Nibaldo C. Inestrosa[1,2*]

[1]Centro de Envejecimiento y Regeneración (CARE), Departamento de Biología Celular y Molecular, Facultad de Ciencias Biológicas, Pontificia Universidad Católica de Chile, Santiago, Chile, 8331150. [2]Center for Healthy Brain Ageing, School of Psychiatry, Faculty of Medicine, University of New South Wales, Sydney, Australia.

* Corresponding author: Dr. Nibaldo C. Inestrosa at CARE, Biomedical Center, Pontificia Universidad Católica de Chile, Av. Alameda 340, Santiago, Chile, postal code 8331150. Phone: + (56)-2-6862724; Fax: + (56)-2-6862959; e-mail: ninestrosa@bio.puc.cl.

Number of pages: 47
Number of figures: 9
Number of Tables: 1
Number of words for Abstract: 225
Number of words for Introduction: 499
Number of words for Discussion: 1450

The authors declare no competing financial interests.

Acknowledgements
We thank Dr. Gail VW Johnson (Department of Anesthesiology, University of Rochester Medical Center, Rochester, NY) for the kind gift of the mito-Cherry plasmid. We also thank Felipe Serrano for the design of the mechanism model and Gloria Méndez for the preparation of primary culture of hippocampal neurons. This work was supported by Grant PFB 12/2007 from the Basal Center for Excellence in Science and Technology (to NCI), and a predoctoral fellowship from Comisión Nacional de Investigación Científica y Tecnológica for MSA.

Abstract

The mitochondrial permeability transition pore (mPTP) is a non-selective pore that is formed and remains open for periods that are highly dependent on the calcium concentration inside the mitochondrial matrix. mPTP has been implicated in the pathogenesis of Alzheimer's disease because amyloid-β peptide (Aβ) oligomers (Aβo) induce its opening, thereby activating mitochondrial-dependent neuronal death cascades. Previous work from our laboratory suggested that canonical Wnt signaling, through the Wnt3a ligand, has a neuroprotective effect against Aβ toxicity, inhibiting the neuronal death induced by Aβ peptide; however, the mechanism by which Wnt signaling activation prevents neuronal death is unclear. To study the cellular steps involved in the neurotoxicity induced by Aβ, we performed live cell imaging in hippocampal neurons to detect specific events related to mitochondrial membrane permeabilization. This last phenomenon was also evaluated by electron microscopy to detect mitochondrial membrane integrity and morphological changes on mitochondria, related to mitochondrial swelling, from hippocampal slices exposed to Aβ in the presence of Wnt3a. We report here that Wnt3a prevents an Aβo-induced cascade of mitochondrial events that leads to neuronal death. This cascade involves: (a) increased mitochondrial calcium, (b) mitochondrial membrane potential loss, (c) cytochrome-c release, (d) mPTP opening and (e) mitochondrial swelling, leading to neuronal death. Thus, our results indicate that the activation of canonical Wnt signaling protects neurons against Aβo damage through the inhibition of mPTP opening.

Introduction

Alzheimer's disease (AD) is a neurodegenerative disorder characterized by memory loss and cognitive decline (Hardy and Selkoe, 2002). Oligomers from amyloid-β peptide (Aβo) are the most neurotoxic species responsible for the neuronal dysfunction in AD (Walsh et al., 2002; Li et al., 2009). Defects at the mitochondrial level have been described in AD patients (Supnet and Bezprozvanny, 2010; Swerdlow et al., 2010) and some studies propose that the Aβ peptide acts inside the mitochondria affecting its membrane permeability through mitochondrial permeability transition pore (mPTP) opening (Du and Yan, 2010a). The mPTP induction, potentiated by an apoptotic stimulus, such as Aβ, or by elevated calcium concentrations, produces an uncontrolled release of this ion from the mitochondria (Celsi et al., 2009) and the permeabilization of the inner membrane, which induces an increased volume of the mitochondria, a phenomenon known as swelling, and the dissipation of the mitochondrial membrane potential, disruption of the membrane and release of pro-apoptotic factors, such as cytochrome-c, into the cytoplasm, activating neuronal death cascades (Petronilli et al., 2001). The study of molecules that are able to prevent the mitochondrial permeability induced by Aβ could lead to the development of tools for the early treatment of neurodegenerative diseases in which mitochondria are involved, such as AD. Previous studies from our laboratory demonstrated that the activation of the canonical Wnt signaling pathway protects neurons against Aβ peptide toxicity (Alvarez et al., 2004; Toledo and Inestrosa, 2010; Vargas et al., 2014), however, the steps that mediate the protective role of Wnt3a are unexplored.

The Wnt/β-catenin pathway is activated by the binding of a Wnt ligand to its Frizzled (Fz) receptor and to the co-receptor LRP5/6, inducing β-catenin accumulation in the cytoplasm to finally translocate to the nucleus to regulate the expression of Wnt target genes (Arrázola et al., 2009; Clevers and Nusse, 2012). Wnt signaling has been implicated in the development and maintenance of the nervous system (Inestrosa and Arenas, 2010) because it regulates synaptogenesis (Salinas and Zou, 2008; Rosso and Inestrosa, 2013) and participates in the adult neurogenesis of the hippocampus (Lie et al., 2005; Varela-Nallar and Inestrosa, 2013). On the other hand, canonical Wnt signaling is involved in neuroprotection against Aβ (Cerpa et al., 2009; De Ferrari et al., 2013) because protects hippocampal neurons from Aβ-induced cell death (Alvarez et al., 2004; Inestrosa and Varela-Nallar, 2014) and also prevents the intracellular calcium increase generated by Aβ, which directly affects mitochondrial calcium levels (Quintanilla et al., 2005; Dinamarca et al., 2010).

We report here that Wnt signaling activation regulates mitochondrial calcium levels altered by Aβo in hippocampal neurons and prevents mitochondrial membrane potential loss, thereby preserving the integrity of mitochondrial membranes, as evidenced by the inhibition of cytochrome-c release, the inactivation of mPTP opening and the prevention of morphological changes (including in size, shape and ultrastructural features) in mitochondria induced by exposure to Aβo. These results suggest that Wnt signaling prevents the mitochondrial swelling, a process characterized by mPTP opening, that is generated by neuron exposure to Aβo.

Materials and Methods

Primary culture of rat hippocampal neurons

The experimental procedures with animals were approved by the Bioethical and Biosafety Committee of the Faculty of Biological Sciences of the Pontificia Universidad Católica de Chile. Rat hippocampal cultures were prepared as described previously (Alvarez et al., 2004; Caceres et al., 1984). Hippocampi from Sprague-Dawley rats at embryonic day 18 were removed, dissected free of meninges in Ca^{2+}/Mg^{2+}-free Hanks' balanced salt solution (HBSS). The tissue was resuspended in HBSS containing 0.25% (wt/vol) trypsin and incubated for 15 min at 37°C. After three rinses with HBSS, the tissue was mechanically dissociated in Dulbecco's modified Eagle's medium (GIBCO, Rockville, MD) supplemented with 10% horse serum (GIBCO), 100 U/ml penicillin and 100 μg/ml streptomycin. Dissociated hippocampal cells were seeded onto poly-L-lysine-coated wells in plating medium. Cultures were maintained at 37°C in 5% CO_2 for 2 h before the plating medium was replaced with neurobasal growth medium (GIBCO) supplemented with B27 (GIBCO), 2 mM L-glutamine, 100 U/ml penicillin and 100 μg/ml streptomycin. On day 2, the cultured neurons were treated with 2 μM cytosine arabinoside (AraC) for 24 h.

Formation of amyloid-β oligomers

Synthetic $A\beta_{1-42}$ peptide corresponding to wild-type human Aβ was obtained from Genemed Synthesis, Inc. (San Francisco, CA). An Aβ peptide stock solution was prepared by dissolving freeze-dried aliquots of Aβ in 1,1,1,3,3,3-hexafluoro-2-propanol (HFIP, Sigma H-8508) at 1 mM, incubated at room temperature for 1 h and lyophilized. For oligomer preparation, the peptide film was dissolved in dimethyl sulfoxide (DMSO, Sigma D2650) at 5 mM and then

diluted into distilled water to a final concentration of 100 μM. The preparation was incubated overnight for Aβ oligomer formation (Klein, 2002). Aβ oligomers were visualized by electron microscopy and analyzed by Tris-Tricine SDS gel electrophoresis, as previously described (Dinamarca et al., 2010; Godoy et al., 2013; Silva-Alvarez et al., 2013).

Mitochondrial and intracellular calcium imaging

For *in vivo* cell imaging, neurons were seeded at a density of 1 x 10^5 cells in 25-mm cover slips and used for the experiments after 14 days *in vitro* (DIV). Hippocampal cells were loaded with the cell-permeant acetoxymethyl ester forms of the visible-wavelength calcium-sensitive dye Rhod2-AM (2 μM) at 4°C, to favor the mitochondrial localization of the probe, for 3 min and then with Fluo3-AM (1 μM) in the presence of pluronic F127 detergent (0.02% final concentration) (Molecular Probes, Carlsbad, CA) for 30 min at 37°C (Peng et al., 1998; Eisner et al., 2010). Cultures were washed with the recording solution, Tyrode Buffer (135 mM NaCl, 5 mM KCl, 1.8 mM $CaCl_2$, 1 mM $MgCl_2$, 10 mM HEPES, 5.6 mM glucose, pH 7.3), and imaged with an Olympus DSU IX81 spinning disk confocal microscope. After a measurement of the basal Rhod2-AM and Fluo3-AM signals, 20 μM Aβo was added at 3 min and the results were registered for 10 min. Rhod2-AM λex/em = 549/578 nm; Fluo3-AM λex/em= 488/526 nm. The estimation of the fluorescence intensity of both probes was presented as the pseudoratio (ΔF/Fo) indicated by: $\Delta F/Fo = (F-F_{base})/ (F_{base}-B)$, where F is the measured fluorescence intensity of the indicator, F_{base} is the fluorescence intensity before the stimulation and B is the background signal determined from the average of areas adjacent to the cells (Dinamarca et al., 2010; Quintanilla et al., 2013). The images were analyzed using NIH ImageJ software.

Mitochondrial membrane potential

Time lapse experiments to detect mitochondrial membrane potential changes ($\Delta\psi_m$) were performed in hippocampal neurons loaded with 50 nM of the fluorescent probe Mitotracker Orange (Molecular Probes) for 30 min at 37°C (Godoy et al., 2013; Silva-Alvarez et al., 2013). Fluorescence variations were analyzed in the same manner as the calcium measurements using an Olympus DSU IX81 spinning disk confocal microscope, considering λex/em = 554/576 nm (Buckman et al., 2001).

Immunofluorescence

Hippocampal neurons were seeded onto poly-L-lysine-coated coverslips in 24-well culture plates at a density of 3.5 x 10^4 cells per well. After treatment, the cells were loaded with 50 nM Mitotracker Orange for 30 min at 37°C. The cells were rinsed twice in PBS and fixed with a freshly prepared solution of 4% paraformaldehyde - 4% sucrose in PBS for 20 min and permeabilized for 5 min with 0.2% Triton X-100 in PBS. After several washes, the cells were incubated with 1% bovine serum albumin (BSA) in PBS (blocking solution) for 30 min at 37°C, followed by an overnight incubation at 4°C with the primary antibody mouse anti-cytochrome-c (BD Pharmingen, San Diego, CA). The cells were washed with PBS and then incubated with an Alexa-conjugated secondary antibody (Molecular Probes) for 30 min at 37°C. The coverslips were mounted in mounting medium (Dako, Glostrup, Denmark). Images were captured with an Olympus FluoView1000 Confocal Microscope and analyzed using NIH ImageJ software.

Neuronal viability assays

Hippocampal neurons plated on polylysine-coated coverslips (30,000 neurons/cover) were treated under different conditions for 24 h. Live and dead neurons were analyzed in non-fixed cells with the LIVE/DEAD Viability/Cytotoxicity Kit for mammalian cells (Molecular) (Saraiva et al., 2010). Apoptotic nuclei were analyzed with Hoechst 33342 stain (Molecular Probes) in fixed cells after the treatments, as previously described (Silva-Alvarez et al., 2013).

Calcein/Cobalt imaging

In vivo detection of mPTP opening was measured using the Image-iT ™ LIVE Mitochondrial Transition Pore Assay Kit (I35103) from Molecular Probes, with some modification according to previous studies (Petronilli et al., 1998; Gillessen et al., 2002). Briefly, hippocampal neurons were seeded at a density of 1 x 10^5 cells in 25-mm cover slips and used for the experiments after 14 DIV. The hippocampal cells were loaded with the labeling mix solution (1 μM calcein-AM, 50 nM Mitotracker Orange, 1 mM $CoCl_2$ and 1 μM Hoechst 33342 dye in Neurobasal media) for 40 min at 37°C. The ex/em peaks of calcein after hydrolysis occur at 494/517 nm. Cytoplasmic signals of calcein were quenched by cobalt without affecting the mitochondrial signal. As a result of stimulation of mPTP opening, calcein was released from the mitochondrial matrix due to the permeabilization of the mitochondrial membranes, which resulted in the redistribution and rapid decay of calcein fluorescence (Petronilli et al., 1999). Hoechst stain (λex/em = 350/461 nm) was not followed in the experiment, but it was used to determine the viability of the neurons before and after Aβo exposure. The mitochondrial calcein staining was checked using a Mitotracker as a mitochondrial positive marker, and mitochondria that presented both labels were used for the analysis. The ionophore ionomycin (0.5 μM), which induced Ca^{2+} overload, was used as a positive control for mPTP induction

(Nicholls and Budd, 2000), and Cyclosporin A (CsA, 20 µM) was used as an inhibitor of the pore opening (Halestrap et al., 1997).

Hippocampal neuron transfection

For mito-Cherry overexpression in cultured hippocampal neurons, we used NeuroMag (OZ Bioscience, Marseille, France) according to the manufacturer's protocol. Briefly, neurons from 12 DIV at 40,000-80,000 cells per well were incubated with non-covalent complexes containing the mito-Cherry plasmid and NeuroMag beads for 15 min over a magnetic plate and additional 45 min without the magnetic plate as previously described (Marchionni et al., 2009; Opazo et al., 2010). After 48 h, the neurons were used for treatments and z-stack image acquisition for 3D reconstruction analysis.

3D image reconstruction

Mitochondrial network images were obtained from mito-Cherry transfected neurons. Z-stack images of 0.35-µm thickness were obtained with a Nikon Eclipse C2si spectral confocal microscope, taking between 15 to 20 frames per neuron, from a total of 6 to 8 neurons per condition, with N=3 independent experiments. The images were reconstructed in 3D isosurface using Imaris software from the Facility of University of Concepción, Chile. The sphericity and volume of each reconstructed mitochondrion were determined as described previously (Picard et al., 2013).

Slice preparation

Hippocampal slices were prepared according to standard procedures from 2-month-old C57BL/6J males mice (http://jaxmice.jax.org/strain/000664.html) (Cerpa et al., 2008; Varela-Nallar et al., 2010). Transverse slices (400 µm) from the dorsal hippocampus were cut under

cold artificial cerebrospinal fluid (ACSF) using a Vibroslice microtome (VSL, WPI) and incubated in oxygenated ACSF for more than one hour at room temperature before treatment.

Mitochondrial Isolation

Mitochondria were isolated from hippocampal slices according to manufacturer's indications, using the Mitochondrial Isolation kit for Tissue (Pierce Biotechnology, Rockford, IL).

Western blot

Isolated mitochondria were lysed in 2% CHAPS in Tris buffered saline (TBS: 25mM Tris, 0.15M NaCl, pH 7.2). The samples (30 μg) were subjected to electrophoresis on 15% SDS-polyacrylamide gels. We used rabbit anti-phosphorylated (Ser9) GSK-3β antibody (Cell signaling Technology Inc., Danvers, MA), mouse anti-GAPDH antibody (Santa Cruz Biotechnology, Inc., Santa Cruz, CA) as a cytoplasmic loading control and rabbit anti-COXIV antibody (Cell Signaling Technology Inc.) as a loading control of mitochondrial fraction.

Electron microscopy

Hippocampal slices were used for electron microscopy analysis, according to standard procedures (Inestrosa et al., 2005; Perkins and McCaffery, 2007; Picard et al., 2013). Briefly, hippocampal slices were treated and directly fixed in 3% glutaraldehyde in 50 mM cacodylate buffer (pH 7.2) for 3 days at room temperature. Then, the slices were treated with 1% osmium tetroxide in cacodylate buffer for 90 min followed by 1% aqueous uranyl acetate, dehydrated in acetone and embedded in Epon resin. The Epon-embedded lamina of the hippocampal slices was cut into small pieces and re-included in the resin. Areas to be examined by electron microscopy (CA1 region of the hippocampus) were selected from 1-μm sections stained with toluidine blue for light microscopy. Ultra-thin sections were cut with a Reichert

Ultramicrotome, placed on 300-mesh copper electron microscopy grids, stained with uranyl acetate and lead citrate (Reynolds, 1963), and examined using a Phillips Tecnai 12 transmission electron microscope at 80 kV from the Facility of the Faculty of Biological Sciences, Pontificia Universidad Católica de Chile. Between 40 to 50 digital images were obtained per treatment, and they were analyzed with ImageJ to manually measure, in a blinded fashion, the mitochondrial area, diameter and perimeter (Song et al., 2004). The ultrastructural features of mitochondria, such as the membrane and cristae integrity, were determined in each mitochondrion at the same time as the measurement of morphological parameters. Membranes or cristae were considered to be intact when the whole structure was preserved and organized and the mitochondria appeared normal, as has been previously described (Sun et al., 2007). Quantitative analysis was performed with n = 3 with GraphPad Prism 5.01.

Quantification and statistical analysis

The data represent the mean and SEM from 3-8 independent experiments for live cell imaging, each with *n*=3-4 replicates. N=3 was used for immunofluorescence, mitochondrial network reconstruction and electron microscopy analysis. *p* values were obtained using a two-way ANOVA test for grouped data, and a one-way ANOVA test for bar graphs, plus a *post hoc* Bonferroni test. Error bars indicate SEM *p<0.01; **p<0.001; ***p<0.0001.

Results

Intracellular and mitochondrial calcium levels are modulated by Wnt signaling activation in neurons that are exposed to Aβ oligomers.

One of the important functions of mitochondria is to control calcium variations inside the cell. A massive and uncontrolled calcium influx into mitochondria directly affects mitochondrial

permeability (Du and Yan, 2010b), inducing mitochondrial membrane potential dissipation, increased membranes permeability and, finally, neuronal death (Celsi et al., 2009). Intracellular calcium levels were evaluated in 14 DIV hippocampal neurons. To determine the neuroprotective effect of Wnt signaling activation, recombinant Wnt3a ligand (rWnt3a, 300 ng/ml) was used. Neurons were treated for 24 h with rWnt3a and loaded with the fluorescent probe Fluo3-AM (1 μM) for 30 min at 37°C. Live cells were analyzed with a spinning disk confocal microscope, and for calcium measurement, the fluorescence intensity was registered during a 3-min period (basal), and then the neurons were stimulated with 20 μM Aβo or vehicle and recorded for an additional 7 min. Figure 1A shows representative pseudocolored images from each treatment immediately before (Figure 1Aa, c) and after 500 s of Aβo exposure (Figure 1Ab, d). Surface plots show increased fluorescence intensity in control neurons exposed to Aβo, which was not observed in Wnt3a pre-treated neurons (Figure 1Aa'-d'). In agreement with a previous study from our laboratory in which the Wnt7a ligand was used to activate Wnt signaling (Quintanilla et al., 2005), the pretreatment of neurons with rWnt3a also prevented the intracellular calcium increase induced by Aβo, evaluated at the soma (Figure 1Ba) and in neurites (Figure 1Bb).

To evaluate mitochondrial calcium levels, neurons were treated with control media and rWnt3a protein and then loaded with Rhod2-AM (2 μM) at 4°C for 3 min plus a recovery period, without a probe, of 30 min at 37°C. Aβo exposure induced a significant increase in the fluorescence intensity compared to the basal period in the same neuron (Figure 2Aa, b) beginning 300 s from the start of the experiment (Figure 2B). This increase was observed specifically in neurites, as shown in Figure 2Ca, b in the magnified cropped image and in the

Figure 1

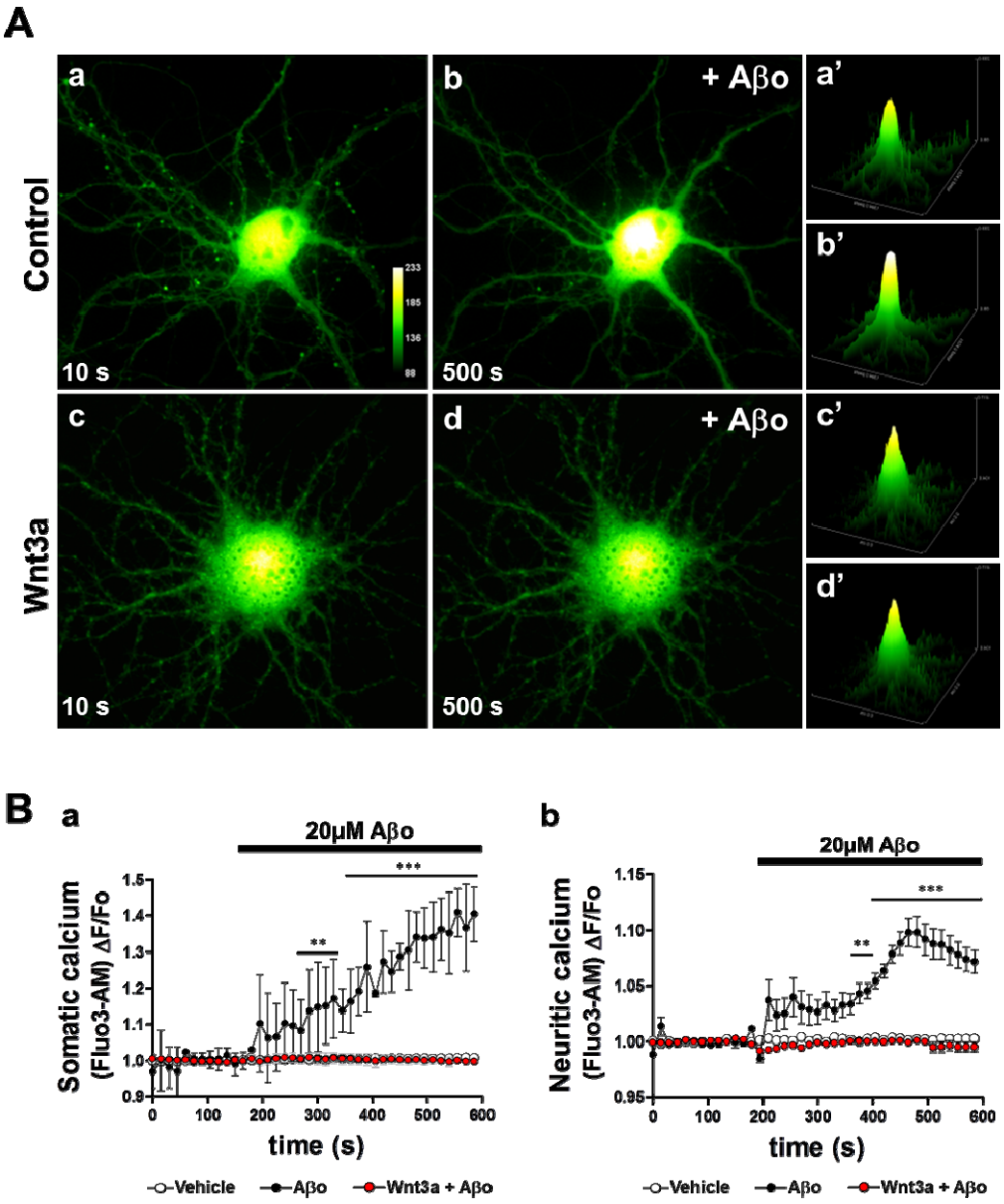

Figure 1. Wnt signaling activation, through *Wnt3a* ligand, prevents intracellular calcium increase induced by Aβ oligomers in cultured hippocampal neurons. 14 DIV hippocampal neurons treated with control media or 300 ng/ml of rWnt3a protein for 24 h and loaded with intracellular calcium indicator Fluo3-AM. **A)** Representative pseudocolored images obtained by Spinning Disk Confocal Microscopy immediately before (a,c) and 500 s after (b,d) Aβo exposure. The respective surface intensity distribution plot are shown in a'-d' images. **B)** Quantification of fluorescence intensity changes ($\Delta F/F_0$) in control and rWnt3a treated neurons in soma (a) and neurites (b). The graphs show the mean ± SEM of n=8 independent experiments. ANOVA test, *post hoc* Bonferroni **p<0.001; *** p<0.0001.

Figure 2

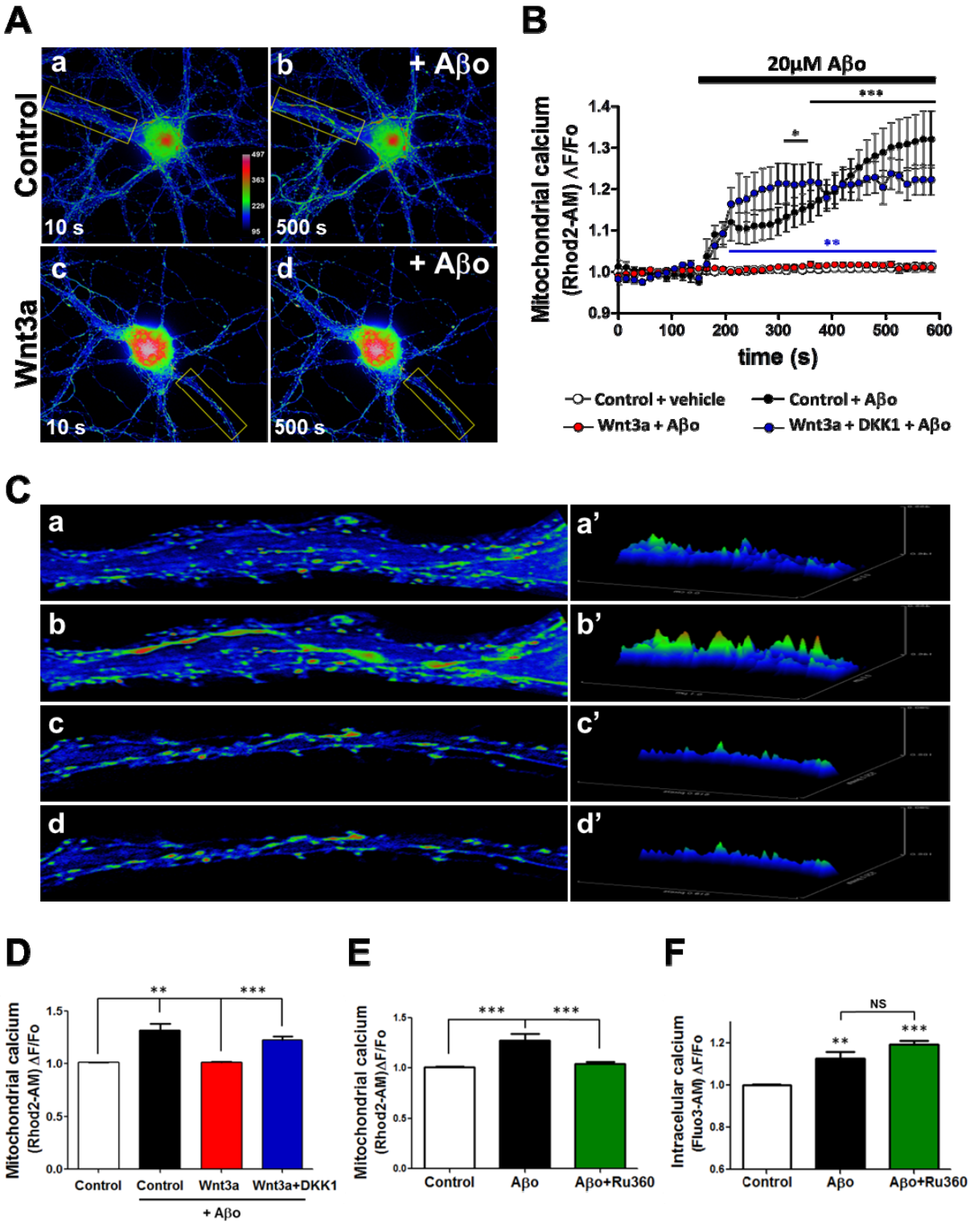
A
a
b
+ Aβo
Control
10 s
500 s
c
d
+ Aβo
Wnt3a
10 s
500 s
B
20μM Aβo
***
*
**
Mitochondrial calcium (Rhod2-AM) ΔF/Fo
1.4
1.3
1.2
1.1
1.0
0.9
0
100
200
300
400
500
600
time (s)
Control + vehicle
Control + Aβo
Wnt3a + Aβo
Wnt3a + DKK1 + Aβo
C
a
a'
b
b'
c
c'
d
d'
D
Mitochondrial calcium (Rhod2-AM) ΔF/Fo
**
***
1.5
1.0
0.5
0.0
Control
Control
Wnt3a
Wnt3a+DKK1
+ Aβo
E
Mitochondrial calcium (Rhod2-AM)ΔF/Fo
***
***
1.5
1.0
0.5
0.0
Control
Aβo
Aβo+Ru360
F
Intracelular calcium (Fluo3-AM) ΔF/Fo
NS
**
***
1.2
1.0
0.8
0.6
Control
Aβo
Aβo+Ru360

Figure 2. Mitochondrial calcium increase induced by Aβ oligomers is prevented by Wnt3a. 14 DIV hippocampal neurons treated with control media or 300 ng/ml of rWnt3a protein for 24 h and loaded with mitochondrial calcium indicator Rhod2-AM. **A)** Pseudocolored images of neurons treated with control medium or rWnt3a and loaded with Rhod2-AM. Images were obtained before (a,c) and after (b,d) the addition of Aβo. **B)** Quantification of fluorescence intensity changes ($\Delta F/F_0$) in time lapse ($\Delta F/F_0$) from control, rWnt3a and rWnt3a+DKK1-treated neurons (DKK1= 100 ng/mL) . Black horizontal bar indicates the addition of Aβo. **C)** Respective cropped images (a-d) and the surface intensity distribution plots (a'-d') show mitochondrial calcium changes in neurites. **D)** Representative graph of the end time point (500s) of the experiment quantified in B) for each condition. **E)** Quantification of changes in mitochondrial fluorescence intensity ($\Delta F/F_0$) at the end of the time lapse experiment in neurons treated with Aβo plus 10 μM Ru360. **F)** Intracellular calcium changes ($\Delta F/F_0$) in response to Aβo in neurons previously treated with Ru360. The graphs show the mean ± SEM of n=6 independent experiments. ANOVA test, *post hoc* Bonferroni *p<0.01; **p<0.001; *** p<0.0001.

surface plots (Figure 2Ca', b'). By contrast, the increase in mitochondrial calcium produced by Aβo in control neurons was not observed in rWnt3a pre-treated neurons (Figure 2Ac, d and Figure 2B). These calcium changes were also evaluated at the neurite level, as shown in the magnification (Figure 2Cc,d) and the surface plots (Figure 2Cc',d'). The mitochondrial calcium levels in rWnt3a neurons after Aβo exposure were always near the control/vehicle levels and were significantly different from those of Aβo-treated neurons (Figure 2B). Figure 2D shows the quantification at the end time point for each treatment compared to the control/basal conditions. The treatment of neurons with the Wnt antagonist Dikkopf-1 (DKK1, 100 ng/mL), which specifically inhibits the Wnt/β-catenin signaling pathway by interacting with LRP5/6 co-receptors (Kawano and Kypta, 2003; Purro et al., 2012), completely abolished the protective effect of Wnt3a against Aβo-induced mitochondrial calcium changes (Figure 2B and Figure 2D). To confirm the specificity of Aβo for the effect observed on mitochondrial calcium levels, we inhibited the calcium uptake by the mitochondria with Ru360, which inhibits the mitochondrial calcium uniporter (MCU) (Ying et al., 1991; Sripetchwandee et al., 2013), the main route for calcium uptake in brain mitochondria (De Stefani et al., 2011; Marchi and Pinton, 2014). The treatment of neurons with 10 μM Ru360 for 30 min significantly inhibited the increase in mitochondrial calcium induced by Aβo (Figure 2E), without affecting the cytoplasmic calcium levels (Figure 2F). These results indicate that the activation of the canonical Wnt signaling pathway through the Wnt3a ligand prevents both intracellular and mitochondrial calcium increases in hippocampal neurons exposed to Aβo.

Aβo induces mitochondrial membrane potential dissipation, which is prevented by canonical Wnt signaling

After determining the effect of Wnt signaling pathway activation on calcium levels in response to 20 μM Aβo, we decided to evaluate whether mitochondrial membrane potential ($_{m}\Delta\psi$) was altered by exposure of hippocampal neurons to Aβo and whether the activation of the canonical Wnt pathway through the Wnt3a ligand was able to prevent those changes. Fourteen DIV neurons were treated as described previously with rWnt3a and loaded with the fluorescent probe Mitotracker Orange (50 nM), which fluoresces according to the mitochondrial membrane potential, for 30 min at 37°C. The incubation of control neurons with Aβo induced a significant loss of $_{m}\Delta\psi$, which was evidenced by the decay of the fluorescence intensity (Figure 3Aa, b). This decrease in mitochondrial membrane potential was less evident in those neurons that had been pre-treated with rWnt3a (Figure 3Ac, d), and these differences between control and Wnt3a treated neurons exposed to Aβo were significant, as shown in Figure 3B and Figure 3C, at the end of the experiment. The inhibition of Wnt signaling with the Wnt antagonists DKK1 and sFRP2 completely inhibited the protective effect of Wnt3a observed on the mitochondrial membrane potential (Figure 3C). These results indicate that the activation of the canonical *Wnt* pathway protects mitochondria, preventing the dissipation of its membrane potential, which is generated by exposure to Aβo oligomers, suggesting that Wnt favors the integrity of the mitochondrial membranes through the stabilization of the mitochondrial membrane potential.

Figure 3

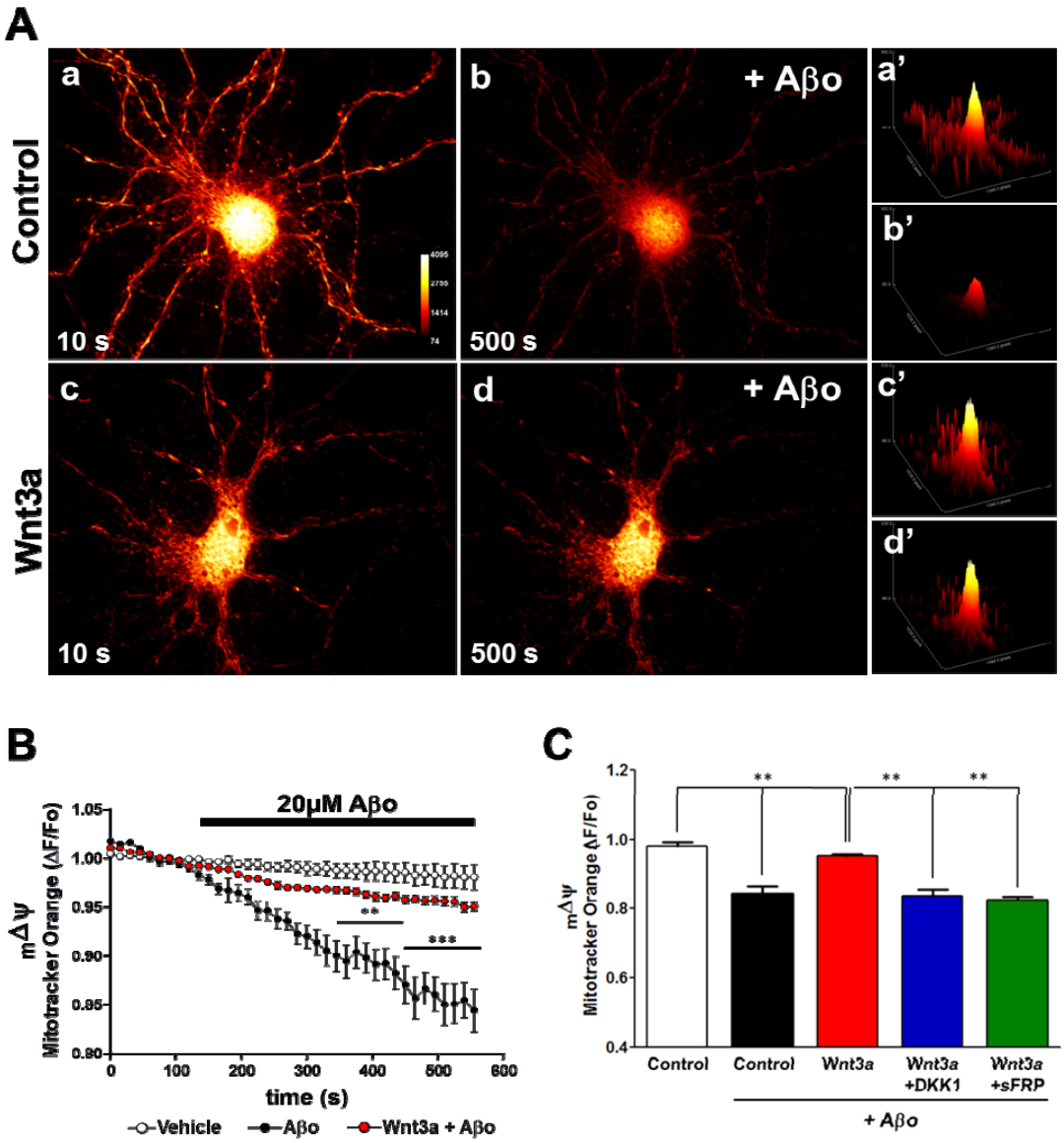

Figure 3. Mitochondrial membrane potential ($_m\Delta\psi$) changes in response to Wnt3a in neurons exposed to Aβo. A) 14 DIV hippocampal neurons treated with control media or rWnt3a protein for 24 h and loaded with Mitotracker Orange. Representative pseudocolored images obtained by Spinning Disk Confocal Microscopy immediately before (a,c) and 500 s after (b,d) Aβo exposure. The respective surface intensity distribution plot are shown in a'-d' images **B)** Quantification of fluorescence intensity changes ($\Delta F/F_0$) in neurites of control and rWnt3a neurons. Black bar indicates the addition of Aβo. **C)** Representative graph of the end time point (500s) of the experiment quantified in D) for each condition, including Wnt inhibitors, DKK1 (100ng/mL) and sFRP2 (250 nM). The graph shows the mean ± SEM of five independent experiments. ANOVA test, *post hoc* Bonferroni **p<0.001; *** p<0.0001.

Cytochrome-c release in hippocampal neurons exposed to Aβo is not produced in the presence of Wnt3a

The loss of mitochondrial membrane potential in Aβo-exposed neurons could be generated as a response of this organelle to mitochondrial membrane permeabilization due to the calcium increase or a direct effect of Aβo. To study whether mitochondrial membranes are permeabilized in response to Aβo, cytochrome-c release from mitochondria to the cytosol was evaluated. Fourteen DIV hippocampal neurons were treated with 5 μM Aβo in the presence or absence of rWnt3a for 24 h. After treatment, cells were incubated with Mitotracker to detect mitochondria, and the neurons were then fixed for immunodetection of cytochrome-c (Figure 4A). Cytochrome-c release was analyzed by the loss of colocalization with mitochondria through the determination of Manders' coefficient M2 (Costes et al., 2004; Manders et al., 1993), which indicates the proportion of cytochrome-c stain over the mitochondria. As shown in Figure 4B and the colocalization analysis (Figure 4C), Aβo induces a significant loss of cytochrome-c localization in mitochondria, which indicates its release from this organelle. By contrast, neurons co-incubated with Aβo and rWnt3a did not present significant changes in Manders' coefficient compared to control conditions. These results indicate that the Wnt3a ligand prevents cytochrome-c release induced by Aβo, suggesting that mitochondrial membranes remain unaltered under these conditions, even in the presence of Aβo in the culture.

Figure 4

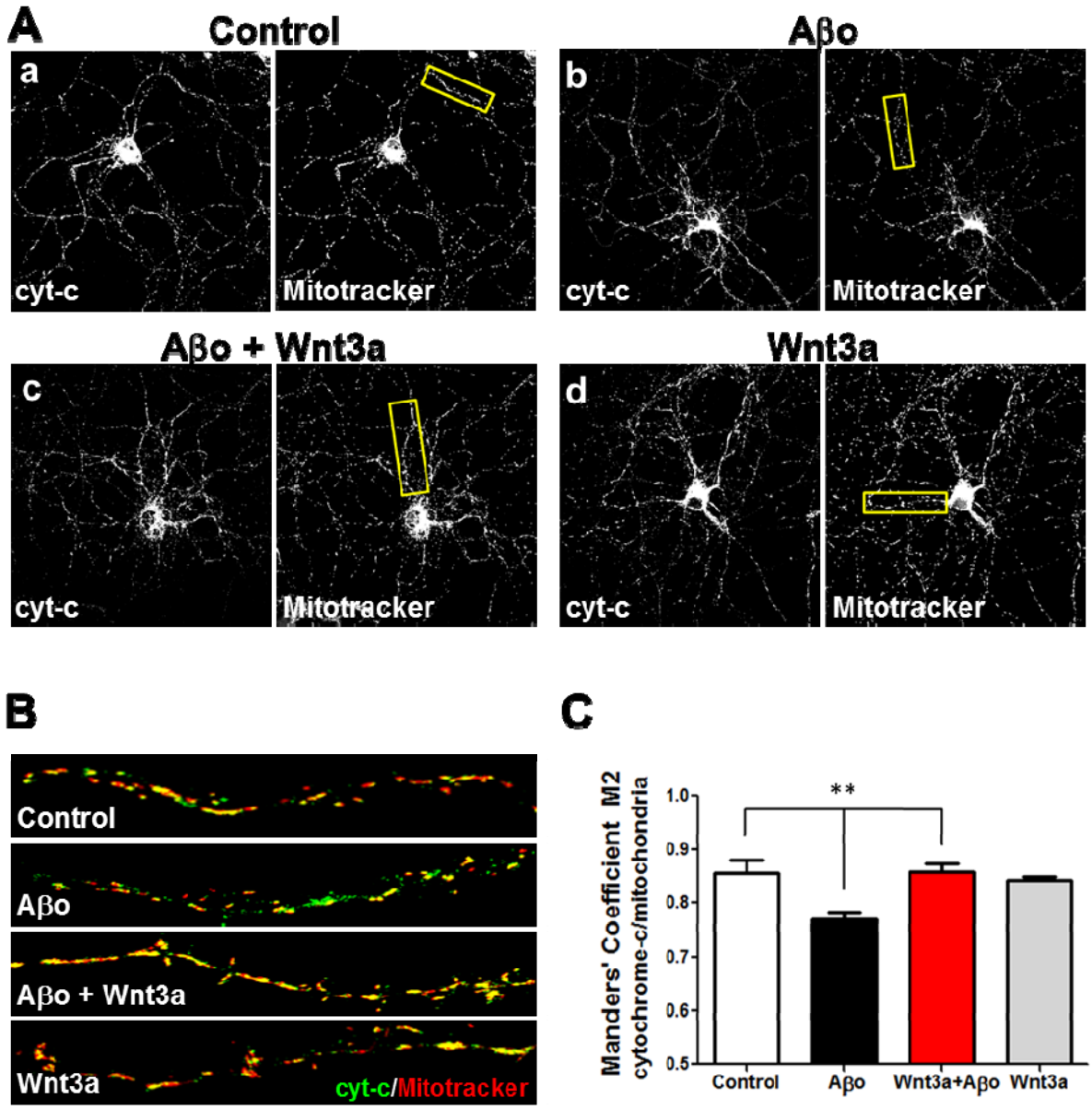

Figure 4. Wnt3a inhibits cytochrome-c release in hippocampal neurons treated with Aβo. **A)** Neurons treated with 5 µM Aβo in the presence or absence of r*Wnt3a* for 24 h were loaded with Mitotracker Orange (50 nM) and then analyzed by immunofluorescence to detect cytochrome-c localization. **B)** Yellow rectangles in A indicate representative magnified neurites to show colocalization between cytochrome-c in green and the mitochondrial marker Mitotracker Orange in red. **C)** Manders' Coefficient M2 was calculated to determine cytochrome-c colocalization with mitochondria. One-way ANOVA test was developed with a *post hoc* Bonferroni **p<0.001. Quantification represents the results of three independent experiments, considering 10-15 neurons analyzed per experiment.

Canonical Wnt signaling activation prevents apoptosis and neuronal death induced by Aβo in hippocampal neurons.

To correlate the described effects on mitochondrial calcium levels, mitochondrial membrane potential and cytochrome-c release with the neuroprotective effect previously described for Wnt3a ligand against Aβ fibrils toxicity (Alvarez et al., 2004), we evaluated the toxicity of Aβo and performed two viability assays: Hoeschst staining to detect apoptotic nuclei (Figure 5A) and the Live/Dead assay as a late marker of neuronal death (Figure 5B). Cultures treated with 5 μM Aβo for 24 h presented neurons with nuclear condensation in contrast to control cultures (Figure 5Aa',b'). Wnt3a treatment significantly prevented the apoptosis induced by Aβo, and the nuclei of these neurons appeared healthy (Figure 5Ac',d'). The graph in Figure 5C shows a significant increase in the percentage of apoptotic nuclei in neurons exposed to Aβo (34.3 ± 2.43%), whereas Wnt3a plus Aβo-treated neurons presented a percentage of apoptotic nuclei similar to control neurons (10.52 ± 0.93%). Similarly, when the Live/Dead assay was performed (Figure 5D), we observed a significant decrease in the percentage of live neurons treated with Aβo compared to controls (45.72 ± 4.44% vs 67.60 ± 4.48%). Neurons that were co-incubated with Aβo and rWnt3a did not show significant differences compared with control neurons (79.94 ± 1.66%) (Figure 5D). These results confirmed the neuroprotective effect that Wnt canonical signaling activation exerts against Aβ toxicity and indicated that the Wnt3a ligand prevents neuronal death induced by the oligomeric forms of Aβ on hippocampal neurons.

Figure 5

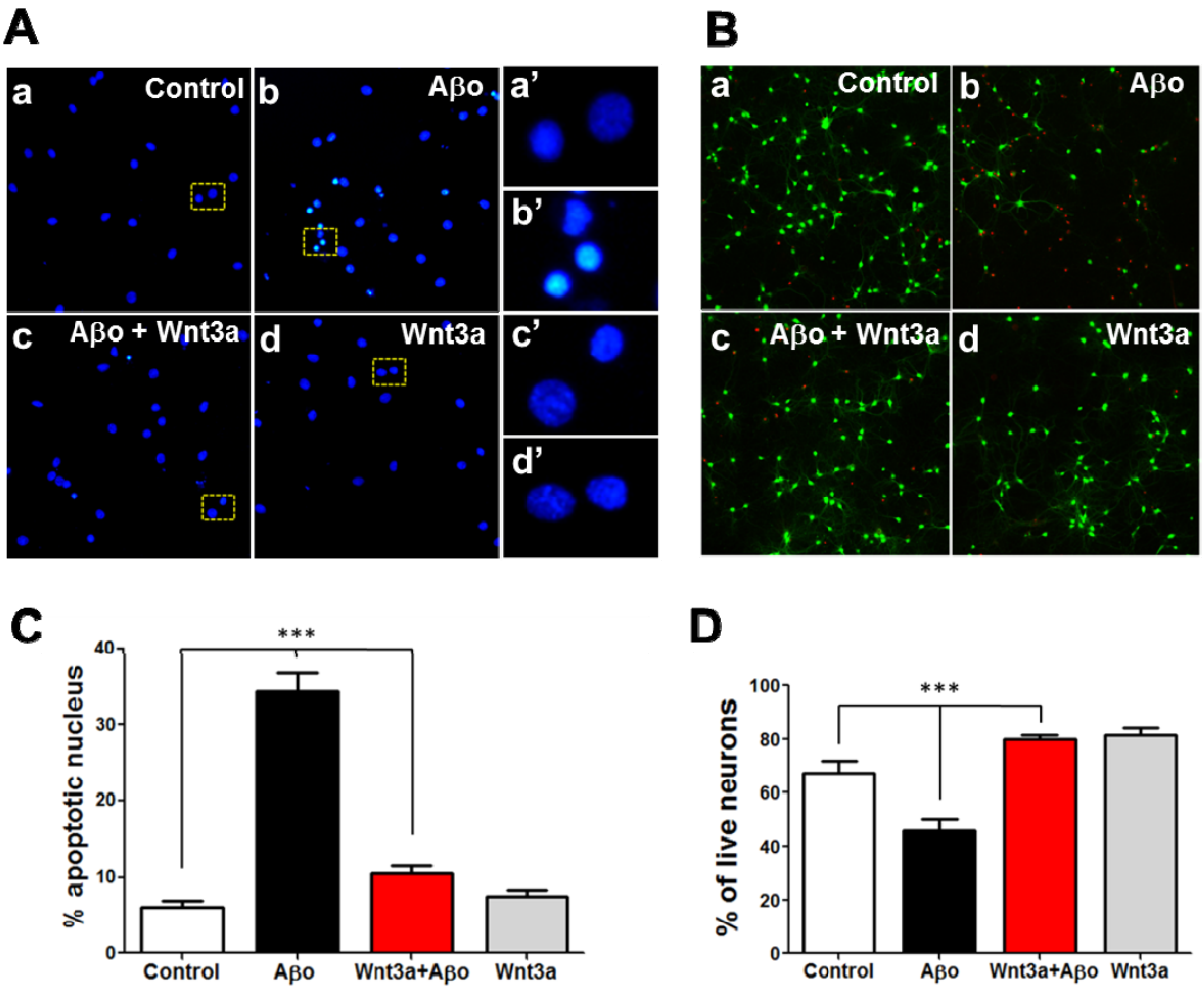

Figure 5. Wnt3a prevents neuronal death induced by Aβo in hippocampal neurons. Neurons were co-incubated with rWnt3a protein and 5μM Aβo for 24 h. **A)** Apoptotic nuclei were detected with Hoechst stain (1μg/ml) in fixed neurons (a-d). Magnification shows representative nucleus of neurons treated with control media (a'), Aβo (b'), rWnt3a+Aβo (c') and rWnt3a alone (d'). **B)** LIVE/DEAD assay. Neurons were loaded with calcein/EthD1 and analyzed in a Fluorescence Microscope. Neurons stained in green (positive for calcein) represent live cells, whereas the red nuclei correspond to death cells. **C)** Quantification of percentage of apoptotic nuclei in each condition. **D)** Quantification of percentage of live neurons (calcein/EthD1 ratio) in response to treatments. Statistical analysis in both experiments was carried out using one-way ANOVA test with a *post hoc* Bonferroni *** p<0,0001. Quantifications represent the results of three independent experiments.

Wnt3a prevents mitochondrial permeability transition pore (mPTP) opening induced by Aβo.

To evaluate the role of mPTP in the toxic effects of Aβo on the mitochondria, we used a direct technique to monitor mPTP opening. This live cell imaging assay was developed by Petronilli et al. in 1998 (Petronilli et al., 1998) and later validated in a neuronal model (Gillessen et al., 2002). Briefly, neurons were incubated with calcein-AM in the presence of cobalt. Under these conditions, cytoplasmic calcein signals were quenched by cobalt without affecting mitochondrial signals. Under mPTP opening stimulation, calcein fluorescence rapidly decay as a result of the permeabilization of mitochondrial membranes. To develop the mPTP assay, 14 DIV hippocampal neurons were treated with control media or rWnt3a for 24 h. Then, the neurons were incubated with a calcein-Co^{2+} mix (1 μM and 1 mM, respectively) for 40 min at 37°C and analyzed immediately by spinning disk confocal microscopy. Representative images for each treatment are shown before (Figure 6Aa, c) and 500 s after exposure to 20 μM Aβo (Figure 6Ab, d). Figures 6Ba-d represent cropped and magnified views indicated by yellow squares under basal conditions for both treatments, control and rWnt3a-treated neurons (Figure 6Aa, c). The images shows that Aβo stimulation resulted in a rapid decay of mitochondrial calcein fluorescence (Figure 6Ba compared to Figure 6Bb), indicating mPTP opening, whereas neurons pre-treated with rWnt3a did not seem to show changes in fluorescence intensity in response to Aβo (6Bc compared to Figure 5Bd). These changes are represented in the graph in Figure 6C, which shows that significant differences between control and rWnt3a-treated neurons in response to Aβo stimulation were evident beginning 300 s after the start of the experiment. The ionophore ionomycin (0.5 μM) was used as a

Figure 6

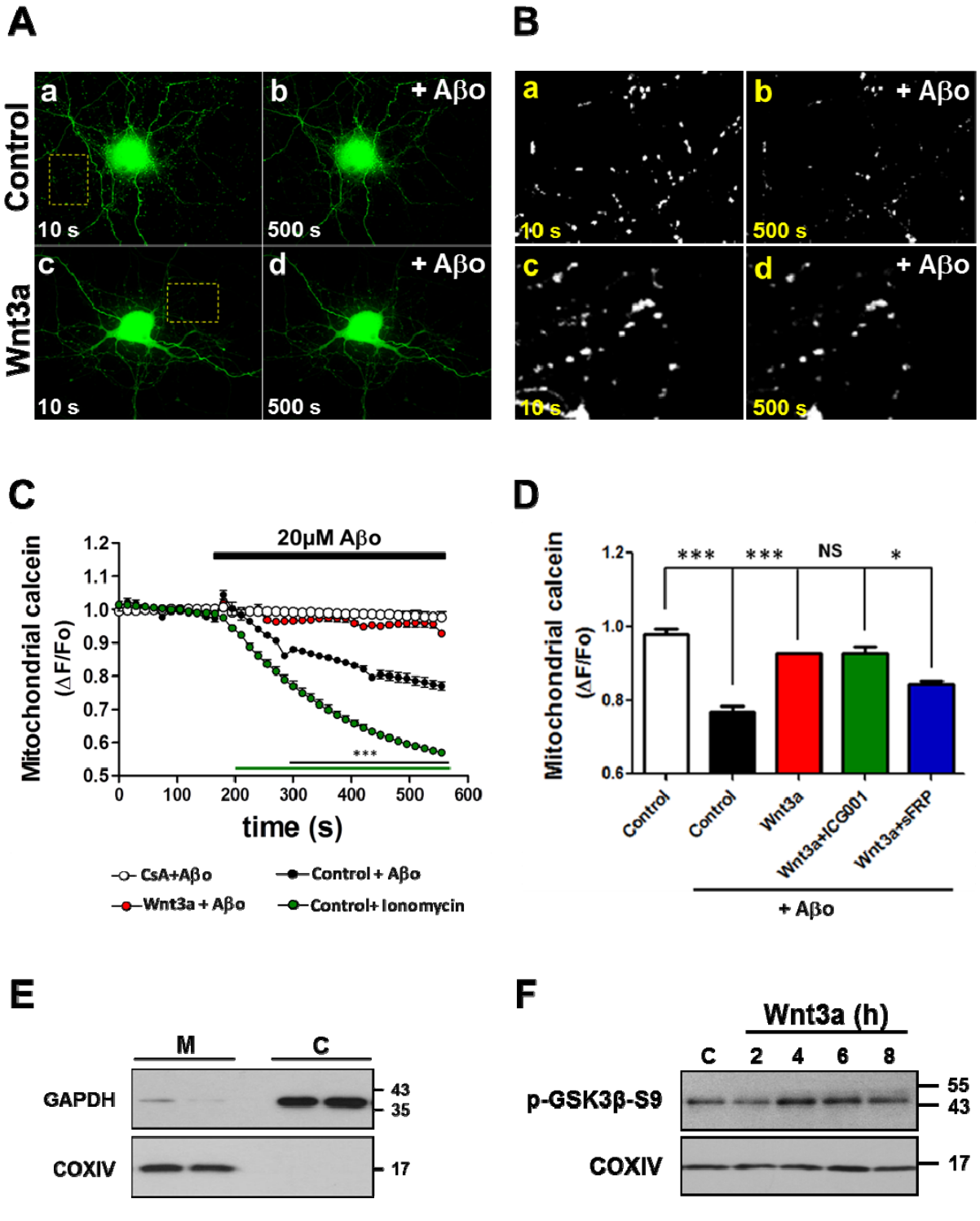
A
B
Control
Wnt3a
a
b
+ Aβo
c
d
10 s
500 s
C
Mitochondrial calcein (ΔF/Fo)
20μM Aβo
time (s)
***
CsA+Aβo
Control + Aβo
Wnt3a + Aβo
Control+ Ionomycin
D
Mitochondrial calcein (ΔF/Fo)
***
***
NS
*
Control
Control
Wnt3a
Wnt3a+ICG001
Wnt3a+sFRP
+ Aβo
E
M
C
GAPDH
COXIV
43
35
17
F
Wnt3a (h)
C
2
4
6
8
p-GSK3β-S9
COXIV
55
43
17

Figure 6. Wnt signaling pathway prevents mitochondrial permeability transition pore (mPTP) opening induced by Aβo in living neurons. A) ***Images represent*** 14 DIV hippocampal neurons treated with rWnt3a protein or control media and loaded with calcein-Co^{2+} to mainly stain mitochondria. Images analysis was carried out in live cells in a spinning disk confocal microscope and the fluorescence intensity decay of mitochondrial calcein was measured to detect the mPTP opening in response to Aβo exposure. **B)** Yellow rectangles from A) indicate the respective magnified images of control (a), Aβo (b), rWnt3a+Aβo (c) and rWnt3a (d) treated neurons to show mitochondrial calcein stain and the changes in response to the different treatments. **C)** Quantification of the fluorescence intensity changes of mitochondrial calcein. Twenty μM CsA and 0.5 μM ionomycin were used as negative and positive controls of mPTP opening, respectively. The graph shows the mean ± SEM of n=7 independent experiments. Black bar indicates the addition of Aβo. Two-way ANOVA test, *post hoc* Bonferroni *** $p<0.0001$. **D)** Representative graph of the end time (500s) of the experiment quantified in C) for each condition, including Wnt inhibitors, ICG-001 (20 μM) and sFRP2 (250 nM). Statistical analysis was developed using one-way ANOVA test, *post hoc* Bonferroni **$p<0.001$; *** $p<0.0001$. **E)** Western blot shows mitochondrial and cytoplasmic fractions isolated from hippocampal slices. "M" fraction corresponds to mitochondria and "C" to cytoplasmic fraction, detected with the loading controls COXIV and GAPDH antibodies, respectively. Each lane corresponds to duplicates. **F)** Western blot analysis shows increased phosphorylated-GSK-3β at Ser9 in the mitochondrial fraction in response to 300 ng/mL of rWnt3a (in hours).

positive control for mPTP opening (Figure 6C, green curve). In addition, 20 μM cyclosporineA (CsA), a specific inhibitor of mPTP (Halestrap et al., 1997), was pre-incubated with neurons for 30 min as a negative control for the mPTP assay in live neurons in response to Aβo (Figure 6C, white curve). By contrast, the inhibition of Wnt signaling with sFRP2 significantly decreased the protective effect of Wnt3a on mPTP opening induced by Aβo, as shown in Figure 6D, which represents the quantification of all conditions at the end time point of the experiment. I order to know whether the Wnt target genes are involved in the Wnt3a effect on the mPTP inhibition, we use ICG001, a Wnt/β-catenin-dependent transcription inhibitor (Emami et al., 2004). Surprisingly we did not find differences compared to Wnt3a+Aβo treatment, which suggests that the protective effect of Wnt3a over mPTP opening is not dependent on *Wnt* target genes. Since previous studies suggest that glycogen synthase kinase-3β (GSK-3β) inhibition, through its phosphorylation at the serine 9 residue, might be involved in cardioprotection against ischemia/reperfusion injury, through the inhibition of mPTP opening (Juhaszova et al., 2004; Nishihara et al., 2007; Gomez et al., 2008), we isolated brain mitochondria from hippocampal slices (Figure 6E) and studied the GSK-3β behavior. Interestingly, canonical Wnt signaling activation induces the phosphorylation of GSK-3β at the same residue, inducing its inhibition and therefore the activation of the Wnt signaling cascade (Stambolic and Woodgett, 1994). According to this, we found that Wnt3a triggers the accumulation of phosphorylated GSK-3β (Ser9) in the mitochondrial fraction (Figure 6F), suggesting that Wnt3a ligand may act upstream of Wnt target genes, probably directly on mitochondria. These results provide direct evidence in live cells that activation of the canonical Wnt signaling pathway through the Wnt3a ligand prevents mPTP opening in

hippocampal neurons exposed to Aβo toxicity, an effect in which GSK-3β inhibition might be involved.

Aβo induce an increase on volume and sphericity of mitochondria which is prevented by Wnt signaling activation. Three-dimensional reconstruction of mitochondrial network.

Several of the classical features of mPTP opening that characterize mitochondria before membrane disruption are the morphological changes that occur during this process, such as crista remodeling and the phenomenon known as swelling, which involves changes in the mitochondrial volume and shape, which cause the rupture of the outer membrane (Bernardi et al., 2006). To evaluate this initial step, we measured the volume and sphericity of mitochondria in response to 5 μM Aβo in the presence or absence of rWnt3a. To accomplish this aim, we performed a 3D reconstruction of mitochondria from hippocampal neurons transfected with mito-Cherry using Imaris software. Figure 7A shows representative reconstructed neurites from neurons treated under the different conditions for 24 h. Aβo-treated neurons showed rounded and more spherical mitochondria than under control conditions. In addition, mitochondria co-treated with rWnt3a and Aβo presented the same normal morphology as control neurons. Quantitative analysis of whole reconstructed neurons indicates that Aβo treatment induced an increase in the sphericity and volume of mitochondria (Figure 7B and Figure 7C, respectively), a change that was significantly prevented by co-incubation with rWnt3a. Together, these results indicate that the presence of the Wnt3a ligand in the hippocampal neuron culture prevents the morphological changes in mitochondria correlated with mPTP opening that are induced by Aβo. These findings are in agreement with

Figure 7

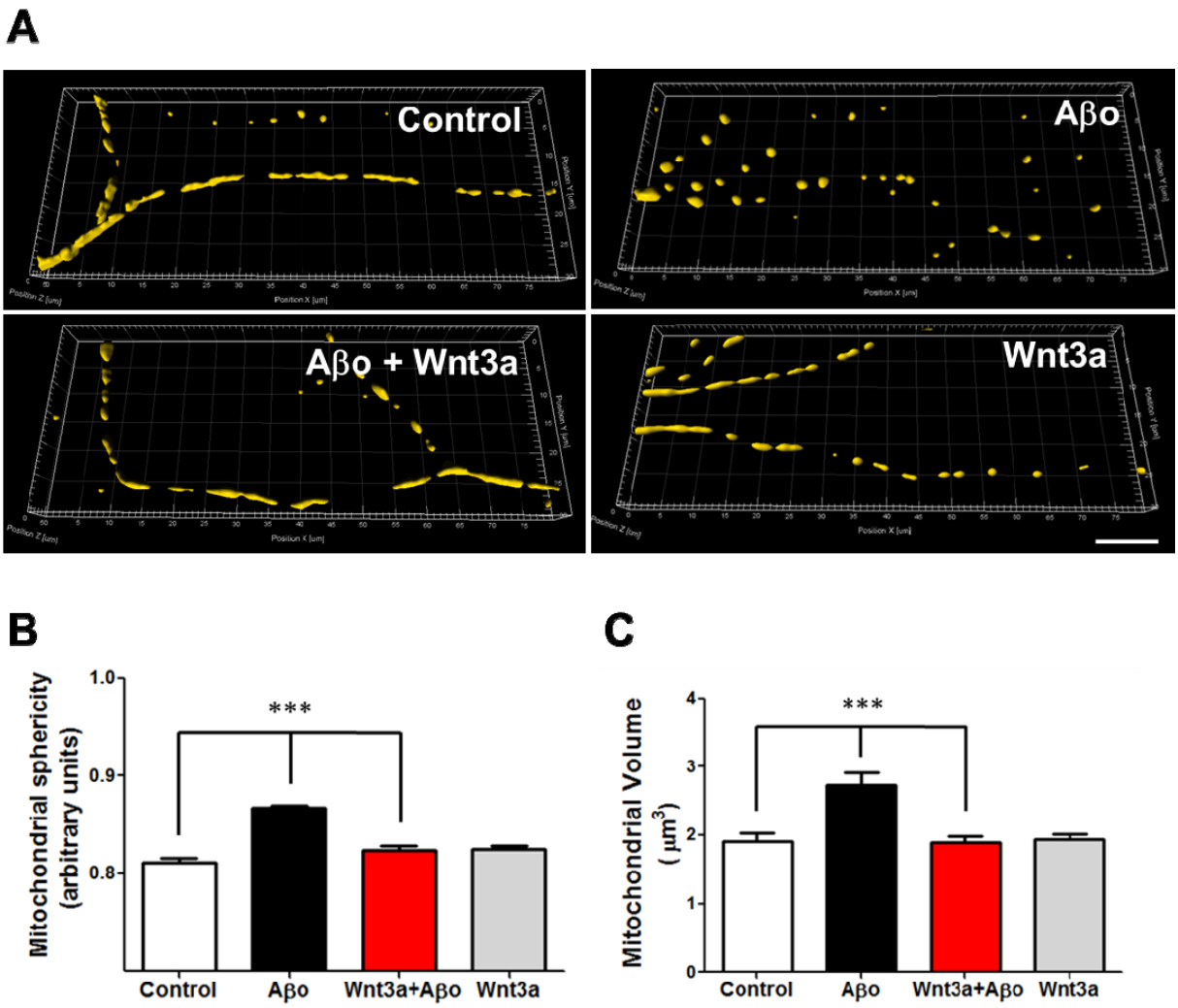

Figure 7. Mitochondrial volume and sphericity changes in response to Aβo and Wnt3a treatments in hippocampal neurons. 14 DIV mito-Cherry-transfected neurons were treated for 24 h with 5μM Aβo and rWnt3a (300 ng/mL) and fixed for 3D reconstruction. **A)** Three-dimensional reconstruction of mitochondria from mito-Cherry neurons. Images show representative mitochondria of a neurite selected from the whole neuron reconstructed (not shown) for each treatment. White bar corresponds to 10 μm. B) Graphs represent the measurements of mitochondrial sphericity (a) and volume (b) performed with the Imaris software used for the mitochondrial network recosntruction. Results are the mean of N=3 independent experiments and the statistical analysis was performed by one-way ANOVA test, *post hoc* Bonferroni *** $p<0.0001$.

the protective effects of Wnt3a against Aβo-dependent mPTP activation that were observed in the live cell experiments.

Aβo disrupts the membrane structure and crista organization of mitochondria from hippocampal slices: The role of Wnt signaling in mitochondrial integrity.

To correlate the previously described effect of Aβo on mPTP opening based on a fluorescence assay in live neurons with disrupted mitochondrial structure, mitochondrial integrity parameters, such as membrane permeabilization and crista organization, were analyzed by electron microscopy. To accomplish this aim, mouse hippocampal slices were incubated for 4 h with control media or rWnt3a protein and then co-incubated with 5 μM Aβo for 1 h. Treated tissues were fixed and used to analyze the mitochondrial integrity by electron microscopy. Microscopic analysis was performed at the CA1 region of the hippocampus (Figure 8Aa). Specifically, we focused on those mitochondria that belonged to synaptic contacts between CA3 axons that projected to CA1 dendrites from the stratum radiatum (Figure 8Ab) because it has recently been suggested that synaptic mitochondria from this region are highly vulnerable in an AD mouse model (Balietti et al., 2013). Figure 8Ac shows a representative image obtained by electron microscopy. The image shows preserved tissue with synaptic contacts, presynaptic vesicles and organelles, such as mitochondria. Ultrastructural analysis of the mitochondria shows a clear deterioration of both the mitochondrial membranes and cristae from slices treated with Aβo, in contrast to control conditions (Figure 8Ba, b). Red arrows indicate the regions of the mitochondria with permeabilized membranes. Vesicular cristae and vesicular swollen mitochondria were observed in Aβo-exposed slices, features of mitochondrial morphological changes that occur during apoptotic processes (Sun et al., 2007).

Figure 8

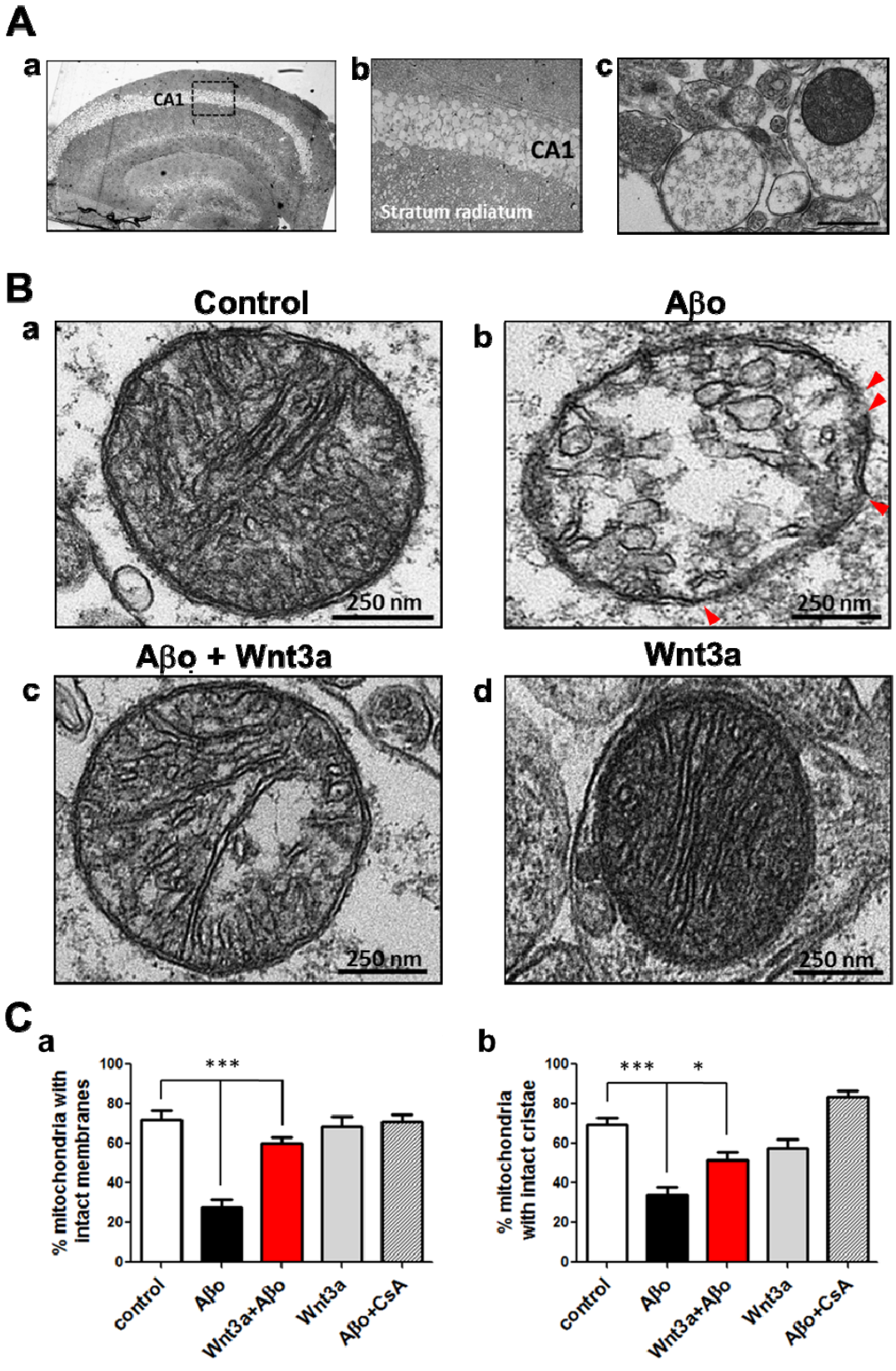
A
a
CA1
b
CA1
Stratum radiatum
c
B
Control
a
250 nm
Aβo
b
250 nm
Aβo + Wnt3a
c
250 nm
Wnt3a
d
250 nm
C
a
% mitochondria with intact membranes
***
control
Aβo
Wnt3a+Aβo
Wnt3a
Aβo+CsA
b
% mitochondria with intact cristae
***
*
control
Aβo
Wnt3a+Aβo
Wnt3a
Aβo+CsA

Figure 8. Wnt3a prevents membrane and cristae disruption generated by Aβo on mitochondria. A) Mouse hippocampal slices (400 μm) were pre-incubated for 4h with rWnt3a and the treated with 5μM Aβo for 1 h. Slices were fixed and processed for electron microscopy analysis. a) Representative slice stained with toluidine blue. Black square shows the CA1 region selected for the analysis. b) 10X zoom from image in (a) shows CA1 neurons. c) Representative image obtained with electron microscopy shows intact tissue and preserved synaptic and mitochondrial structures. **B)** Electron microscopy. Representative images of mitochondria are shown for each treatment. Red arrows indicate disrupted mitochondrial membranes. Bars correspond to 250 nm. **C)** Ultrastructural analysis. a) Mitochondrial membrane integrity was analyzed. Graph shows the percentage of mitochondria that exhibit intact membranes. b) Mitochondrial cristae integrity analysis is represented in the graph that shows the percentage of mitochondria with intact mitochondria. Statistical analysis from three independent slices treated, one-way ANOVA test with *post hoc* Bonferroni * $p< 0.01$, *** $p<0,0001$.

Moreover, these changes were not observed in mitochondria from slices treated with Wnt3a ligand plus Aβo (Figure 8Bc). Treatment with rWnt3a protein alone did not generate any changes in mitochondrial structure compared to the control situation (Figure 8Bd), and treatment with CsA, the mPTP inhibitor, plus Aβo completely prevented the morphological changes generated by the Aβ peptide (Figure 8C). Quantification of the images indicates that the percentage of mitochondria with intact membranes and cristae was significantly lower in Aβo-treated slices than in control samples, with values of 44.8 ± 8.1% and 35.5 ± 6.1%, respectively, whereas slices treated with rWnt3a plus Aβo did not show a significant decrease in the proportions of either intact membrane or cristae (12.1 ± 2.1% and 17.6 ± 3.1%, respectively) compared to controls (Figure 8C). These results indicate that the activation of the canonical Wnt signaling pathway prevents mitochondrial membrane permeabilization and crista disorganization, favoring the maintenance of mitochondrial integrity as a defense against the damage generated by Aβo toxicity.

Mitochondrial swelling induced by Aβo is prevented by Wnt canonical signaling activation.

For an in-depth analysis of the mitochondrial morphological changes that occur during the swelling phenomenon, more specific morphological parameters that change under mPTP opening were analyzed, such as mitochondrial area, perimeter and diameter (Figure 9 and Table 1), which are measures of mitochondrial size and shape (Song et al., 2004; Barrientos et al., 2011). Figure 9Aa shows control mitochondria with compact morphology, intact membranes, organized cristae and a synaptic distribution of mitochondria in both pre- and post-synaptic terminals. Aβo treatment induced dramatic changes in mitochondrial size. Many mitochondria were greatly enlarged and swollen compared to control mitochondria (Figure

Figure 9

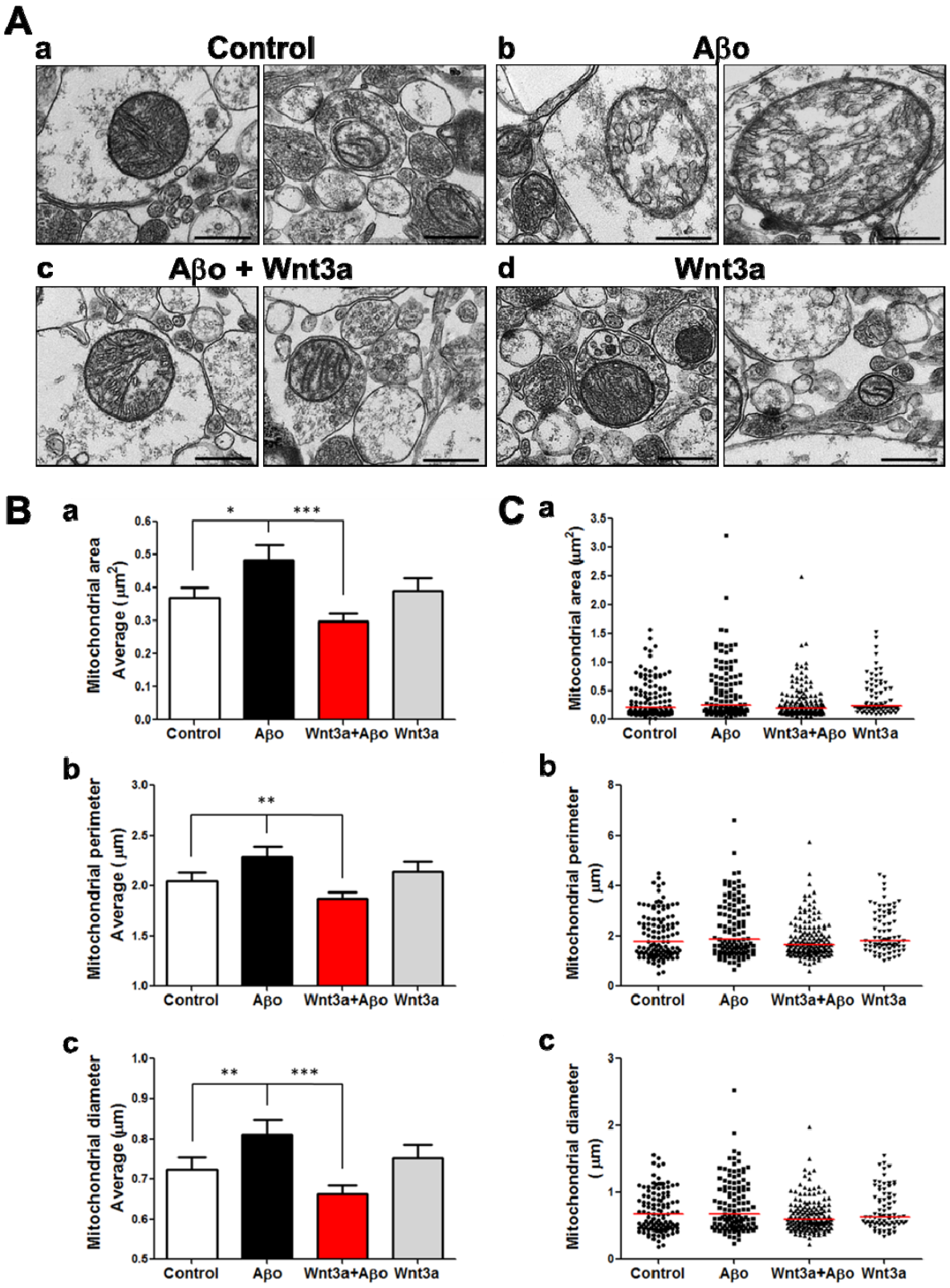
A
a Control
b Aβo
c Aβo + Wnt3a
d Wnt3a
B
a
Mitochondrial area Average (μm²)
b
Mitochondrial perimeter Average (μm)
c
Mitochondrial diameter Average (μm)
Control
Aβo
Wnt3a+Aβo
Wnt3a
C
a
Mitocondrial area (μm²)
b
Mitochondrial perimeter (μm)
c
Mitochondrial diameter (μm)

Figure 9. Mitochondrial morphological changes induced by Aβo are prevented by Wnt canonical signaling activation. A) Electron microscopy. Representative images obtained from the electron microscope show different mitochondrial morphologies for each condition. Bars correspond to 500 nm. One-way ANOVA test, *post hoc* Bonferroni *p<0.01; **p<0.001; *** p<0.0001. **B)** Morphological changes analysis. Bar graphs represent the average area, perimeter and diameter of mitochondria in each condition. **C)** Scatter plots. Graphs indicate the distribution of area, perimeter and diameter of each analyzed mitochondria inside the whole mitochondrial population. Red horizontal bars represent median values of each morphological parameter analyzed.

Table 1

Group	Control	Aβo	Aβo + rWnt3a	rWnt3a
***n* =**	113	118	152	76
Minimum	0.015	0.033	0.025	0.079
25% Percentil	0.127	0.14	0.1343	0.1795
		(+10.2) [a]	***(+5.7)*** [a]	***(+41.3)*** [a]
Median	0.214	0.2545	0.1915	0.2395
		(+18.9) [a]	***(-10.5)*** [a]	***(+11.9)*** [a]
75% Percentil	0.542	0.743	0.3465	0.559
		(+37.1) [a]	***(-36.1)*** [a]	***(+3.1)*** [a]
Maximum	1.571	3.209	2.481	1.523
		(+104.2) [a]	***(+57.9)*** [a]	***(-3.0)*** [a]
Mean	0.3682	0.4828	0.2978	0.3906
		(+31.1) [a]	***(-19.1)*** [a]	***(+6.1)*** [a]
SD	0.3344	0.4922	0.2976	0.324
SEM	0.03146	0.04531	0.02414	0.03716

Table 1. Percentile values and statistical analysis of mitochondrial area from electron microscopy images. Table represents a percentile-grouped analysis for each treatment. The values are represented in micrometers^2 (μm^2) and "a" corresponds to the percentage of increase of each group values when compared to corresponding Control group.

9Ab). rWnt3a treatment prevented these changes, and the mitochondria had the same normal shape as under control conditions with or without Aβo (Figure 9Ac, d). As shown in Table 1, the mean area per mitochondrion for the Aβo group was 0.4828 μm^2, in contrast to 0.3682, 0.2978 and 0.3906 μm^2 for the control, Wnt3a+Aβo and Wnt3a groups, respectively. For the measurements of the perimeter, the mean value per mitochondrion for the Aβo group was 2.284 μm, in contrast to 2.046, 1.873 and 2.146 μm for the control, Wnt3a+Aβo and Wnt3a groups, respectively. The mean diameter per mitochondrion for the Aβo group was 0.8103 μm, in contrast to 0.7242, 0.6634 and 0.7521 μm for the control, Wnt3a+Aβo and Wnt3a groups, respectively. According to the one-way ANOVA, the mean for each parameter of the Aβo group was significantly different from the mean for each parameter for the other groups (Figure 9B). Compared to the control group, the mean values for the Aβo group increased by 31.1% for mitochondrial area, 11.6% for perimeter and 11.9% for diameter. As demonstrated in the scatter graphs (Figure 9C), the increases in the mean values for the Aβo group were a reflection of an increase in the size of a subset of mitochondria in the upper 50th percentile rather than an upward shift of the entire population. This result is demonstrated in Table 1 (table not shown for perimeter and diameter), by the 37.1% and 104.2% increases in the 75th percentile and maximum values, respectively, for mitochondrial area; the 16.9% and 46.6% respective increases in perimeter; and the 12.9% and 61.4% increases in the mitochondrial diameter in the Aβo group vs. the control group, compared to the negligible changes in the minimum values and only 10.2%, 4.7% and 5.8% increases in the lower 25th percentile for mitochondrial area, perimeter and diameter, respectively. This detailed analysis suggests that the structural and morphological changes that occur in mitochondria exposed to Aβo are

correlated with mitochondrial swelling (Cha et al., 2012). By contrast, mitochondria from the Wnt3a+Aβo group did not present these morphological alterations and therefore are structurally similar to those mitochondria from the control group. In conclusion, the analysis indicates that Wnt3a treatment prevents the increases in mitochondrial area, perimeter and diameter induced by Aβo exposure (Figure 9), preventing mitochondrial *swelling* and therefore mPTP opening.

Discussion

Previous studies from our laboratory have shown that activation of the canonical Wnt signaling pathway has a neuroprotective role against Aβ toxicity (Cerpa et al., 2009; Inestrosa and Varela-Nallar, 2014); however, there is no direct evidence that explains the mechanism by which this signaling protects neurons from cell death or whether this neuroprotective effect is due to the role of Wnt signaling in the regulation of cell death cascades that are initiated in the mitochondria. In this study, we found that the activation of Wnt signaling through the Wnt3a ligand prevents the mPTP opening induced by the toxicity of Aβo (Figure 6A), as well as inhibits all of the consequent effects, such as the membrane potential loss (Figure 3), mitochondrial morphological changes (Figure 7 and Figure 9), mitochondrial structure disruption (Figure 8), and cytochrome-c release (Figure 4) and, therefore, neuronal death (Figure 5).

It is well documented that Aβ induces the activation of mPTP in an AD mouse model (Du et al., 2008) and *in vitro* (Moreira et al., 2001; Parks et al., 2001; Shevtzova et al., 2001) and that this activation and the subsequent mitochondrial and neuronal damage depend on the direct

interaction of Aβ with CypD (Du et al., 2008), the main component of the mPTP (Baines et al., 2005; Schinzel et al., 2005). The detailed structure of the mPTP is not well established, but it is proposed to be mainly formed by the voltage-dependent anion channel (VDAC) at the outer membrane, the adenine nucleotide translocase (ANT) at the inner membrane, and cyclophilin D (CypD) in the mitochondrial matrix (Halestrap, 2009) which is to date the only protein component that is essential for the activation of this pore (Basso et al., 2005; Kato et al., 2009). Moreover, in AD transgenic mice, CypD deficiency attenuates the cellular death induced by Aβ and improves memory and synaptic function (Du et al., 2008).

Calcium overload in mitochondria can also induce mPTP opening (Szalai et al., 1999; Celsi et al., 2009), and in agreement with this, it is very well established that calcium plays an important role in the neurotoxicity of AD in mouse models (LaFerla, 2002; Stutzmann et al., 2007) and *in vitro*, because it has been demonstrated that Aβ aggregates prepared from Aβ synthetic peptides induce calcium increases in cultured hippocampal neurons, which directly impacts the mitochondrial calcium levels (Dinamarca et al., 2010). We evaluated whether our Aβo preparation was able to induce mitochondrial calcium changes in neurons and whether this modulation was prevented by the activation of Wnt signaling. We observed that Aβo increased mitochondrial calcium levels specifically at the neurites of neurons (Figure 1C). These compartmentalized effects of Aβo on mitochondrial calcium changes could be explained by the specific sensitivity of synaptic mitochondria (rather than non-synaptic mitochondria) to calcium overload, which cause them to more readily undergo a permeability transition (Brown et al., 2006). In addition, synaptic mitochondria are more sensitive to direct Aβ damage, affecting trafficking and transport to specific regions of the neurons where more

energy is required, which would make those mitochondria more sensitive to mPTP (Du et al., 2010, 2012). In the same way, the CypD levels of synaptic mitochondria are also important in the sensitivity of synaptic mitochondria to Aβ damage, and high CypD content makes those mitochondria more vulnerable to permeability transitions (Naga et al., 2007). Interestingly, Aβ-mediated synaptic damage to neurons required Wnt antagonist components, such as DKK1 (Purro et al., 2012), another piece of evidence that suggests that the modulation of Wnt signaling activity could be important in regulating Aβ toxicity on neuronal function and viability.

How could Wnt signaling be regulating the permeability transition and pore activation? Our results indicate that the Wnt3a ligand prevents mPTP opening induced by Aβo in live neurons (Figure 6). The ability of Wnt signaling to prevent the mPTP induction produced by Aβ could be mediated by two different mechanisms: 1) controlling intracellular calcium variations generated by Aβ, as has been previously suggested (Quintanilla et al., 2005; Dinamarca et al., 2010); or 2) regulating the direct effect of Aβo on mPTP formation and activation (Du et al., 2010). According to this, several mPTP modulators have been described that also act through the interaction with mPTP components (Eliseev et al., 2009; Rasola et al., 2010; Saraiva et al., 2010). One of these modulators is Bcl-2, an anti-apoptotic protein (Kuwana and Newmeyer, 2003), which is downregulated in AD models (Paradis et al., 1996). Our previous studies shown that Bcl-2 is a Wnt target gene in hippocampal neurons (Fuentealba et al., 2004) and also participates in mitochondrial stabilization against Aβ damage (Fuenzalida et al., 2007). In relation to mPTP-induced apoptosis, Bcl-2 has been shown to prevent cell death through interaction with the main component of the pore, CypD (Eliseev et al., 2009), giving a novel

protective function to CypD. Despite this evidence, we observed that the inhibition of permeability transition mediated by the Wnt3a ligand was not dependent on the activation of Wnt target genes transcription because ICG-001 treatment did not abolish the protective Wnt effect on permeability transition inhibition (Figure 6D), strengthening the idea that this effect is not related to the Bcl-2 action. In has been reported that GSK-3β, one of the main components of the Wnt signaling pathway, is able to translocate to the mitochondria and to act on its inactive form (phosphorylated at serine 9) with one of the components of mPTP, the adenine nucleotide translocase, ANT (Nishihara et al., 2007; Gomez et al., 2008; Juhaszova et al., 2009) . This interaction is correlated with a 60% decrease in the interaction between CypD and ANT, which is necessary for mPTP opening (Miura et al., 2009; Zorov et al., 2009; Miura and Tanno, 2010). Our results showing an increase in the mitochondrial content of phosphorylated-GSK-3β (Figure 7F) is consistent with the idea that the inhibition of GSK-3β mediates the Wnt3a function on mPTP regulation and suggest a possible mechanism to explain how Wnt could modulate mPTP opening and therefore the mitochondrial permeability induced by Aβ (Figure 10). However, further analysis of the interaction between phosphorylated-GSK-3β with CypD will be required to characterize this possible mechanism.

The rapid mPTP opening observed with Aβo (Figure 6C) was correlated with the kinetics of mitochondrial membrane potential dissipation (Figure 3B) and also with the ultrastructural changes observed by electron microscopy (Figure 8) and the cytochrome-c release from the mitochondria (Figure 4), as has been previously described (Moreira et al., 2002). Three-dimensional reconstruction of mitochondria exposed to Aβo indicated that those mitochondria undergo morphological changes correlated with mitochondrial permeability transitions (Figure 7), such as changes in mitochondrial shape, which included an increase in the sphericity

Figure 10

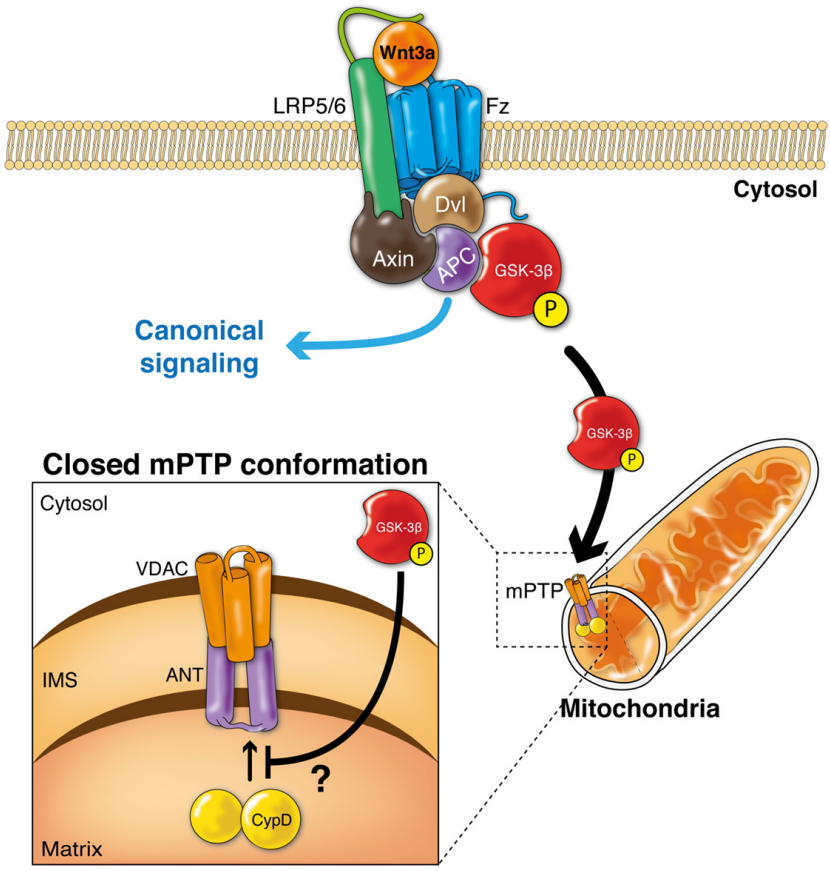

Figure 10. Proposed mechanism for the action of Wnt3a in the regulation of mitochondrial mPTP opening. Wnt signaling is activated by the binding of the Wnt3a ligand to its Fz receptor and the co-receptor LRP5/6. This interaction activates Dvl, which causes the dissociation of the destruction complex, which involves Axin, APC and GSK-3β proteins, to prevent β-catenin degradation through the proteasome, therefore inducing its accumulation in the cytoplasm to finally translocate to the nucleus to regulate the expression of Wnt target genes. This signaling is known as the canonical Wnt signaling pathway, however Wnt can also acts through another signaling mediator: the GSK-3β, which participates beyond β-catenin and therefore in a Wnt target genes transcription-independent manner (Wu and Pan, 2010). Wnt signaling activation produces GSK-3β phosphorylation at the Serine 9 residue to inhibit the kinase. In our proposed model, this inhibited GSK-3β accumulates into the mitochondria in response to Wnt signaling activation through Wnt3a ligand. The mitochondrial p-GSK-3β and its accumulation into this organelle have been implicated in the inhibition of mPTP opening by its binding with ANT. This interaction also correlates with the inhibition of the binding between ANT and CypD that is necessary for the conformation and opening of the mPTP. Fz: Frizzled, Dvl: Dishevelled, APC: adenomatous polyposis coli, GSK-3β: glycogen synthase kinase-3β, p-GSK-3β: phosphorylated GSK-3β at Ser9, ANT: adenine nucleotide translocase, CypD: cyclophilin D.

(Figure 7B) and in the volume of each mitochondrion (Figure 7C) (Bernardi et al., 2006). In agreement with the inhibition of the mPTP opening that we observed with the canonical Wnt signaling activation, we also showed here that these morphological changes were completely prevented by Wnt3a (Figure 8 and Figure 9). A detailed analysis of these parameters was conducted by electron microscopy to correlate these protective effects in an *in vivo* model using hippocampal slices from mouse brains, specifically at the CA1 region of the hippocampus (Figure 8A). We evaluated these changes at this particular zone because it has been reported that mitochondria and synapses from the CA1 show early sensitivity to damage in an AD context (Balietti et al., 2013). As we expected, we observed dramatic changes in mitochondrial integrity (Figure 8B) and morphology (Figure 9) in slices that were exposed to Aβo for only 1 h. As we saw before, 1 h of Aβo exposure is enough to affect the synapses of hippocampal neurons, disrupting the clustering of the post-synaptic protein PSD-95 (Inestrosa et al., 2013), which is correlated with the fact that synaptic mitochondria are also more sensitive than non-synaptic mitochondria (Brown et al., 2006). The ultrastructural study performed here indicates that the activation of Wnt signaling prevents membrane disruption and cristae disorganization of mitochondria exposed to Aβo, as has been described for the APP/PS1 transgenic mouse model of the AD (Kim et al., 2012), supporting the idea that Wnt prevents mitochondrial membrane permeability because those parameters that we evaluated are classical features observed during the swelling phenomenon induced by mPTP, which finally leads to apoptotic processes and to neuronal death (Sun et al., 2007).

In conclusion, the data showed here present a novel mechanism by which canonical Wnt signaling protects neurons from Aβo toxicity. This mechanism involves inhibiting mPTP opening and all of its consequences, thereby preventing the neuronal death observed in AD.

This study suggests a possible new approach for the treatment of AD and opens a new line of study in the field of Wnt signaling in neuroprotection.

References

Alvarez AR, Godoy J a, Mullendorff K, Olivares GH, Bronfman M, Inestrosa NC (2004) Wnt-3a overcomes beta-amyloid toxicity in rat hippocampal neurons. Exp Cell Res 297:186–196.

Arrázola MS, Varela-Nallar L, Colombres M, Toledo EM, Cruzat F, Pavez L, Assar R, Aravena A, González M, Montecino M, Maass A, Martínez S, Inestrosa NC (2009) Calcium/calmodulin-dependent protein kinase type IV is a target gene of the Wnt/beta-catenin signaling pathway. J Cell Physiol 221:658–667.

Baines CP, Kaiser RA, Purcell NH, Blair NS, Osinska H, Hambleton MA, Brunskill EW, Sayen MR, Gottlieb RA, Dorn GW, Robbins J, Molkentin JD (2005) Loss of cyclophilin D reveals a critical role for mitochondrial permeability transition in cell death. Nature 434:658–662.

Balietti M, Giorgetti B, Casoli T, Solazzi M, Tamagnini F, Burattini C, Aicardi G, Fattoretti P (2013) Early selective vulnerability of synapses and synaptic mitochondria in the hippocampal CA1 region of the Tg2576 mouse model of Alzheimer's disease. J Alzheimers Dis 34:887–896.

Barrientos SA, Martinez NW, Yoo S, Jara JS, Zamorano S, Hetz C, Twiss JL, Alvarez J, Court FA (2011) Axonal degeneration is mediated by the mitochondrial permeability transition pore. J Neurosci 31:966–978.

Basso E, Fante L, Fowlkes J, Petronilli V, Forte M a, Bernardi P (2005) Properties of the permeability transition pore in mitochondria devoid of Cyclophilin D. J Biol Chem 280:18558–18561.

Bernardi P, Krauskopf A, Basso E, Petronilli V, Blachly-Dyson E, Blalchy-Dyson E, Di Lisa F, Forte M a (2006) The mitochondrial permeability transition from in vitro artifact to disease target. FEBS J 273:2077–2099.

Bravo R, Vicencio JM, Parra V, Troncoso R, Munoz JP, Bui M, Quiroga C, Rodriguez AE, Verdejo HE, Ferreira J, Iglewski M, Chiong M, Simmen T, Zorzano A, Hill J a, Rothermel B a, Szabadkai G, Lavandero S (2011) Increased ER-mitochondrial coupling promotes mitochondrial respiration and bioenergetics during early phases of ER stress. J Cell Sci 124:2143–2152.

Brown MR, Sullivan PG, Geddes JW (2006) Synaptic mitochondria are more susceptible to Ca2+overload than nonsynaptic mitochondria. J Biol Chem 281:11658–11668.

Buckman JF, Hernández H, Kress GJ, Votyakova T V, Pal S, Reynolds IJ (2001) MitoTracker labeling in primary neuronal and astrocytic cultures: influence of mitochondrial membrane potential and oxidants. J Neurosci Methods 104:165–176.

Caceres A, Banker G, Steward O, Binder L, Payne M (1984) MAP2 is localized to the dendrites of hippocampal neurons which develop in culture. Brain Res 315:314–318.

Celsi F, Pizzo P, Brini M, Leo S, Fotino C, Pinton P, Rizzuto R (2009) Mitochondria, calcium and cell death: a deadly triad in neurodegeneration. Biochim Biophys Acta 1787:335–344.

Cerpa W, Godoy J a, Alfaro I, Farías GG, Metcalfe MJ, Fuentealba R, Bonansco C, Inestrosa NC (2008) Wnt-7a modulates the synaptic vesicle cycle and synaptic transmission in hippocampal neurons. J Biol Chem 283:5918–5927.

Cerpa W, Toledo EM, Varela-Nallar L, Inestrosa NC (2009) The role of Wnt signaling in neuroprotection. Drug News Perspect 22:579–591.

Cha M-Y, Han S-H, Son SM, Hong H-S, Choi Y-J, Byun J, Mook-Jung I (2012) Mitochondria-specific accumulation of amyloid β induces mitochondrial dysfunction leading to apoptotic cell death. PLoS One 7:e34929.

Clevers H, Nusse R (2012) Wnt/β-catenin signaling and disease. Cell 149:1192–1205.

Costes S V, Daelemans D, Cho EH, Dobbin Z, Pavlakis G, Lockett S (2004) Automatic and quantitative measurement of protein-protein colocalization in live cells. Biophys J 86:3993–4003.

De Ferrari G, Avila M, Medina M, Pérez-Palma E, Bustos B, Alarcón M (2013) Wnt/β-Catenin Signaling in Alzheimer's Disease. CNS Neurol Disord Drug Targets.

De Stefani D, Raffaello A, Teardo E, Szabò I, Rizzuto R (2011) A forty-kilodalton protein of the inner membrane is the mitochondrial calcium uniporter. Nature 476:336–340.

Dinamarca MC, Sagal JP, Quintanilla RA, Godoy JA, Arrázola MS, Inestrosa NC (2010) Amyloid-beta-Acetylcholinesterase complexes potentiate neurodegenerative changes induced by the Abeta peptide. Implications for the pathogenesis of Alzheimer's disease. Mol Neurodegener 5:4.

Du H, Guo L, Fang F, Chen D, Sosunov A a, McKhann GM, Yan Y, Wang C, Zhang H, Molkentin JD, Gunn-Moore FJ, Vonsattel JP, Arancio O, Chen JX, Yan S Du (2008)

Cyclophilin D deficiency attenuates mitochondrial and neuronal perturbation and ameliorates learning and memory in Alzheimer's disease. Nat Med 14:1097–1105.

Du H, Guo L, Yan S, Sosunov A a, McKhann GM, Yan SS (2010) Early deficits in synaptic mitochondria in an Alzheimer's disease mouse model. Proc Natl Acad Sci U S A 107:18670–18675.

Du H, Guo L, Yan SS (2012) Synaptic mitochondrial pathology in Alzheimer's disease. Antioxid Redox Signal 16:1467–1475.

Du H, Yan SS (2010a) Mitochondrial permeability transition pore in Alzheimer's disease: cyclophilin D and amyloid beta. Biochim Biophys Acta 1802:198–204.

Du H, Yan SS (2010b) Mitochondrial medicine for neurodegenerative diseases. Int J Biochem Cell Biol 42:560–572.

Eisner V, Parra V, Lavandero S, Hidalgo C, Jaimovich E (2010) Mitochondria fine-tune the slow Ca(2+) transients induced by electrical stimulation of skeletal myotubes. Cell Calcium 48:358–370.

Eliseev R a, Malecki J, Lester T, Zhang Y, Humphrey J, Gunter TE (2009) Cyclophilin D interacts with Bcl2 and exerts an anti-apoptotic effect. J Biol Chem 284:9692–9699.

Emami KH, Nguyen C, Ma H, Kim DH, Jeong KW, Eguchi M, Moon RT, Teo J-L, Oh SW, Kim HY, Moon SH, Ha JR, Kahn M (2004) A small molecule inhibitor of beta-catenin/CREB-binding protein transcription [corrected]. Proc Natl Acad Sci U S A 101:12682–12687.

Fuentealba R a, Farias G, Scheu J, Bronfman M, Marzolo MP, Inestrosa NC (2004) Signal transduction during amyloid-beta-peptide neurotoxicity: role in Alzheimer disease. Brain Res Brain Res Rev 47:275–289.

Fuenzalida K, Quintanilla R, Ramos P, Piderit D, Fuentealba R a, Martinez G, Inestrosa NC, Bronfman M (2007) Peroxisome proliferator-activated receptor gamma up-regulates the Bcl-2 anti-apoptotic protein in neurons and induces mitochondrial stabilization and protection against oxidative stress and apoptosis. J Biol Chem 282:37006–37015.

Gillessen T, Grasshoff C, Szinicz L (2002) Mitochondrial permeability transition can be directly monitored in living neurons. Biomed Pharmacother 56:186–193.

Godoy JA, Allard C, Arrázola MS, Zolezzi JM, Inestrosa NC (2013) SIRT1 Protects Dendrites, Mitochondria and Synapses from Aβ Oligomers in Hippocampal Neurons. J Alzheimers Dis Park 03.

Gomez L, Paillard M, Thibault H, Derumeaux G, Ovize M (2008) Inhibition of GSK3beta by postconditioning is required to prevent opening of the mitochondrial permeability transition pore during reperfusion. Circulation 117:2761–2768.

Halestrap AP (2009) What is the mitochondrial permeability transition pore? J Mol Cell Cardiol 46:821–831.

Halestrap AP, Connern CP, Griffiths EJ, Kerr PM (1997) Cyclosporin A binding to mitochondrial cyclophilin inhibits the permeability transition pore and protects hearts from ischaemia/reperfusion injury. Mol Cell Biochem 174:167–172.

Hardy J, Selkoe DJ (2002) The amyloid hypothesis of Alzheimer's disease: progress and problems on the road to therapeutics. Science 297:353–356.

Inestrosa NC, Arenas E (2010) Emerging roles of Wnts in the adult nervous system. Nat Rev Neurosci 11:77–86.

Inestrosa NC, Godoy J a, Vargas JY, Arrazola MS, Rios J a, Carvajal FJ, Serrano FG, Farias GG (2013) Nicotine prevents synaptic impairment induced by amyloid-β oligomers through α7-nicotinic acetylcholine receptor activation. Neuromolecular Med 15:549–569.

Inestrosa NC, Godoy JA, Quintanilla R a, Koenig CS, Bronfman M (2005) Peroxisome proliferator-activated receptor gamma is expressed in hippocampal neurons and its activation prevents beta-amyloid neurodegeneration: role of Wnt signaling. Exp Cell Res 304:91–104.

Inestrosa NC, Varela-Nallar L (2014) Wnt signaling in the nervous system and in Alzheimer's disease. J Mol Cell Biol 6:64–74.

Juhaszova M, Zorov DB, Kim S, Pepe S, Fu Q, Fishbein KW, Ziman BD, Wang S, Ytrehus K, Antos CL, Olson EN, Sollott SJ (2004) Glycogen synthase kinase-3β mediates convergence of protection signaling to inhibit the mitochondrial permeability transition pore. 113.

Juhaszova M, Zorov DB, Yaniv Y, Nuss HB, Wang S, Sollott SJ (2009) Role of glycogen synthase kinase-3beta in cardioprotection. Circ Res 104:1240–1252.

Kato M, Akao M, Matsumoto-Ida M, Makiyama T, Iguchi M, Takeda T, Shimizu S, Kita T (2009) The targeting of cyclophilin D by RNAi as a novel cardioprotective therapy: evidence from two-photon imaging. Cardiovasc Res 83:335–344.

Kawano Y, Kypta R (2003) Secreted antagonists of the Wnt signalling pathway. J Cell Sci 116:2627–2634.

Kim MJ, Huh YH, Choi KJ, Jun S, Je a R, Chae H, Lee C, Kweon H-S (2012) Ultrastructural Abnormalities in APP/PSEN1 Transgenic Mouse Brain as the Alzheimer's Disease Model. Korean J Microsc 42:179–185.

Klein WL (2002) Abeta toxicity in Alzheimer's disease: globular oligomers (ADDLs) as new vaccine and drug targets. Neurochem Int 41:345–352.

Kuwana T, Newmeyer DD (2003) Bcl-2-family proteins and the role of mitochondria in apoptosis. Curr Opin Cell Biol 15:691–699.

LaFerla FM (2002) Calcium dyshomeostasis and intracellular signalling in Alzheimer's disease. Nat Rev Neurosci 3:862–872.

Li S, Hong S, Shepardson NE, Walsh DM, Shankar GM, Selkoe D (2009) Soluble oligomers of amyloid beta protein facilitate hippocampal long-term depression by disrupting neuronal glutamate uptake. Neuron 62:788–801.

Lie D-C, Colamarino S a, Song H-J, Désiré L, Mira H, Consiglio A, Lein ES, Jessberger S, Lansford H, Dearie AR, Gage FH (2005) Wnt signalling regulates adult hippocampal neurogenesis. Nature 437:1370–1375.

Manders EMM, Verbeek FJ, Aten JA (1993) Measurement of co-localization of objects in dual-colour confocal images. J Microsc 169:375–382.

Marchi S, Pinton P (2014) The mitochondrial calcium uniporter complex: molecular components, structure and physiopathological implications. J Physiol 592:829–839.

Marchionni I, Kasap Z, Mozrzymas JW, Sieghart W, Cherubini E, Zacchi P (2009) New insights on the role of gephyrin in regulating both phasic and tonic GABAergic inhibition in rat hippocampal neurons in culture. Neuroscience 164:552–562.

Miura T, Nishihara M, Miki T (2009) Drug development targeting the glycogen synthase kinase-3beta (GSK-3beta)-mediated signal transduction pathway: role of GSK-3beta in myocardial protection against ischemia/reperfusion injury. J Pharmacol Sci 109:162–167.

Miura T, Tanno M (2010) Mitochondria and GSK-3beta in cardioprotection against ischemia/reperfusion injury. Cardiovasc Drugs Ther 24:255–263.

Moreira PI, Santos MS, Moreno A, Oliveira C (2001) Amyloid beta-peptide promotes permeability transition pore in brain mitochondria. Biosci Rep 21:789–800.

Moreira PI, Santos MS, Moreno A, Rego AC, Oliveira C (2002) Effect of amyloid beta-peptide on permeability transition pore: a comparative study. J Neurosci Res 69:257–267.

Naga KK, Sullivan PG, Geddes JW (2007) High cyclophilin D content of synaptic mitochondria results in increased vulnerability to permeability transition. J Neurosci 27:7469–7475.

Nicholls DG, Budd SL (2000) Mitochondria and neuronal survival. Physiol Rev 80:315–360.

Nishihara M, Miura T, Miki T, Tanno M, Yano T, Naitoh K, Ohori K, Hotta H, Terashima Y, Shimamoto K (2007) Modulation of the mitochondrial permeability transition pore complex in GSK-3beta-mediated myocardial protection. J Mol Cell Cardiol 43:564–570.

Opazo F, Punge A, Bückers J, Hoopmann P, Kastrup L, Hell SW, Rizzoli SO (2010) Limited intermixing of synaptic vesicle components upon vesicle recycling. Traffic 11:800–812.

Paradis E, Koutroumanis M, Goodyer C (1996) Amyloid ␤ Peptide of Alzheimer ' s Disease Downregulates Bcl-2 and Upregulates Bax Expression in Human Neurons. 16:7533–7539.

Parks JK, Smith TS, Trimmer P a, Bennett JP, Parker WD (2001) Neurotoxic Abeta peptides increase oxidative stress in vivo through NMDA-receptor and nitric-oxide-synthase mechanisms, and inhibit complex IV activity and induce a mitochondrial permeability transition in vitro. J Neurochem 76:1050–1056.

Peng TI, Jou MJ, Sheu SS, Greenamyre JT (1998) Visualization of NMDA receptor-induced mitochondrial calcium accumulation in striatal neurons. Exp Neurol 149:1–12.

Perkins EM, McCaffery JM (2007) Conventional and immunoelectron microscopy of mitochondria. Methods Mol Biol 372:467–483.

Petronilli V, Miotto G, Canton M, Brini M, Colonna R, Bernardi P, Di Lisa F (1999) Transient and long-lasting openings of the mitochondrial permeability transition pore can be monitored directly in intact cells by changes in mitochondrial calcein fluorescence. Biophys J 76:725–734.

Petronilli V, Miotto G, Canton M, Colonna R, Bernardi P, Di Lisa F (1998) Imaging the mitochondrial permeability transition pore in intact cells. Biofactors 8:263–272.

Petronilli V, Penzo D, Scorrano L, Bernardi P, Di Lisa F (2001) The mitochondrial permeability transition, release of cytochrome c and cell death. Correlation with the duration of pore openings in situ. J Biol Chem 276:12030–12034.

Picard M, White K, Turnbull DM (2013) Mitochondrial morphology, topology, and membrane interactions in skeletal muscle: a quantitative three-dimensional electron microscopy study. J Appl Physiol 114:161–171.

Purro S a, Dickins EM, Salinas PC (2012) The secreted Wnt antagonist Dickkopf-1 is required for amyloid β-mediated synaptic loss. J Neurosci 32:3492–3498.

Quintanilla RA, Jin YN, von Bernhardi R, Johnson GVW (2013) Mitochondrial permeability transition pore induces mitochondria injury in Huntington disease. Mol Neurodegener 8:45.

Quintanilla RA, Muñoz FJ, Metcalfe MJ, Hitschfeld M, Olivares G, Godoy J a, Inestrosa NC (2005) Trolox and 17beta-estradiol protect against amyloid beta-peptide neurotoxicity by

a mechanism that involves modulation of the Wnt signaling pathway. J Biol Chem 280:11615–11625.

Rasola A, Sciacovelli M, Chiara F, Pantic B, Brusilow WS, Bernardi P (2010) Activation of mitochondrial ERK protects cancer cells from death through inhibition of the permeability transition. Proc Natl Acad Sci U S A 107:726–731.

Reynolds ES (1963) The use of lead citrate at high pH as an electron-opaque stain in electron microscopy. J Cell Biol 17:208–212.

Rosso SB, Inestrosa NC (2013) WNT signaling in neuronal maturation and synaptogenesis. Front Cell Neurosci 7:103.

Salinas PC, Zou Y (2008) Wnt signaling in neural circuit assembly. Annu Rev Neurosci 31:339–358.

Saraiva LM, Seixas da Silva GS, Galina A, Da-Silva WS, Klein WL, Ferreira ST, De Felice FG (2010) Amyloid-β triggers the release of neuronal hexokinase 1 from mitochondria. PLoS One 5:e15230.

Schinzel AC, Takeuchi O, Huang Z, Fisher JK, Zhou Z, Rubens J, Hetz C, Danial NN, Moskowitz M a, Korsmeyer SJ (2005) Cyclophilin D is a component of mitochondrial permeability transition and mediates neuronal cell death after focal cerebral ischemia. Proc Natl Acad Sci U S A 102:12005–12010.

Shevtzova EF, Kireeva EG, Bachurin SO (2001) Effect of beta-amyloid peptide fragment 25-35 on nonselective permeability of mitochondria. Bull Exp Biol Med 132:1173–1176.

Silva-Alvarez C, Arrázola MS, Godoy J a, Ordenes D, Inestrosa NC (2013) Canonical Wnt signaling protects hippocampal neurons from Aβ oligomers: role of non-canonical Wnt-5a/Ca(2+) in mitochondrial dynamics. Front Cell Neurosci 7:97.

Song DD, Shults CW, Sisk A, Rockenstein E, Masliah E (2004) Enhanced substantia nigra mitochondrial pathology in human alpha-synuclein transgenic mice after treatment with MPTP. Exp Neurol 186:158–172.

Sripetchwandee J, Sanit J, Chattipakorn N, Chattipakorn SC (2013) Mitochondrial calcium uniporter blocker effectively prevents brain mitochondrial dysfunction caused by iron overload. Life Sci 92:298–304.

Stambolic V, Woodgett JR (1994) Mitogen inactivation of glycogen synthase kinase-3 beta in intact cells via serine 9 phosphorylation. Biochem J 303 (Pt 3:701–704.

Stutzmann GE, Smith I, Caccamo A, Oddo S, Parker I, Laferla F (2007) Enhanced ryanodine-mediated calcium release in mutant PS1-expressing Alzheimer's mouse models. Ann N Y Acad Sci 1097:265–277.

Sun MG, Williams J, Munoz-Pinedo C, Perkins G a, Brown JM, Ellisman MH, Green DR, Frey TG (2007) Correlated three-dimensional light and electron microscopy reveals transformation of mitochondria during apoptosis. Nat Cell Biol 9:1057–1065.

Supnet C, Bezprozvanny I (2010) Neuronal calcium signaling, mitochondrial dysfunction, and Alzheimer's disease. J Alzheimers Dis 20 Suppl 2:S487–98.

Swerdlow RH, Burns JM, Khan SM (2010) The Alzheimer's disease mitochondrial cascade hypothesis. J Alzheimers Dis 20 Suppl 2:S265–79.

Szalai G, Krishnamurthy R, Hajnóczky G (1999) Apoptosis driven by IP(3)-linked mitochondrial calcium signals. EMBO J 18:6349–6361.

Toledo EM, Inestrosa NC (2010) Activation of Wnt signaling by lithium and rosiglitazone reduced spatial memory impairment and neurodegeneration in brains of an

APPswe/PSEN1DeltaE9 mouse model of Alzheimer's disease. Mol Psychiatry 15:272–285, 228.

Varela-Nallar L, Alfaro IE, Serrano FG, Parodi J, Inestrosa NC (2010) Wingless-type family member 5A (Wnt-5a) stimulates synaptic differentiation and function of glutamatergic synapses. Proc Natl Acad Sci U S A 107:21164–21169.

Varela-Nallar L, Inestrosa NC (2013) Wnt signaling in the regulation of adult hippocampal neurogenesis. Front Cell Neurosci 7:100.

Vargas JY, Fuenzalida M, Inestrosa NC (2014) In vivo Activation of Wnt Signaling Pathway Enhances Cognitive Function of Adult Mice and Reverses Cognitive Deficits in an Alzheimer's Disease Model. J Neurosci 34:2191–2202.

Walsh DM, Klyubin I, Fadeeva J V, Cullen WK, Anwyl R, Wolfe MS, Rowan MJ, Selkoe DJ (2002) Naturally secreted oligomers of amyloid beta protein potently inhibit hippocampal long-term potentiation in vivo. Nature 416:535–539.

Wu D, Pan W (2010) GSK3: a multifaceted kinase in Wnt signaling. Trends Biochem Sci 35:161–168.

Ying WL, Emerson J, Clarke MJ, Sanadi DR (1991) Inhibition of mitochondrial calcium ion transport by an oxo-bridged dinuclear ruthenium ammine complex. Biochemistry 30:4949–4952.

Zorov DB, Juhaszova M, Yaniv Y, Nuss HB, Wang S, Sollott SJ (2009) Regulation and pharmacology of the mitochondrial permeability transition pore. Cardiovasc Res 83:213–225.

3. CHAPTER II

The next section presents a detailed description of two specific techniques performed in this thesis to detect mPTP opening and mitochondrial swelling. The results and protocols described here are part of the Research Objective N° 2 and allowed the preparation of the manuscript that is presented below.

This work is going to be published in the series *"Methods in Molecular Biology"* by Humana Press/Springer Science + Business Media, edited by John Walker and corresponds to the Chapter 7 of the volume *Neuronal Cell Death - Methods and Protocols*, which was edited by Laura Lossi and Adalberto Merighi, from the University of Turin and Istituto Nazionale di Neuroscienze (INN), Turin, Italy.

The chapter that is presented below is entitled: *Monitoring Mitochondrial Membranes Permeability in Live Neurons and Mitochondrial Swelling through Electron Microscopy Analysis*, by Arrázola MS and Inestrosa NC. Here, we described the development of a live cell imaging assay to detect mitochondrial permeability transition, through the loading of live neurons with calcein/cobalt; and the development of a detailed analysis of morphological and ultrastructural changes that mitochondria undergo during this process, evaluated by electron microscopy.

Monitoring Mitochondrial Membranes Permeability in Live Neurons and Mitochondrial Swelling through Electron Microscopy Analysis

Macarena S. Arrázola, and Nibaldo C. Inestrosa

Abstract

Maintenance of mitochondrial membrane integrity is essential for mitochondrial function and neuronal viability. Apoptotic stimulus or calcium overload lead to mitochondrial permeability transition pore (mPTP) opening and induce mitochondrial *swelling*, a common feature of mitochondrial membrane permeabilization. The first phenomenon can be evaluated in cells loaded with the dye calcein-AM quenched by cobalt, and mitochondrial *swelling* can be detected by electron microscopy through the analysis of mitochondrial membrane integrity. Here, we described a live cell imaging assay to detect mitochondrial permeability transition and the development of a detailed analysis of morphological and ultrastructural changes that mitochondria undergo during this process.

Key words: mitochondrial permeability transition, mitochondrial swelling, live cell imaging, mitochondrial membrane permeabilization, electron microscopy, mitochondrial calcein, cobalt, quenching, mitochondrial ultractructure.

Running head: Mitochondrial permeability transition assay and mitochondrial swelling

1. Introduction

Mitochondria are membranous enclose organelles present in all cellular types, including neurons, where participate in several vital processes, such as cellular bioenergetics, metabolism and calcium homeostasis *(1, 2)*. Calcium regulation is essential for the synaptic function of a neuron *(3)* and therefore for its viability *(4)*. Calcium ions influx into neurons is regulated by different cellular compartments, including the endoplasmic reticulum and mitochondria *(5)*. Calcium overload into mitochondria has been described as an inductor of the mitochondrial permeability transition *(6)*, which is a phenomenon characterized by the formation of large conductance permeability transition pores (mPTP) that make the mitochondrial membrane abruptly permeable to solutes up to 1,500 Da, resulting in the loss of mitochondrial membrane potential *(7)*. The permeabilization of the mitochondrial inner membrane induces morphological changes in this organelle, including increased volume, a phenomenon known as swelling, membranes disruption, cristae disorganization and the release of pro-apoptotic factors to the cytoplasm, to finally activate neuronal death cascades *(8, 9)*. For this reason, the maintenance of the structural integrity and function of mitochondria is crucial for their proper function and, therefore, for neuronal viability.

Mitochondrial swelling can be detected *in vitro* with a spectrophotometric assay from isolated mitochondria, as previously described *(10)*, however the amount of material required to obtain high quality purification is a limiting step when the experimental model in use is a primary culture of neurons. For this reason, we describe here a direct live cell imaging technique to monitor the mPTP opening, and the development of a detailed data analysis. This assay was developed by Petronilli et al. in 1998 *(11)* and, later, validated in a neuronal model *(12)*. The assay is based on the loading of living neurons with a calcein-AM/cobalt mix to quench the

cytosolic signal of calcein, but leaving intact the mitochondrial stain. The exposure of neurons to mPTP inductors, such as the ionophore ionomycin *(13),* or to calcium overload results in the decay of the mitochondrial calcein fluorescence, indicating mitochondrial permeability transition. Mitochondrial swelling can be also detected through the study of certain ultrastructural parameters by transmission electron microscopy (14). We describe here a detailed analysis to evaluate morphological changes in mitochondria exposed to permeability transition.

2. Materials

2.1. Mitochondrial Permeability Transition by Live Cell Imaging

1. Glass coverslips of 25 mm diameter (Marienfeld GmbH & Co. KG, Lauda - Königshofen, Germany).
2. 1X Neurobasal Medium (Gibco®, Life Technologies™, Carlsbad, CA).
3. B27 supplement (Gibco®, Life Technologies™).
4. DMSO (Sigma Chemicals, St. Louis, MO).
5. Stock probes: 1mM Calcein-AM, 10 μM Mitotracker Orange CMTMRos and 1 mM Hoechst 33342 (all from Molecular Probes®, Life Technologies™, Carlsbad, CA) in DMSO. Store at -20 °C protected from light.
6. 1mM Cobalt (II) chloride hexahydrate ($CoCl_2$ x $6H_2O$) stock solution: To prepare 5 mL dissolve 1.1897 g in 5 mL of sterile distilled water. Store at -20 °C protected from light.
7. Tyrode buffer: 135mM NaCl, 5mM KCl, 1.8mM $CaCl_2$, 1mM $MgCl_2$, 10 mM HEPES, 5.6 mM glucose, pH to 7.3 with concentrated HCl. To prepare 0.5 L weigh 3.944 g NaCl, 0.186 g KCl, 0.132 g $CaCl_2$, 1.19 g HEPES and 0.280 g glucose and transfer to a 0.5 L

glass beaker containing 300 mL distilled water. Mix and then add 500 µL 1M $MgCl_2$. Adjust pH with HCl and make up to 0.5 L. Make aliquots of 50 mL in Falcon tubes or glass bottles and store at -20 °C. Defrost 1 aliquot of Tyrode buffer for the assay, use it along the day and then discard. For calcium free experiments do not add $CaCl_2$ to the preparation. *See* **Note 1**.

8. Confocal microscope with appropriate laser sources (see below).

2.2. Mitochondrial Swelling Detection from Electron Microscopy Analysis

1. Cold artificial cerebrospinal fluid (ACSF): 124 mM NaCl, 2.69 mM KCl, 1.25 mM KH_2PO_4, 1.3 mM $MgSO_4$, 2.6 mM $NaHCO_3$, 10 mM glucose, 2.5 mM $CaCl_2$. To prepare a 10x stock solution of ACSF, weigh 72.466 g NaCl, 2.006 g KCl, 1.701 g KH_2PO_4, 1.565 g $MgSO_4$ or 3.203 g $MgSO_4$ x $7H_2O$, 21.843 g $NaHCO_3$ and 19.817 g glucose. Mix and make up to 1 L. To prepare 1x ACSF solution, dilute 100 mL of the 10x stock solution in 900 mL of distilled water. Oxygenate the solution by bubbling with an O_2/CO_2 mix for 10 min and adjust pH to 7.4 with NaOH/HCl 1N. Add 0.368 g $CaCl_2$ x $2H_2O$ and make up to 1L. Check again the pH and if it is necessary readjust pH to 7.4.
2. Cell strainer 70 µm nylon (BD Biosciences, Bedford, MA).
3. Six-well plates for cell culture.
4. Silicon tubes.
5. 0.1 M cacodylate buffer, pH 7.2 with HCl: Dissolve 2.14 g of sodium cacodylate in 80 mL of distilled water. Adjust pH to 7.2 and then make up to 100 mL with distilled water.
6. Fixative solution: 2.5% glutaraldehyde (e.g. Sigma Chemicals): Dilute 1 mL of 25% glutaraldehyde stock solution into 9 mL of 0.1 M cacodylate buffer, pH 7.2.

7. 1% osmium tetroxide (OsO_4): Dilute 25 mL of a 4% osmium tetroxide stock solution (Sigma Chemicals) with 75 mL of distilled water. Store at 4°C.
8. 1% uranyl acetate [$UO_2(OCOCH_3)_2 \times 2H_2O$]: Weigh 10 mg uranyl acetate and dissolve in 1 mL distilled water.
9. Epon resin (e.g. EMbed-812, Electron Microscopy Sciences, Hatfield, PA).
10. 4% uranyl acetate [$UO_2(OCOCH_3)_2 \times 2H_2O$]: Weigh 0.4 g of uranyl acetate and dissolve in 10 mL pure methanol.
11. Lead citrate staining solution: mix 1.33 g $Pb(NO_3)2$, 1.76 g $Na_3(C_6H_507) \times 2H_20$ and 30 mL distilled water in a 50 mL volumetric flask. Shake vigorously for 1 min and allow standing with intermittent shaking. After 30 min add 8.0 mL 1 N NaOH and make up to 50 mL with distilled water. Mix until lead citrate dissolves. The final pH is 12.0.
12. Cooper grids for electron microscopy (e.g. Ted Pella Inc., Redding, CA).
13. Biosafety cabinet.
14. CO_2 incubator.
15. Vibrating microtome.
16. Ultramicrotome.
17. Transmission electron microscope.

3. Methods

For live cell imaging, all procedures are carried out at 37 °C and under sterilized conditions unless otherwise specified.

3.1. Mitochondrial Permeability Transition by Live Cell Imaging

1. Seed neurons on glass coverslips of 25 mm diameter in a 35 mm dish or in the available format (*see* **Note 2**). Neurons are maintained in Neurobasal medium supplemented with B27 at 37 °C in an incubator with 5% CO_2.
2. For live cell imaging, load the cells with the fluorescent probes (*see* **Note 3**). In this step work with the cells in a biosafety cabinet protected from light. Before removing the cells from the incubator, prepare the loading mix: add 1µL of 1 mM calcein-AM stock solution, 1 µL of 1 M $CoCl_2$ and 5 µL of 10µM Mitotracker Orange in 993 µL of Neurobasal medium to make 1 mL. Final mix concentration is 1µM calcein-AM, 1 mM $CoCl_2$, 50 nM Mitotracker Orange (*see* **Note 4**). Hoechst dye can also be added to the loading mix to evaluate neuronal viability if necessary. *See* **Note 5**.
3. Wash cells twice with 1 mL Neurobasal medium without supplements (*see* **Note 6**). For 25 mm covers add 1 mL of loading mix to the dish and incubate neurons at 37 °C for 30 min, protected from light.
4. Remove the loaded neurons from the incubator and wash twice with 1 mL of Neurobasal medium, working in a biosafety cabinet. Change medium to Tyrode buffer and incubate cells for 10 min at 37 °C to equilibrate probes.
5. Transfer the cover to the microscope room and assemble the system as shown in Fig. 1A, B. Use little amounts of solid paraffin between both sides of the cover to fix it at the microscope system. *See* **Note 7**.
6. Set microscope parameters to start the mPTP live cell assay. For a spinning disk confocal microscope, use Texas Red filter to detect Mitotracker fluorescence, FITC for calcein-AM and UV filter for Hoechst, or set the adequate excitation/emission wavelengths depending on the microscope used (*see* **Note 8**). Water immersion objectives are recommendable for

Figure 1

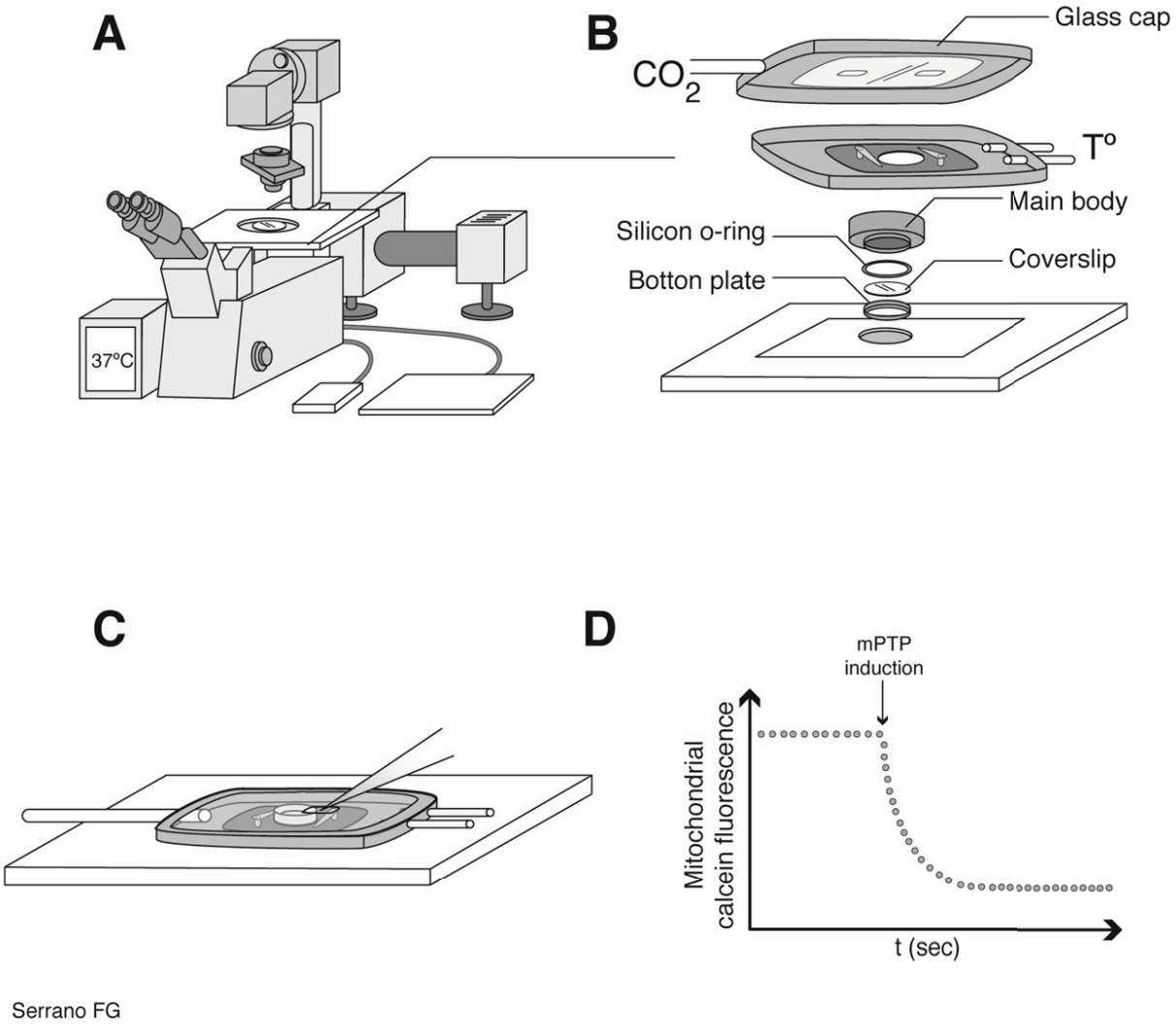

Fig. 1. Sample assembly for live cell imaging assay. A) Microscope system equipped for live cell assays. B) Neurons seeded on a glass coverslip mounted in the microscope chamber with CO_2 and temperature regulation. The glass cap is used to maintain the gas pressure and the temperature at 37 °C. C) Closed chamber ready to use and for the stimulation of neurons. D) Graphical representation of a common record obtained along the experiment after mPTP induction, i.e. with ionomycin. Mitochondrial calcein fluorescence decay is usually observed under mitochondrial permeability transition conditions.

live cell imaging assays. Set temperature to 37 °C and the gas pressure to ensure a constant flux of 5% CO_2 in the culture chamber of the microscope.

7. Set the time of the experiment and the interval between each digital image. It is recommendable to measure fluorescence changes for 15 min at least, with an image acquisition time of 10-15 sec between each frame. Measure a baseline for 3 min and then add the stimulus (Fig. 1C) (*see* **Note 9**). Finally, check the focus and start the experiment. It is recommendable to perform positive and negative controls of the mitochondrial permeability transition pore opening to check the efficiency of the assay. See **Note 10**.
8. For image analysis use the NIH ImageJ software and install the "Delta F" plugin. Follow the sequential steps to analyze fluorescence changes on the images: Open the image with Image J > Image > Stacks > Z project, type the number of images corresponding to the basal line, i.e. a 3 min baseline corresponds to 180 sec, if images were taken every 15 sec, and then the first 12 images correspond to the baseline; so type 1 in the start slice box and 12 in the stop slice > OK. This step creates an average image of the baseline.
9. Run "Delta F" plugin to determine fluorescence changes from the image stacks: Plugins > Stacks – T-functions > Delta F. A new image called "Delta F" is generated from this step. To obtain the value of ΔF/Fo (variation of the fluorescence between each image compared to the baseline) follow the next steps on Image J: Process > Image calculator, on Image 1 select the Delta F image created in the previous step; operation: Divide; and Image 2 is the average image created first > Yes. A new image is created called "Result of Delta F". From this image select a neurite with the polygon selection tool and perform the analysis: Images > Stacks > Plot z-axis Profile. A "Results" window is displayed with the mean fluorescence values corresponding to each time point. Plot the data to obtain

fluorescence changes along the live cell imaging assay, as shown Fig 1D. Repeat this step with each neurite selected until complete around 8-10 neurites per neuron.

10. Fluorescence analysis can be done with the mitochondrial calcein images to detect mPTP opening and also with those obtained from the Mitotracker loading, to detect mitochondrial membrane potential changes in response to the same stimulus (Fig. 2).

3.2. Mitochondrial swelling detection from electron microscopy analysis.

1. Prepare brain slices from rat or mouse brain *(15, 16)*. Cut transverse slices of 400 μm under cold ACSF using a vibrating microtome.
2. Incubate the slices in oxygenated ACSF for more than one hour at room temperature before treatment.
3. For slices treatment, mount the slices in a 6-well plate modified as shown in Fig. 3, to keep each dish oxygenated (*see* **Note 11**). Dilute all treatments in ACSF in an appropriate volume to maintain slices immersed and avoid its contact with the air. This step is carried out at room temperature.
4. After treatment, transfer the slices one by one, with a soft brush or tweezers, to an Eppendorf tube containing 1 mL of the fixative and fix for 6 h. *See* **Note 12**.
5. After fixation, wash the slices with 1 mL of 0.1 M cacodylate buffer, pH 7.2 for 18 h at 4 °C.
6. Perform a secondary fixation with 1% osmium tetroxide for 90 min and then wash with 3 washes, 5 min each in distilled water.
7. Stain samples with 1% aqueous uranyl acetate for 60 min.
8. Dehydrate samples in acetone following these sequential steps: 1 x 50%, 1 x 70%, 2 x 95% and 3 x 100% acetone, 20 min each.

Figure 2

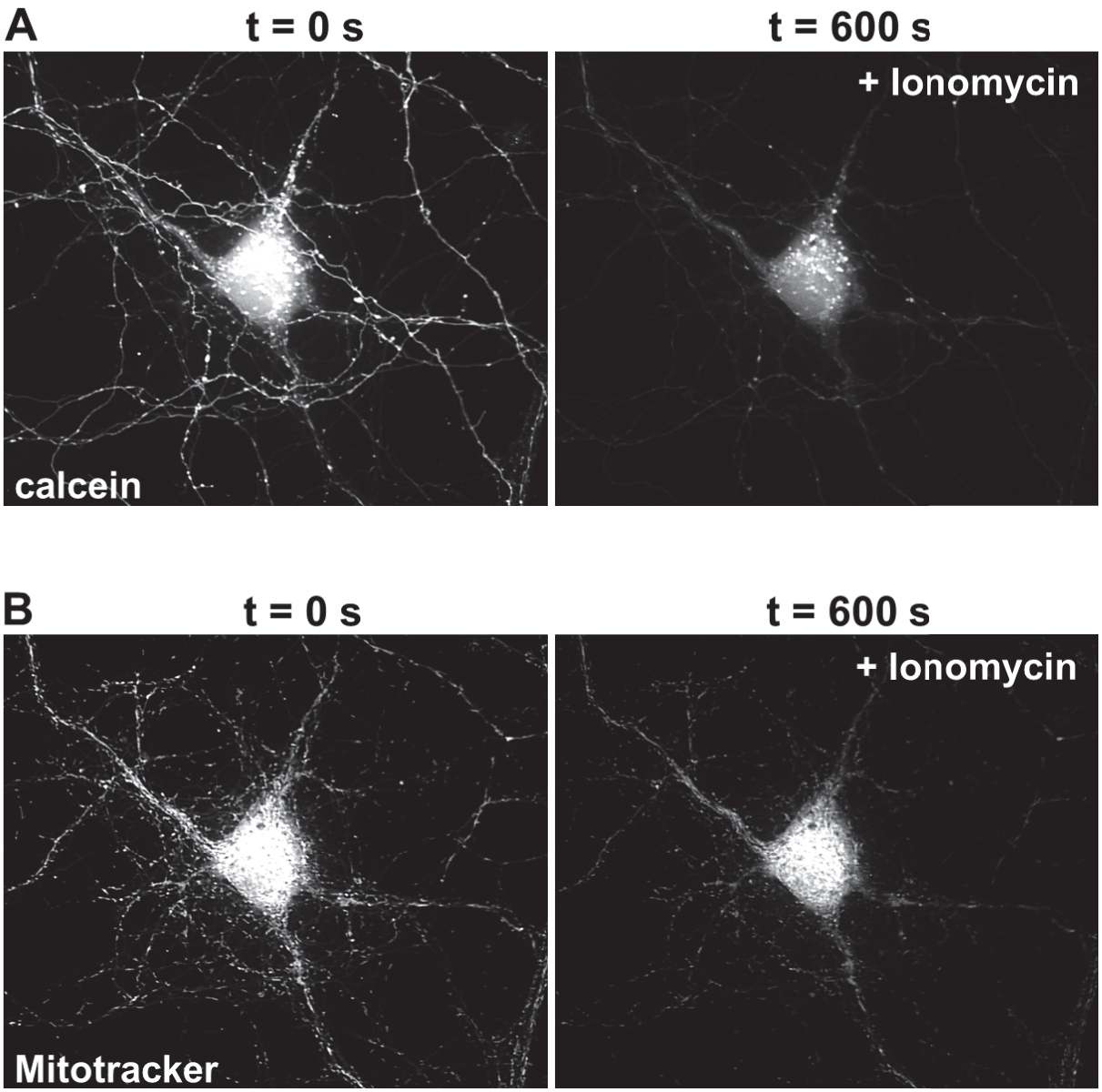

Fig. 2. Images obtained from the mPTP live cell imaging assay. Neurons were loaded with the loading Mix, containing calcein-AM, cobalt and Mitotracker Orange. A) Images show mitochondrial calcein fluorescence dissipation on neurons exposed to 0.5 μM ionomycin which indicates mitochondrial permeability transition. Images show fluorescence changes at the beginning (t=0) and at the end (t=600) of the experiment. B) Images show the mitochondrial membrane potential loss in the same neuron shows in A) under ionomycin stimulus.

9. Place samples in 1:1 Epon:acetone overnight and embed them in 100% Epon resin into a mold. Place mold containing samples in 60 °C oven for 24 h to polymerize.
10. Cut ultra-thin sections (60-70 nm) with an ultramicrotome and collect them on 300-mesh copper electron microscopy grids (Fig. 3). Stain with 4% uranyl acetate for 2 min and lead citrate for 5 min *(17)*.
11. Examine the samples in a transmission electron microscope. For morphological analysis of mitochondria is recommendable to capture digital images with a 16.500 – 20.000 x magnification.
12. For mitochondrial ultrastuctural analysis take 40-50 digital images per sample and evaluate membrane integrity of each mitochondrion by manually detecting structural abnormalities. Mitochondria with an overall intact structure are considered healthy, but loss of membrane continuity is considered an index of disruption. The same approach is applicable to cristae integrity analysis (Fig. 4).
13. To evaluate mitochondrial swelling, measure morphological parameters, such as area, diameter and perimeter *(18)* with ImageJ software. Set scale parameters in ImageJ: Analyze > Set scale > introduce distance in pixels and unit of length. *See* **Note 13**.
14. Set the parameters to be measured in ImageJ: Analyze > Set measurements > click in, Area, Perimeter and Feret's diameter.
15. Measure mitochondrial morphology with the polygon selection tool of ImageJ by surrounding each mitochondrion and press Ctrl+M on the keyboard to display the Results window. Plot the results in a column graph and as a scatter plot graph to analyze the whole population of mitochondria. *See* **Note 14**.

Figure 3

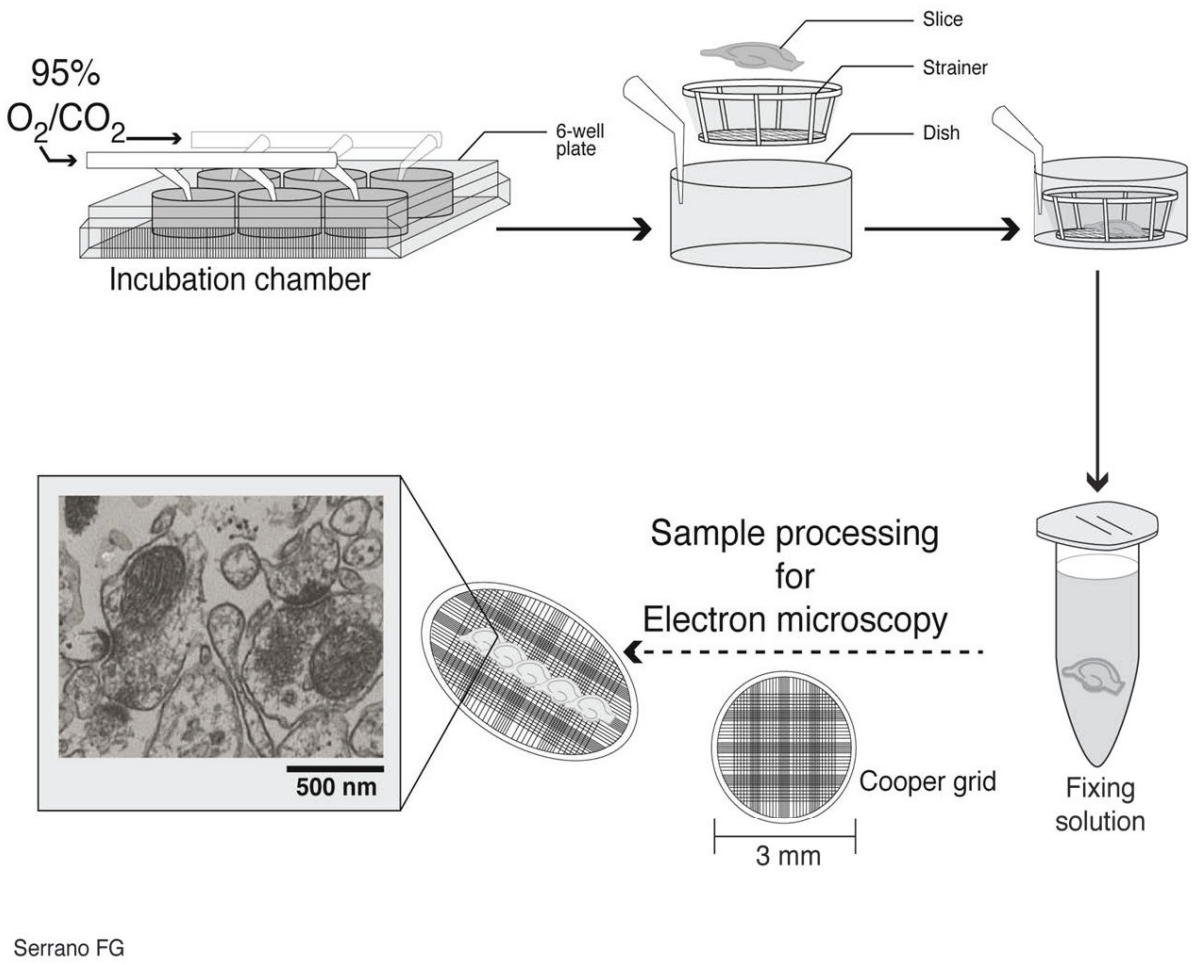

Fig. 3. Slice preparation and treatment for electron microscopy. Incubation chamber is used to treat slices separately. Each well contains a cell strainer to keep slices protected from bubbles generated by the oxygenation system. After the incubation time, slices are immersed in fixing solution, processed for electron microscopy and sequentially collected on copper grids for electron microscopy analysis. A representative image obtain with the microscope is shown at the end of the flowchart.

Figure 4

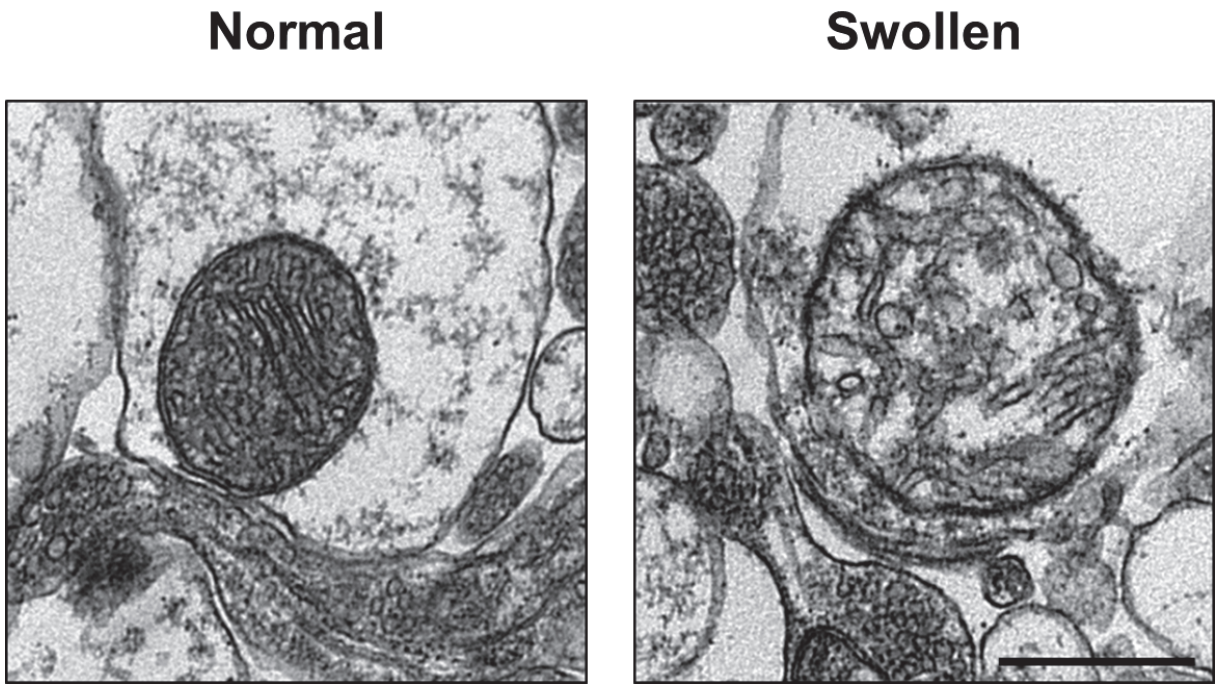

Fig. 4. Mitochondrial swelling detection by electron microscopy. Images show normal mitochondria with intact membrane and cristae (left picture) and a swollen mitochondrion (right picture) which is larger than normal and also displays membrane disruption and cristae disorganization, the common features of mitochondrial swelling by permeability transition. Bar = 500 nm.

4. Notes

1. To maintain the osmolarity of the Tyrode buffer under calcium free conditions, add 3.997 g NaCl to the preparation instead 3.944 g, to change the concentration from 135 mM to 136.8 mM NaCl.
2. Glass coverslips of other diameters may be used depending on the chamber that is going to be mounted to the microscope stage for the live cell assay. Some microscopes have chamber adaptors for 12, 25 or 40 mm diameter coverslip. If the microscope does not have chamber adaptors for different coverslip size, glass bottom dishes can also be used to seed cells.
3. Try to load just one cover per assay to avoid fluorescence decay during the time waiting between each experiment.
4. Other Mitotrackers could be used to evaluate the mitochondrial membrane potential during the mPTP live cell assay, as Mitotracker Red CMXRos, but higher concentration of this probe is needed (between 200 nM to 1 μM). It is also important to check the bleaching of the probe depending on the microscope available.
5. Add 1μL of 1 mM Hoechst 33342 dye to 1 mL of loading mix. It is recommendable to measure Hoechst stain only at the beginning and at the end of the experiment and not along it to avoid probes bleaching.
6. If the cells were previously treated before the live imaging experiment, it is necessary to wash them to eliminate the stimulus. Also it is important to wash the cells to deplete them from B27, since it could interfere with the stimulus that is going to be used for the live cell assay.

7. Put the paraffin only at the edges of the cover to maintain an adequate cellular field to observe at the microscope. Some systems are magnetically sealed and do not need paraffin.
8. Hoechst λ ex/em = 350/461 nm. The ex/em peaks of calcein after hydrolysis are 494/517 nm. Mitotracker Orange λ ex/em = 554/576 nm.
9. For live cell imaging, the stimulus can be added manually with a micropipette or through a peristaltic pump.
10. Use 0.5 μM of the ionophore ionomycin, as a positive control of mitochondrial permeability transition. A loss of mitochondrial calcein is appreciated when this stimulus is added. As a negative control, incubate neurons for 30 min at 37 °C with 20 μM cyclosporin A (CsA) to inhibit mPTP opening before the stimulus. A control of probe bleaching is also needed. To evaluate this issue, measure the fluorescence of the probe for the duration of the experiment by simply adding vehicle.
11. An oxygenated dish can be manually made by introducing silicone tubes adapted to a white pipette tip. Fix the tip to the inside wall of the dish until the middle of the well and connect the tube to the oxygen. Be sure to keep a constant oxygen flux along the experiment, avoiding bubbles directly on the slices. Mount the slices into a cell strainer (usually used for organotypic cultures) inside each dish. Under these conditions slices can be maintained between 6 to 8 h without affecting cell viability (see **Fig. 3**).
12. Prepare a fresh fixing solution every time you need it and only in the amount that is necessary for each experiment. Do not freeze.
13. To determine distance in pixels, measure the length of the scale bar using the straight line selections tool of ImageJ and then open the set scale window and introduce the following

parameters: *distance in pixels* is automatically determined by the software when the scale bar is measured with the straight line tool; the *known distance* corresponds to the length of the scale bar measured from the image; and the *unit length* also depends on the scale bar unit usually in µm. Click on "Global", and the final scale should be in pixel/µm.

14. The scatter plot graphs allow a deep analysis of the data, because they can be divided by percentiles to determine which population is affected by a determined treatment, as previously described (*see* 18).

Acknowledgments

This work was supported by grants from the Basal Center of Excellence in Aging and Regeneration (CONICYT – PFB 12/2007) and FONDECYT N° 1120156 to NCI, and a pre-doctoral fellowship from CONICYT to MSA.

References

1. Kann, O., Schuchmann, S., Buchheim, K. et al. (2003) Coupling of neuronal activity and mitochondrial metabolism as revealed by NAD(P)H fluorescence signals in organotypic hippocampal slice cultures of the rat. *Neuroscience* **119**, 87–100.
2. Celsi, F., Pizzo, P., Brini, M. et al. (2009) Mitochondria, calcium and cell death: a deadly triad in neurodegeneration. *Biochim Biophys Acta* **1787**, 335–344.
3. Vos, M., Lauwers, E., and Verstreken, P. (2010) Synaptic mitochondria in synaptic transmission and organization of vesicle pools in health and disease. *Front Synaptic Neurosci* **2**, 139.

4. Newmeyer, D.D., and Ferguson-Miller, S. (2003) Mitochondria: releasing power for life and unleashing the machineries of death *Cell* **112**, 481–490.

5. Gunter, T.E., and Gunter, K.K. (2001) Uptake of calcium by mitochondria: transport and possible function. *IUBMB Life* **52**, 197–204.

6. Lemasters, J.J., Theruvath, T.P., Zhong, Z. et al. (2009) Mitochondrial calcium and the permeability transition in cell death. *Biochim Biophys Acta* **1787**, 1395–1401.

7. Rao, V.K., Carlson, E. A, and Yan S.S. (2013) Mitochondrial permeability transition pore is a potential drug target for neurodegeneration. *Biochim. Biophys. Acta* doi: 10.1016/j.bbadis.2013.09.003.

8. Galluzzi, L., Blomgren, K., andKroemer G. (2009) Mitochondrial membrane permeabilization in neuronal injury. *Nat Rev Neurosci* **10**, 481–494.

9. Petronilli, V., Penzo, D., Scorrano, L. et al. (2001) The mitochondrial permeability transition, release of cytochrome c and cell death. Correlation with the duration of pore openings in situ. *J Biol Chem* **276**, 12030–12034.

10. Schinzel, A.C., Takeuchi, O., Huang, Z. et al. (2005) Cyclophilin D is a component of mitochondrial permeability transition and mediates neuronal cell death after focal cerebral ischemia. *Proc Natl Acad Sci USA* **102**, 12005–12010.

11. Petronilli, V., Miotto, G., Canton, M. et al. (1998) Imaging the mitochondrial permeability transition pore in intact cells. *Biofactors* **8**, 263–272.

12. Gillessen, T., Grasshoff, C., and Szinicz, L. (2002) Mitochondrial permeability transition can be directly monitored in living neurons. *Biomed Pharmacother* **56**, 186–193.

13. Abramov, A.Y., and Duchen M.R. (2003) Actions of ionomycin, 4-BrA23187 and a novel electrogenic Ca2+ ionophore on mitochondria in intact cells. *Cell Calcium* **33**, 101–112.

14. Sun, M.G., Williams, J., Munoz-Pinedo, C. et al. (2007) Correlated three-dimensional light and electron microscopy reveals transformation of mitochondria during apoptosis. *Nat Cell Biol* **9**, 1057–1065.

15. Cerpa, W., Godoy, J.A., Alfaro, I. et al. (2008) Wnt-7a modulates the synaptic vesicle cycle and synaptic transmission in hippocampal neurons. *J Biol Chem* **283**, 5918–5927.

16. Varela-Nallar, L., Alfaro, I.E., Serrano, F.G. et al. (2010) Wingless-type family member 5A (Wnt-5a) stimulates synaptic differentiation and function of glutamatergic synapses. *Proc Natl Acad Sci USA* **107**, 21164–21169.

17. Reynolds, E.S. (1963) The use of lead citrate at high pH as an electron-opaque stain in electron microscopy. *J Cell Biol* **17**, 208–212.

18. Song, D.D., Shults, C.W., Sisk, A. et al. (2004) Enhanced substantia nigra mitochondrial pathology in human alpha-synuclein transgenic mice after treatment with MPTP. *Exp Neurol* **186**, 158–172.

4. DISCUSSION

Even though it is well demonstrated that Wnt signaling is involved in processes related to neuroprotection in AD (Cerpa et al., 2009; Inestrosa and Varela-Nallar, 2014), there is no direct evidence explaining the mechanism by which this signaling protects neurons from cell death or whether this neuroprotective effect is due to the role of Wnt signaling in the regulation of cell death cascades, and even which are the cellular steps that mediate this protective effect. Since cell death is mainly regulated at the mitochondria and this organelle is one of the early targets directly affected in AD (Eckert et al., 2010; Johri and Beal, 2012; Reddy, 2007) we decided to study whether Wnt signaling activation exerts its protective role through preventing mitochondrial damage. Because mitochondrial function declines with the progression of the disease (Swerdlow et al., 2010), and due to its function directly depends on the mitochondrial membrane integrity and the preservation of its structure (Kroemer et al., 2007), we explored the role of Wnt signaling in the regulation of mitochondrial permeability and whether this regulation is a result of the inhibition of one of the main mechanisms involved in this process: the mPTP opening. This hypothesis allows us to propose that the regulation of the mitochondrial permeability through Wnt signaling is related to the protection against Aβ-induced neuronal death. In this study, we found that the activation of Wnt signaling through the Wnt3a ligand prevents the mPTP opening induced by the toxicity of Aβo in hippocampal neurons, as well as inhibits all of the consequent effects that affect

mitochondria, such as the loss of membrane potential, mitochondrial morphological changes, mitochondrial structure disruption, and cytochrome-c release and, therefore, neuronal death.

4.1. Wnt signaling and Aβo-induced neuronal death

The activation of Wnt signaling pathway has been physiologically implicated in fundamental processes of the development, maintenance and function of the central nervous system (CNS) (Inestrosa and Arenas, 2010). Beyond its essential role in cell proliferation, tissue patterning, cell fate, migration, morphogenesis and synaptic function (Zou and Salinas, 2014), Wnt signaling has been related to cell survival and neurodegeneration (Harvey and Marchetti, 2014; Oliva et al., 2013). For several years, our laboratory has been studying the role of Wnt signaling in the neurodegeneration observed in AD. The first time that canonical Wnt signaling was related to AD was by De Ferrari and Inestrosa in 2000, and they proposed that sustained loss of Wnt signaling function may lead to AD (De Ferrari and Inestrosa, 2000). Later, they showed that Aβ fibrils induce the destabilization of endogenous levels of β-catenin, which were recovered with lithium (De Ferrari et al., 2003), a pharmacological inhibitor of GSK-3β, and therefore and inductor of Wnt signaling activation (Klein and Melton, 1996). Subsequent studies from our laboratory demonstrated that the direct activation of the canonical Wnt signaling, through the Wnt3a ligand, prevents neuronal death induce by Aβ fibrils and that this activation also rescue the levels of Wnt-related proteins, such as β-catenin, which were down-regulated by Aβ toxicity (Alvarez et al., 2004), indicating that Wnt signaling activation plays a key role in neuroprotection against Aβ-induced neuronal death. To reproduce the protective role of Wnt3a against Aβ-induced neuronal death we performed two viability assays: Hoechst staining to detect apoptotic nuclei and the Live/Dead assay as a late

marker of neuronal death, however, unlike the studies previously described, we use Aβ oligomers instead of fibrils to induce cell death, since currently this state of aggregation is considered as the most toxic species related to the neuronal and cognitive damage described in AD (Cleary et al., 2005; Walsh et al., 2000). The Aβo preparation was analyzed by tris-tricine geles to confirm the presence of low molecular weight oligomers (dimers to tetramers) and through electron microscopy to observed their structure (Apendix 1A, B). These Aβo produce a 50% decrease in neuronal viability, which was significant from 5 μM Aβo, evaluated at 24 h treatment (Apendix 1C). With these conditions we performed most of the experiments in hippocampal neurons and brain slices to induce Aβo-dependent damage. As we expected, Wnt signaling activation with recombinant Wnt3a significantly prevented the apoptosis and therefore the neuronal death induced by Aβ. These results confirmed the neuroprotective effect that Wnt canonical signaling activation generates against Aβ toxicity, particularly against the oligomeric forms of Aβ.

4.2. Wnt signaling and its regulation of mitochondrial calcium levels

One of the important functions of mitochondria is to control calcium variations inside the cell. A massive and uncontrolled calcium influx into mitochondria directly affects mitochondrial permeability (Du and Yan, 2010b) through the mPTP opening (Szalai et al., 1999), inducing mitochondrial membrane potential dissipation, increased membranes permeability and, finally, neuronal death (Celsi et al., 2009). In agreement with this, it is very well established that calcium plays an important role in the neurotoxicity of AD in mouse models (LaFerla, 2002; Stutzmann et al., 2007) and *in vitro*, because it has been demonstrated that Aβ aggregates, prepared from Aβ synthetic peptides, induce intracellular calcium

increase, which directly impacts the mitochondrial calcium levels (Dinamarca et al., 2010; Supnet and Bezprozvanny, 2010). Previous studies related to the role of Wnt signaling in the regulation of Aβ-induced intracellular calcium increase have shown that the early activation of Wnt signaling, with the canonical ligand Wnt7a, prevents the intracellular calcium increase generated by Aβ fibrils (Quintanilla et al., 2005) and oligomers (Dinamarca et al., 2010) in hippocampal neurons. They also showed that these oligomers affect the calcium buffering function of the mitochondria, because they produce calcium overload into the organelle, however it has not been explored whether Wnt signaling is able to prevent this calcium increase into mitochondria and if this process is involved in the neuroprotective role of this signaling pathway against Aβ toxicity in AD. The results indicate that our Aβo preparation was able to induce mitochondrial calcium changes in neurons, which was prevented in the presence of the uniporter inhibitor Ru360 (Ying et al., 1991), with no effect over intracellular calcium levels induced by Aβo. This mitochondrial calcium change was specifically observed at the neurites of neurons. These compartmentalized effects of Aβo on mitochondrial calcium changes could be explained by the specific sensitivity of synaptic mitochondria (rather than non-synaptic mitochondria) to calcium overload, which cause them to more readily undergo a permeability transition (Brown et al., 2006), which is in agreement with recent observations that indicate that synaptic mitochondria are more sensitive to direct Aβ damage, affecting the trafficking and transport of the mitochondria to specific regions of the neurons where more energy is required, even making those mitochondria more sensitive to mPTP (Du et al., 2012). In the same way, the CypD levels of synaptic mitochondria are also important in the sensitivity of those mitochondria to Aβ damage and it has been described that high CypD content in synaptic mitochondria makes them more vulnerable to permeability transitions

(Naga et al., 2007). Interestingly, and related to the results obtained in this work about the capability of Wnt3a to prevent mitochondrial calcium overload induced by Aβo, it has been demonstrated that the synaptic damage mediated by Aβ in neurons required Wnt antagonist components, such as Dickkopf-1 (DKK1) (Purro et al., 2012), another piece of evidence that suggests that the modulation of Wnt signaling activity could be important in regulating Aβ toxicity on neuronal function and viability. In agreement with this idea, we observed that the inhibition of canonical Wnt signaling with DKK1 plus Aβo resulted in an increase in mitochondrial calcium at the soma (Apendix 2), where we did not initially observe significant changes with Aβo alone, which suggests that the inhibition of endogenous Wnt signaling could be potentiating the effect of Aβo over the modulation of mitochondrial calcium levels and, in this manner, could be participating in the regulation of the permeability transition induced by Aβ.

4.3. Wnt signaling as a novel regulator of mitochondrial permeability

There are several described events that occur as a consequence of the mitochondrial permeability transition triggered in AD (Moreira et al., 2001). When the IMM is disrupted, because of the formation of the mPTP, mitochondria undergo some structural changes that finally affect its function and therefore, the cellular decision between life or death (Newmeyer and Ferguson-Miller, 2003). The loss of mΔΨ and the release of proapototic factors from the mitochondria to the cytoplasm are key processes related to mPTP formation and opening (Petronilli et al., 2001). For this reason, we decided to analyze, in the first instance, both events under Aβo treatment in the neurons in which Wnt signaling was previously activated. Our results indicate that Wnt3a prevents both, the Aβo-induced mΔΨ dissipation and the

release of cytochrome-c from the inner space to the cytoplasm. The rapid decay of mΔΨ observed was correlated with the kinetic of the mPTP opening. This phenomenon was directly evaluated by a live cell imaging assay based on mitochondrial calcein dissipation, as a result of the mPTP opening, as was described previously (Gillessen et al., 2002; Petronilli et al., 1998) and as is detailed in the Chapter II of this thesis. Interestingly, Wnt signaling activation also prevents the mPTP induction in a similar way as the mPTP inhibitor, cyclosporin A (CsA) (Halestrap et al., 1997), suggesting a possible mechanism by which Wnt signaling could regulate neuronal death. All of these mitochondrial alterations related to the mitochondrial membranes permeability are associated with morphological changes that mitochondria undergo during mPTP opening (Moreira et al., 2002).

4.4. Ultrastructural changes of mitochondria during permeability transition.

The permeabilization of the IMM induces morphological changes in the mitochondria, including an increased size and volume, because of water and solutes exchange during mPTP opening, known as *swelling*, the disruption of both membranes and cristae disorganization. All of these events are classical features that mitochondria present in neurons undergoing cell death (Sun et al., 2007). To correlate the inhibition of mPTP opening mediated by Wnt signaling activation with these mitochondrial morphological alterations that are generated by Aβ in AD, we performed three-dimensional reconstruction of the mitochondrial network from hippocampal neurons transfected with mito-Cherry. We observed that neurons exposed to Aβo presented mitochondria with increased sphericity and volume, morphological changes correlated with mitochondrial permeability transition (Bernardi et al., 2006). We also observed that these morphological changes were completely prevented by Wnt3a.

A detailed analysis of these parameters was conducted by electron microscopy to correlate these protective effects in an *in vivo* model using hippocampal slices from mouse brains, specifically at the CA1 region of the hippocampus. We evaluated these changes at this particular zone because it has been reported that mitochondria and synapses from the CA1 show early sensitivity to damage in AD (Balietti et al., 2013). As we expected, we observed dramatic changes in the mitochondrial integrity and morphology in slices that were exposed to Aβo for only 1 h. As has been seen before, 1 h of Aβo exposure is enough to affect the synapses of hippocampal neurons, disrupting the clustering of PSD-95 (Inestrosa et al., 2013), which is correlated with the fact that synaptic mitochondria are also more sensitive than non-synaptic mitochondria (Brown et al., 2006). The morphological analysis from the electron microscopy images showed that mitochondria from Aβ-exposed neurons present increased area, diameter and perimeter, confirming our previous results in cultured hippocampal neurons, through the 3D reconstruction. We were also able to prevent these changes by the preincubation of the slices with Wnt3a, reaffirming the idea that Wnt signaling activation prevents mPTP opening and therefore the morphological changes that mitochondria undergo during this phenomenon. The ultrastructural study indicated that the activation of Wnt signaling prevents membrane disruption and cristae disorganization of mitochondria exposed to Aβo, features that have been described for the APP/PS1 transgenic mouse model of the AD (Kim et al., 2012), and that we were able to prevent also with CsA, supporting the idea that Wnt prevents mitochondrial membrane permeability, preventing the mitochondrial swelling induced by mPTP opening, which finally leads to apoptotic processes and to neuronal death (Sun et al., 2007).

4.5. How could Wnt signaling regulate the permeability transition and pore activation?

It is well documented that Aβ induces the activation of mPTP in an AD mouse model (Du et al., 2008) and *in vitro* (Moreira et al., 2001; Parks et al., 2001; Shevtzova et al., 2001) and that this activation and the subsequent mitochondrial and neuronal damage depends in part on the Aβ interaction with CypD, the main component of the mPTP (Baines et al., 2005; Schinzel et al., 2005), which is to date the only protein component that is essential for the activation of this pore (Basso et al., 2005; Kato et al., 2009).

Our results indicate that the Wnt3a ligand prevents mPTP opening induced by Aβo in live neurons. The ability of Wnt signaling to prevent the mPTP induction produced by Aβ could be mediated by two different mechanisms: 1) controlling intracellular calcium variations generated by Aβ, as has been previously suggested (Dinamarca et al., 2010; Quintanilla et al., 2005); or 2) regulating the direct effect of Aβo on mPTP formation and activation (Du et al., 2010). However, there are several sources of evidence that suggest that canonical Wnt signaling activation could regulate mitochondrial membrane permeability directly through the inhibition of the mPTP formation. For example, it has been reported that GSK-3β, one of the main components of the Wnt signaling pathway, is able to translocate to the mitochondria and to act on its inactive form (phosphorylated at serine 9) with one of the components of the mPTP, the adenine nucleotide translocase, ANT (Gomez et al., 2008; Juhaszova et al., 2009; Nishihara et al., 2007). This interaction has been correlated with a 60% decrease in the interaction between CypD and ANT, which is necessary for mPTP opening (Miura and Tanno, 2010; Miura et al., 2009; Zorov et al., 2009). Interestingly, canonical Wnt signaling activation induces the phosphorylation of GSK-3β at the same residue (Ser-9), inducing its inhibition and therefore the activation of the Wnt signaling cascade (Stambolic and Woodgett, 1994). These

findings suggest a possible mechanism to explain how Wnt could modulate mPTP opening and therefore the mitochondrial permeability induced by Aβ. Our results showing an increase in the mitochondrial content of phosphorylated-GSK-3β are consistent with the idea that the inhibition of GSK-3β mediates the Wnt3a function on mPTP regulation and suggest an explanation about the possible mechanism by which Wnt inhibits the mPTP opening and the subsequent lethal events generated in neurons, triggered by the mitochondrial permeability induced by Aβ. However, further analysis of the interaction between phosphorylated-GSK-3β with CypD or ANT will be required to better characterize this possible mechanism.

4.6. Other mPTP modulators and its association with GSK-3β

Several mPTP modulators have been described because they interact with the mPTP components or directly regulate the binding between the components of the pore (Eliseev et al., 2009; Rasola et al., 2010a; Saraiva et al., 2010). The real situation is that all of the regulators that have been described can interact with some of the main components of the mPTP or affect or facilitate its interaction, to finally modulate mitochondrial membrane permeability and cell viability. An example is the mitochondrial hexokinase II (HKII) which when is detached from the mitochondria, by a selective HK peptide, induces the mPTP opening and cell death (Chiara et al., 2008). Mitochondrial HKII regulates mPTP induction through the delivery of a survival signal that stabilizes the mPTP in the closed conformation, whereas HKII detachment from mitochondria would propagates a conformational change to molecules of the inner mitochondrial membrane, eventually leading to pore opening (Rasola et al., 2010b). Other mPTP modulator is the survival kinase Akt, which surprisingly regulates HKII by promoting its binding to mitochondria, through HKII phosphorylation (Miyamoto et

al., 2008). Interestingly and in agreement with our proposal, Akt also phosphorylates GSK-3β to inactivate it, which has been described to favor the association of HKII to the OMM. By contrast activation of GSK-3β was shown to induce release of HKII, enhancing susceptibility to cell death (Robey and Hay, 2006).

Another described modulator of mPTP formation is the pro-apoptotic protein Bax, which belongs to the Bcl-2 family proteins (Chipuk et al., 2010). Bax interacts with ANT (Marzo et al., 1998) and both cooperate to control de mitochondrial-dependent apoptosis (Marzo, 1998). On the other hand, Bcl-2 proteins have also been described to interact with VDAC (Rasola et al., 2010b) and the balance in the interaction between pro- and anti-apoptotic proteins with VDAC controls the sensitivity of mitochondria to mPTP induction (Mathupala et al., 2006). Once again, it has been proposed that GSK-3β can control this balance through VDAC phosphorylation, which would displace Bcl-2 from its interaction with VDAC, favoring the binding between VDAC and the pro-apoptotic Bax/Bak proteins, and therefore the mPTP induction (Mathupala et al., 2006). It has been shown that GSK-3β interact with VDAC (Nishihara et al., 2007) and interestingly in AD, GSK-3β phosphorylates VDAC which is correlated with HKII and anti-apoptotic Bcl-2 family proteins dissociation from VDAC and mitochondrial permeability transition in AD neurons (Reddy, 2013). These are other pieces of evidence that suggest that the regulation of GSK-3β activity could be important in the control of neuronal sensitivity to mPTP induction, and reinforce the idea that Wnt could inhibit mPTP formation through GSK-3β inhibition.

As was mentioned before, the anti-apoptotic protein Bcl-2 (Kuwana and Newmeyer, 2003) is another mPTP regulator and has been shown to prevent cell death through its interaction with the main component of the pore, CypD (Eliseev et al., 2009), giving a novel

protective function to CypD. Interestingly, Bcl-2 is downregulated in AD models (Paradis et al., 1996) and has been described as a Wnt target gene in hippocampal neurons (Fuentealba et al., 2004) and also participates in mitochondrial stabilization against Aβ damage (Fuenzalida et al., 2007). Despite this evidence, we observed that the inhibition of permeability transition, mediated by the Wnt3a ligand, was not dependent on the activation of Wnt target genes transcription because the treatment of neurons with ICG-001, a Wnt/β-catenin-dependent transcription inhibitor (Emami et al., 2004), did not abolish the protective Wnt effect on the inhibition of permeability transition, strengthening the idea that this effect could be mediated by the modulation of GSK-3β (Nishihara et al., 2007) rather than Wnt-dependent genes. Further analysis of the interaction between phosphorylated-GSK-3β with CypD/ANT/VDAC complex will be required to better characterize this possible mechanism.

Altogether, the data shown so far propose a novel mechanism by which canonical Wnt signaling protects neurons from Aβo toxicity. This mechanism involves the inhibition of mPTP opening and all of its consequences, thereby preventing the neuronal death observed in AD. This study suggests a possible new approach for the treatment of AD and opens a new line of study in the field of the role of Wnt signaling in neuroprotection.

5. CONCLUSIONS

The results presented in this thesis allow us to formulate the following conclusions:

1. Wnt3a ligand prevents the intracellular and mitochondrial calcium increase induced by Aβo in hippocampal neurons, which is prevented by the canonical Wnt signaling inhibitor, Dickopf-1.

2. Aβo produce mΔΨ dissipation in live neurons, which is prevented by the pretreatment with Wnt3a. Inhibition of Wnt signaling enables Wnt3a ligand to rescue the loss of the mΔΨ.

3. Wnt signaling activation through Wnt3a ligand prevents both, the cytochrome-c release from the mitochondrial and the neuronal death induced by Aβo.

4. Wnt3a prevents the mitochondrial membrane permeability through the inhibition of Aβo-induced mPTP opening, by a mechanism that is independent on the Wnt target genes transcription, suggesting the participation of a non-conventional Wnt signaling in the regulation of the mPTP.

5. Wnt3a induces increased levels of inactivated GSK-3β at the mitochondria, suggesting a possible mechanism on the regulation of mPTP inhibition mediated by Wnt signaling.

6. Wnt signaling activation prevents morphological and ultrastructural changes that mitochondria undergo during the mitochondrial swelling induced by Aβo in cultured hippocampal neurons and in hippocampal slices.

6. APPENDICES

Appendix 1

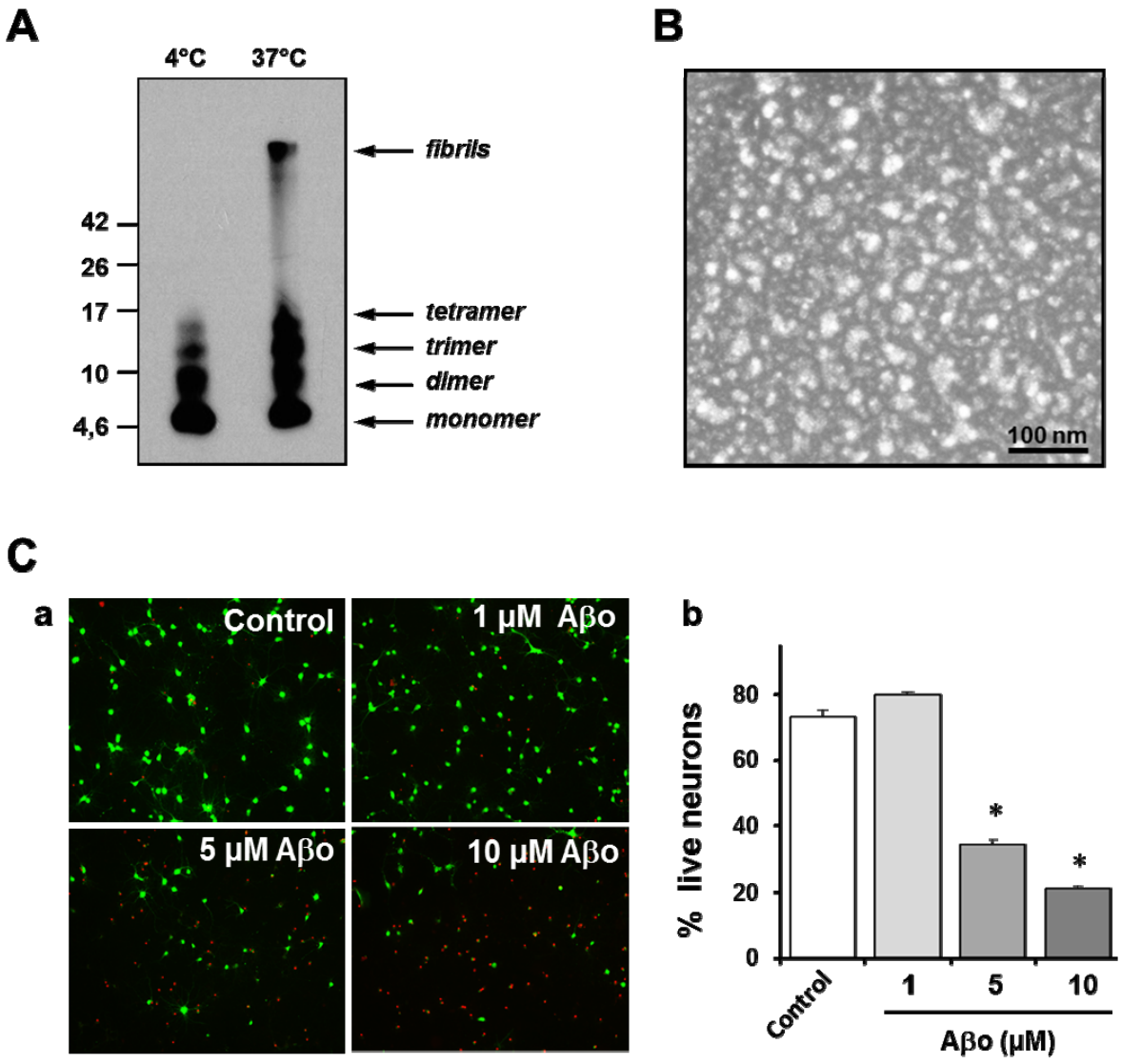

Apendix 1. Characterization of Aβo preparation and neuronal viability. A) Tris-tricine SDS-PAGE analysis of Aβ aggregates prepared at 4°C and at 37°C. First lane shows low-range molecular weight species, corresponding to dimers, trimers and tetramers. Second lane indicates the presence of Aβ fibrils under these conditions. B) Electron microscopy analysis shows oligomeric structures from Aβ preparation at 4°C. Bar represents 100 nm. C) LIVE/DEAD viability assay performed with the Aβo preparation in hippocampal neurons treated for 24 h. a) Calcein positive neurons (green) correspond to live cells in the culture and EthD1 positive cells (red nuclei) represent death neurons. b) Quantification of the percentage of live neurons in response to Aβo exposure compared to control neurons. Student T-test, * $p<0,01$ (n=3).

Appendix 2

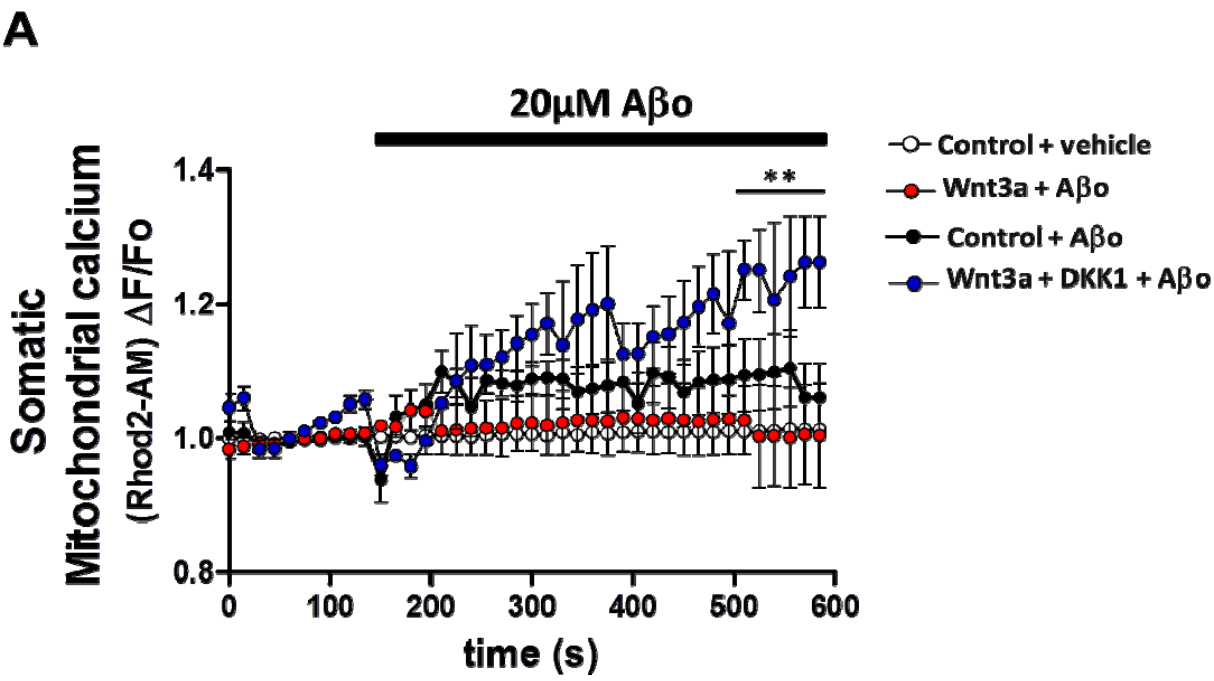

Apendix 2. Mitochondrial calcium measurement at the soma in hippocampal neurons. Fourteen DIV hippocampal neurons were loaded with the mitochondrial calcium indicator, Rhod2-AM at 4°C to favor mitochondrial loading of the probe. A) Quantification of changes in mitochondrial fluorescence intensity ($\Delta F/F_0$) in a time lapse experiment to detect mitochondrial calcium changes in the soma of hippocampal neurons in response to 20 µM Aβo. Neurons were previously treated with: control media, rWnt3a (300ng/ml), or rWnt3a plus DKK1 (DKK1 = 100 ng/ml), for 24h and then exposed to Aβo. Black bar indicates the addition of Aβo. The graph shows the mean ± SEM of n=3 independent experiments. ANOVA test, *post hoc* Bonferroni **p<0.001.

7. REFERENCES

Alford, S., Frenguelli, B.G., Schofield, J.G., and Collingridge, G.L. (1993). Characterization of Ca2+ signals induced in hippocampal CA1 neurones by the synaptic activation of NMDA receptors. J. Physiol. *469*, 693–716.

Alvarez, A.R., Godoy, J. a, Mullendorff, K., Olivares, G.H., Bronfman, M., and Inestrosa, N.C. (2004). Wnt-3a overcomes beta-amyloid toxicity in rat hippocampal neurons. Exp. Cell Res. *297*, 186–196.

Arrázola, M.S., Varela-Nallar, L., Colombres, M., Toledo, E.M., Cruzat, F., Pavez, L., Assar, R., Aravena, A., González, M., Montecino, M., et al. (2009). Calcium/calmodulin-dependent protein kinase type IV is a target gene of the Wnt/beta-catenin signaling pathway. J Cell Physiol. *221*, 658–667.

Babcock, D.F., Herrington, J., Goodwin, P.C., Park, Y.B., and Hille, B. (1997). Mitochondrial participation in the intracellular Ca2+ network. J. Cell Biol. *136*, 833–844.

Baines, C.P., Kaiser, R.A., Purcell, N.H., Blair, N.S., Osinska, H., Hambleton, M.A., Brunskill, E.W., Sayen, M.R., Gottlieb, R.A., Dorn, G.W., et al. (2005). Loss of cyclophilin D reveals a critical role for mitochondrial permeability transition in cell death. Nature *434*, 658–662.

Balietti, M., Giorgetti, B., Casoli, T., Solazzi, M., Tamagnini, F., Burattini, C., Aicardi, G., and Fattoretti, P. (2013). Early selective vulnerability of synapses and synaptic mitochondria in the hippocampal CA1 region of the Tg2576 mouse model of Alzheimer's disease. J Alzheimers Dis. *34*, 887–896.

Basso, E., Fante, L., Fowlkes, J., Petronilli, V., Forte, M.A., and Bernardi, P. (2005). Properties of the permeability transition pore in mitochondria devoid of Cyclophilin D. J Biol Chem *280*, 18558–18561.

Bates, K.A., Verdile, G., Li, Q.-X., Ames, D., Hudson, P., Masters, C.L., and Martins, R.N. (2009). Clearance mechanisms of Alzheimer's amyloid-beta peptide: implications for therapeutic design and diagnostic tests. Mol. Psychiatry *14*, 469–486.

Bernardi, P., Krauskopf, A., Basso, E., Petronilli, V., Blachly-Dyson, E., Blalchy-Dyson, E., Di Lisa, F., and Forte, M. a (2006). The mitochondrial permeability transition from in vitro artifact to disease target. FEBS J. *273*, 2077–2099.

Berridge, M.J. (1998). Neuronal calcium signaling. Neuron *21*, 13–26.

Berridge, M.J. (2011). Calcium signalling and Alzheimer's disease. Neurochem. Res. *36*, 1149–1156.

Bezprozvanny, I., and Mattson, M.P. (2008). Neuronal calcium mishandling and the pathogenesis of Alzheimer's disease. Trends Neurosci. *31*, 454–463.

Brown, M.R., Sullivan, P.G., and Geddes, J.W. (2006). Synaptic mitochondria are more susceptible to Ca2+overload than nonsynaptic mitochondria. J. Biol. Chem. *281*, 11658–11668.

Canevari, L., Clark, J.B., and Bates, T.E. (1999). beta-Amyloid fragment 25-35 selectively decreases complex IV activity in isolated mitochondria. FEBS Lett. *457*, 131–134.

Caspersen, C., Wang, N., Yao, J., Sosunov, A., Chen, X., Lustbader, J.W., Xu, H.W., Stern, D., McKhann, G., and Yan, S. Du (2005). Mitochondrial Abeta: a potential focal point for neuronal metabolic dysfunction in Alzheimer's disease. FASEB J. *19*, 2040–2041.

Celsi, F., Pizzo, P., Brini, M., Leo, S., Fotino, C., Pinton, P., and Rizzuto, R. (2009). Mitochondria, calcium and cell death: a deadly triad in neurodegeneration. Biochim Biophys Acta. *1787*, 335–344.

Cerpa, W., Dinamarca, M.C., and Inestrosa, N.C. (2008). Structure-function implications in Alzheimer's disease: effect of Abeta oligomers at central synapses. Curr. Alzheimer Res. *5*, 233–243.

Cerpa, W., Toledo, E.M., Varela-Nallar, L., and Inestrosa, N.C. (2009). The role of Wnt signaling in neuroprotection. Drug News Perspect. *22*, 579–591.

Chen, J.X., and Yan, S.S. (2010). Role of mitochondrial amyloid-beta in Alzheimer's disease. J. Alzheimers. Dis. *20 Suppl 2*, S569–78.

Cheung, K.-H., Shineman, D., Müller, M., Cárdenas, C., Mei, L., Yang, J., Tomita, T., Iwatsubo, T., Lee, V.M.-Y., and Foskett, J.K. (2008). Mechanism of Ca2+ disruption in Alzheimer's disease by presenilin regulation of InsP3 receptor channel gating. Neuron *58*, 871–883.

Chiara, F., Castellaro, D., Marin, O., Petronilli, V., Brusilow, W.S., Juhaszova, M., Sollott, S.J., Forte, M., Bernardi, P., and Rasola, A. (2008). Hexokinase II detachment from

mitochondria triggers apoptosis through the permeability transition pore independent of voltage-dependent anion channels. PLoS One *3*, e1852.

Chipuk, J.E., Moldoveanu, T., Llambi, F., Parsons, M.J., and Green, D.R. (2010). The BCL-2 family reunion. Mol. Cell *37*, 299–310.

Chow, V.W., Mattson, M.P., Wong, P.C., and Gleichmann, M. (2010). An overview of APP processing enzymes and products. Neuromolecular Med. *12*, 1–12.

Cleary, J.P., Walsh, D.M., Hofmeister, J.J., Shankar, G.M., Kuskowski, M. a, Selkoe, D.J., and Ashe, K.H. (2005). Natural oligomers of the amyloid-beta protein specifically disrupt cognitive function. Nat. Neurosci. *8*, 79–84.

Clevers, H., and Nusse, R. (2012). Wnt/β-catenin signaling and disease. Cell *149*, 1192–1205.

Connern, C.P., and Halestrap, a P. (1994). Recruitment of mitochondrial cyclophilin to the mitochondrial inner membrane under conditions of oxidative stress that enhance the opening of a calcium-sensitive non-specific channel. Biochem. J. *302 (Pt 2*, 321–324.

Demuro, A., Parker, I., and Stutzmann, G.E. (2010). Calcium signaling and amyloid toxicity in Alzheimer disease. J. Biol. Chem. *285*, 12463–12468.

Devi, L., and Anandatheerthavarada, H.K. (2010). Mitochondrial trafficking of APP and alpha synuclein: Relevance to mitochondrial dysfunction in Alzheimer's and Parkinson's diseases. Biochim. Biophys. Acta *1802*, 11–19.

Devi, L., Prabhu, B.M., Galati, D.F., Avadhani, N.G., and Anandatheerthavarada, H.K. (2006). Accumulation of amyloid precursor protein in the mitochondrial import channels of human Alzheimer's disease brain is associated with mitochondrial dysfunction. J. Neurosci. *26*, 9057–9068.

Dinamarca, M.C., Cerpa, W., Garrido, J., Hancke, J.L., and Inestrosa, N.C. (2006). Hyperforin prevents beta-amyloid neurotoxicity and spatial memory impairments by disaggregation of Alzheimer's amyloid-beta-deposits. Mol. Psychiatry *11*, 1032–1048.

Dinamarca, M.C., Colombres, M., Cerpa, W., Bonansco, C., and Inestrosa, N.C. (2008). Beta-amyloid oligomers affect the structure and function of the postsynaptic region: role of the Wnt signaling pathway. Neurodegener. Dis. *5*, 149–152.

Dinamarca, M.C., Sagal, J.P., Quintanilla, R.A., Godoy, J.A., Arrázola, M.S., and Inestrosa, N.C. (2010). Amyloid-beta-Acetylcholinesterase complexes potentiate neurodegenerative changes induced by the Abeta peptide. Implications for the pathogenesis of Alzheimer's disease. Mol. Neurodegener. *5*, 4.

Du, H., and Yan, S.S. (2010a). Mitochondrial permeability transition pore in Alzheimer's disease: cyclophilin D and amyloid beta. Biochim Biophys Acta. *1802*, 198–204.

Du, H., and Yan, S.S. (2010b). Mitochondrial medicine for neurodegenerative diseases. Int J Biochem Cell Biol. *42*, 560–572.

Du, H., Guo, L., Fang, F., Chen, D., Sosunov, A. a, McKhann, G.M., Yan, Y., Wang, C., Zhang, H., Molkentin, J.D., et al. (2008). Cyclophilin D deficiency attenuates mitochondrial and neuronal perturbation and ameliorates learning and memory in Alzheimer's disease. Nat Med. *14*, 1097–1105.

Du, H., Guo, L., Yan, S., Sosunov, A. a, McKhann, G.M., and Yan, S.S. (2010). Early deficits in synaptic mitochondria in an Alzheimer's disease mouse model. Proc Natl Acad Sci U S A. *107*, 18670–18675.

Du, H., Guo, L., and Yan, S.S. (2012). Synaptic mitochondrial pathology in Alzheimer's disease. Antioxid. Redox Signal. *16*, 1467–1475.

Eckert, A., Schulz, K.L., Rhein, V., and Götz, J. (2010). Convergence of amyloid-beta and tau pathologies on mitochondria in vivo. Mol. Neurobiol. *41*, 107–114.

Eliseev, R. a, Malecki, J., Lester, T., Zhang, Y., Humphrey, J., and Gunter, T.E. (2009). Cyclophilin D interacts with Bcl2 and exerts an anti-apoptotic effect. J. Biol. Chem. *284*, 9692–9699.

Emami, K.H., Nguyen, C., Ma, H., Kim, D.H., Jeong, K.W., Eguchi, M., Moon, R.T., Teo, J.-L., Oh, S.W., Kim, H.Y., et al. (2004). A small molecule inhibitor of beta-catenin/CREB-binding protein transcription [corrected]. Proc. Natl. Acad. Sci. U. S. A. *101*, 12682–12687.

Farías, G.G., Alfaro, I.E., Cerpa, W., Grabowski, C.P., Godoy, J. a, Bonansco, C., and Inestrosa, N.C. (2009). Wnt-5a/JNK signaling promotes the clustering of PSD-95 in hippocampal neurons. J. Biol. Chem. *284*, 15857–15866.

De Ferrari, G. V, and Inestrosa, N.C. (2000). Wnt signaling function in Alzheimer's disease. Brain Res. Brain Res. Rev. *33*, 1–12.

De Ferrari, G. V, Chacón, M. a, Barría, M.I., Garrido, J.L., Godoy, J. a, Olivares, G., Reyes, a E., Alvarez, a, Bronfman, M., and Inestrosa, N.C. (2003). Activation of Wnt signaling rescues neurodegeneration and behavioral impairments induced by beta-amyloid fibrils. Mol. Psychiatry *8*, 195–208.

Ferreira, S.T., Vieira, M.N.N., and De Felice, F.G. (2007). Soluble protein oligomers as emerging toxins in Alzheimer's and other amyloid diseases. IUBMB Life *59*, 332–345.

Fuentealba, R. a, Farias, G., Scheu, J., Bronfman, M., Marzolo, M.P., and Inestrosa, N.C. (2004). Signal transduction during amyloid-beta-peptide neurotoxicity: role in Alzheimer disease. Brain Res Brain Res Rev. *47*, 275–289.

Fuenzalida, K., Quintanilla, R., Ramos, P., Piderit, D., Fuentealba, R. a, Martinez, G., Inestrosa, N.C., and Bronfman, M. (2007). Peroxisome proliferator-activated receptor gamma up-regulates the Bcl-2 anti-apoptotic protein in neurons and induces mitochondrial stabilization and protection against oxidative stress and apoptosis. J Biol Chem. *282*, 37006–37015.

Gillessen, T., Grasshoff, C., and Szinicz, L. (2002). Mitochondrial permeability transition can be directly monitored in living neurons. Biomed Pharmacother. *56*, 186–193.

Gomez, L., Paillard, M., Thibault, H., Derumeaux, G., and Ovize, M. (2008). Inhibition of GSK3beta by postconditioning is required to prevent opening of the mitochondrial permeability transition pore during reperfusion. Circulation *117*, 2761–2768.

Haass, C., and Selkoe, D.J. (2007). Soluble protein oligomers in neurodegeneration: lessons from the Alzheimer's amyloid beta-peptide. Nat. Rev. Mol. Cell Biol. *8*, 101–112.

Halestrap, A.P. (2009). What is the mitochondrial permeability transition pore? J Mol Cell Cardiol. *46*, 821–831.

Halestrap, A.P., Connern, C.P., Griffiths, E.J., and Kerr, P.M. (1997). Cyclosporin A binding to mitochondrial cyclophilin inhibits the permeability transition pore and protects hearts from ischaemia/reperfusion injury. Mol Cell Biochem. *174*, 167–172.

Hansson Petersen, C. a, Alikhani, N., Behbahani, H., Wiehager, B., Pavlov, P.F., Alafuzoff, I., Leinonen, V., Ito, A., Winblad, B., Glaser, E., et al. (2008). The amyloid beta-peptide is imported into mitochondria via the TOM import machinery and localized to mitochondrial cristae. Proc. Natl. Acad. Sci. U. S. A. *105*, 13145–13150.

Hardy, J., and Selkoe, D.J. (2002). The amyloid hypothesis of Alzheimer's disease: progress and problems on the road to therapeutics. Science (80-.). *297*, 353–356.

Hardy, J.A., and Higgins, G.A. (1992). Alzheimer's disease: the amyloid cascade hypothesis. Science *256*, 184–185.

Harvey, K., and Marchetti, B. (2014). Regulating Wnt signaling: a strategy to prevent neurodegeneration and induce regeneration. J. Mol. Cell Biol. *6*, 1–2.

Inestrosa, N.C., and Arenas, E. (2010). Emerging roles of Wnts in the adult nervous system. Nat Rev Neurosci. *11*, 77–86.

Inestrosa, N.C., and Varela-Nallar, L. (2014). Wnt signaling in the nervous system and in Alzheimer's disease. J Mol Cell Biol. *6*, 64–74.

Inestrosa, N.C., Godoy, J. a, Vargas, J.Y., Arrazola, M.S., Rios, J. a, Carvajal, F.J., Serrano, F.G., and Farias, G.G. (2013). Nicotine prevents synaptic impairment induced by amyloid-β oligomers through α7-nicotinic acetylcholine receptor activation. Neuromolecular Med. *15*, 549–569.

Johri, A., and Beal, M.F. (2012). Mitochondrial dysfunction in neurodegenerative diseases. J. Pharmacol. Exp. Ther. *342*, 619–630.

Juhaszova, M., Zorov, D.B., Yaniv, Y., Nuss, H.B., Wang, S., and Sollott, S.J. (2009). Role of glycogen synthase kinase-3beta in cardioprotection. Circ. Res. *104*, 1240–1252.

Kato, M., Akao, M., Matsumoto-Ida, M., Makiyama, T., Iguchi, M., Takeda, T., Shimizu, S., and Kita, T. (2009). The targeting of cyclophilin D by RNAi as a novel cardioprotective therapy: evidence from two-photon imaging. Cardiovasc. Res. *83*, 335–344.

Kim, M.J., Huh, Y.H., Choi, K.J., Jun, S., Je, a R., Chae, H., Lee, C., and Kweon, H.-S. (2012). Ultrastructural Abnormalities in APP/PSEN1 Transgenic Mouse Brain as the Alzheimer's Disease Model. Korean J. Microsc. *42*, 179–185.

Klein, P.S., and Melton, D.A. (1996). A molecular mechanism for the effect of lithium on development. Proc. Natl. Acad. Sci. U. S. A. *93*, 8455–8459.

Kroemer, G., Galluzzi, L., and Brenner, C. (2007). Mitochondrial Membrane Permeabilization in Cell Death. 99–163.

Kuwana, T., and Newmeyer, D.D. (2003). Bcl-2-family proteins and the role of mitochondria in apoptosis. Curr. Opin. Cell Biol. *15*, 691–699.

LaFerla, F.M. (2002). Calcium dyshomeostasis and intracellular signalling in Alzheimer's disease. Nat Rev Neurosci. *3*, 862–872.

Lambert, M.P., Barlow, A.K., Chromy, B.A., Edwards, C., Freed, R., Liosatos, M., Morgan, T.E., Rozovsky, I., Trommer, B., Viola, K.L., et al. (1998). Diffusible, nonfibrillar ligands derived from Abeta1-42 are potent central nervous system neurotoxins. Proc. Natl. Acad. Sci. U. S. A. *95*, 6448–6453.

Li, S., Hong, S., Shepardson, N.E., Walsh, D.M., Shankar, G.M., and Selkoe, D. (2009). Soluble oligomers of amyloid beta protein facilitate hippocampal long-term depression by disrupting neuronal glutamate uptake. Neuron *62*, 788–801.

Lie, D.-C., Colamarino, S. a, Song, H.-J., Désiré, L., Mira, H., Consiglio, A., Lein, E.S., Jessberger, S., Lansford, H., Dearie, A.R., et al. (2005). Wnt signalling regulates adult hippocampal neurogenesis. Nature *437*, 1370–1375.

Lindholm, D., Wootz, H., and Korhonen, L. (2006). ER stress and neurodegenerative diseases. Cell Death Differ. *13*, 385–392.

Lustbader, J.W., Cirilli, M., Lin, C., Xu, H.W., Takuma, K., Wang, N., Caspersen, C., Chen, X., Pollak, S., Chaney, M., et al. (2004). ABAD directly links Abeta to mitochondrial toxicity in Alzheimer's disease. Science *304*, 448–452.

Manczak, M., Anekonda, T.S., Henson, E., Park, B.S., Quinn, J., and Reddy, P.H. (2006). Mitochondria are a direct site of A beta accumulation in Alzheimer's disease neurons: implications for free radical generation and oxidative damage in disease progression. Hum. Mol. Genet. *15*, 1437–1449.

Marks, A.R. (1997). Intracellular calcium-release channels: regulators of cell life and death. Am. J. Physiol. *272*, H597–605.

Marzo, I. (1998). Bax and Adenine Nucleotide Translocator Cooperate in the Mitochondrial Control of Apoptosis. Science (80-.). *281*, 2027–2031.

Marzo, I., Brenner, C., Zamzami, N., Susin, S.A., Beutner, G., Brdiczka, D., Rémy, R., Xie, Z.H., Reed, J.C., and Kroemer, G. (1998). The permeability transition pore complex: a target for apoptosis regulation by caspases and bcl-2-related proteins. J. Exp. Med. *187*, 1261–1271.

Masliah, E., Mallory, M., Alford, M., DeTeresa, R., Hansen, L.A., McKeel, D.W., and Morris, J.C. (2001). Altered expression of synaptic proteins occurs early during progression of Alzheimer's disease. Neurology *56*, 127–129.

Mathupala, S.P., Ko, Y.H., and Pedersen, P.L. (2006). Hexokinase II: cancer's double-edged sword acting as both facilitator and gatekeeper of malignancy when bound to mitochondria. Oncogene *25*, 4777–4786.

Mattson, M.P. (2004). Pathways towards and away from Alzheimer's disease. Nature *430*, 631–639.

Mattson, M.P., Cheng, B., Davis, D., Bryant, K., Lieberburg, I., and Rydel, R.E. (1992). beta-Amyloid peptides destabilize calcium homeostasis and render human cortical neurons vulnerable to excitotoxicity. J. Neurosci. *12*, 376–389.

McLean, C.A., Cherny, R.A., Fraser, F.W., Fuller, S.J., Smith, M.J., Beyreuther, K., Bush, A.I., and Masters, C.L. (1999). Soluble pool of Abeta amyloid as a determinant of severity of neurodegeneration in Alzheimer's disease. Ann. Neurol. *46*, 860–866.

Miura, T., and Tanno, M. (2010). Mitochondria and GSK-3beta in cardioprotection against ischemia/reperfusion injury. Cardiovasc Drugs Ther *24*, 255–263.

Miura, T., Nishihara, M., and Miki, T. (2009). Drug development targeting the glycogen synthase kinase-3beta (GSK-3beta)-mediated signal transduction pathway: role of GSK-3beta in myocardial protection against ischemia/reperfusion injury. J. Pharmacol. Sci. *109*, 162–167.

Miyamoto, S., Murphy, A.N., and Brown, J.H. (2008). Akt mediates mitochondrial protection in cardiomyocytes through phosphorylation of mitochondrial hexokinase-II. Cell Death Differ. *15*, 521–529.

Moreira, P.I., Santos, M.S., Moreno, A., and Oliveira, C. (2001). Amyloid beta-peptide promotes permeability transition pore in brain mitochondria. Biosci. Rep. *21*, 789–800.

Moreira, P.I., Santos, M.S., Moreno, A., Rego, A.C., and Oliveira, C. (2002). Effect of amyloid beta-peptide on permeability transition pore: a comparative study. J. Neurosci. Res. *69*, 257–267.

Moreira, P.I., Santos, M.S., and Oliveira, C.R. (2007). Alzheimer's disease: a lesson from mitochondrial dysfunction. Antioxid. Redox Signal. *9*, 1621–1630.

Morgan, C., Colombres, M., Nuñez, M.T., and Inestrosa, N.C. (2004). Structure and function of amyloid in Alzheimer's disease. Prog. Neurobiol. *74*, 323–349.

Mucke, L., Masliah, E., Yu, G.Q., Mallory, M., Rockenstein, E.M., Tatsuno, G., Hu, K., Kholodenko, D., Johnson-Wood, K., and McConlogue, L. (2000). High-level neuronal expression of abeta 1-42 in wild-type human amyloid protein precursor transgenic mice: synaptotoxicity without plaque formation. J. Neurosci. *20*, 4050–4058.

Muirhead, K.E. a, Borger, E., Aitken, L., Conway, S.J., and Gunn-Moore, F.J. (2010). The consequences of mitochondrial amyloid beta-peptide in Alzheimer's disease. Biochem. J. *426*, 255–270.

Naga, K.K., Sullivan, P.G., and Geddes, J.W. (2007). High cyclophilin D content of synaptic mitochondria results in increased vulnerability to permeability transition. J. Neurosci. *27*, 7469–7475.

Newmeyer, D.D., and Ferguson-Miller, S. (2003). Mitochondria: releasing power for life and unleashing the machineries of death. Cell *112*, 481–490.

Nishihara, M., Miura, T., Miki, T., Tanno, M., Yano, T., Naitoh, K., Ohori, K., Hotta, H., Terashima, Y., and Shimamoto, K. (2007). Modulation of the mitochondrial permeability transition pore complex in GSK-3beta-mediated myocardial protection. J Mol Cell Cardiol. *43*, 564–570.

Oliva, C. a, Vargas, J.Y., and Inestrosa, N.C. (2013). Wnts in adult brain: from synaptic plasticity to cognitive deficiencies. Front. Cell. Neurosci. *7*, 224.

Paradis, E., Koutroumanis, M., and Goodyer, C. (1996). Amyloid Peptide of Alzheimer ' s Disease Downregulates Bcl-2 and Upregulates Bax Expression in Human Neurons. *16*, 7533–7539.

Parks, J.K., Smith, T.S., Trimmer, P. a, Bennett, J.P., and Parker, W.D. (2001). Neurotoxic Abeta peptides increase oxidative stress in vivo through NMDA-receptor and nitric-oxide-synthase mechanisms, and inhibit complex IV activity and induce a mitochondrial permeability transition in vitro. J. Neurochem. *76*, 1050–1056.

Paula-Lima, A.C., Adasme, T., SanMartín, C., Sebollela, A., Hetz, C., Carrasco, M.A., Ferreira, S.T., and Hidalgo, C. (2011). Amyloid β-peptide oligomers stimulate RyR-mediated Ca2+ release inducing mitochondrial fragmentation in hippocampal neurons and prevent RyR-mediated dendritic spine remodeling produced by BDNF. Antioxid. Redox Signal. *14*, 1209–1223.

Petronilli, V., Miotto, G., Canton, M., Colonna, R., Bernardi, P., and Di Lisa, F. (1998). Imaging the mitochondrial permeability transition pore in intact cells. Biofactors. *8*, 263–272.

Petronilli, V., Penzo, D., Scorrano, L., Bernardi, P., and Di Lisa, F. (2001). The mitochondrial permeability transition, release of cytochrome c and cell death. Correlation with the duration of pore openings in situ. J Biol Chem. *276*, 12030–12034.

Purro, S. a, Dickins, E.M., and Salinas, P.C. (2012). The secreted Wnt antagonist Dickkopf-1 is required for amyloid β-mediated synaptic loss. J. Neurosci. *32*, 3492–3498.

Quintanilla, R.A., Muñoz, F.J., Metcalfe, M.J., Hitschfeld, M., Olivares, G., Godoy, J. a, and Inestrosa, N.C. (2005). Trolox and 17beta-estradiol protect against amyloid beta-peptide neurotoxicity by a mechanism that involves modulation of the Wnt signaling pathway. J. Biol. Chem. *280*, 11615–11625.

Rao, V.K., Carlson, E. a, and Yan, S.S. (2013). Mitochondrial permeability transition pore is a potential drug target for neurodegeneration. Biochim. Biophys. Acta.

Rasola, A., Sciacovelli, M., Chiara, F., Pantic, B., Brusilow, W.S., and Bernardi, P. (2010a). Activation of mitochondrial ERK protects cancer cells from death through inhibition of the permeability transition. Proc. Natl. Acad. Sci. U. S. A. *107*, 726–731.

Rasola, A., Sciacovelli, M., Pantic, B., and Bernardi, P. (2010b). Signal transduction to the permeability transition pore. FEBS Lett. *584*, 1989–1996.

Reddy, P.H. (2006). Amyloid precursor protein-mediated free radicals and oxidative damage: implications for the development and progression of Alzheimer's disease. J. Neurochem. *96*, 1–13.

Reddy, P.H. (2007). Mitochondrial dysfunction in aging and Alzheimer's disease: strategies to protect neurons. Antioxid. Redox Signal. *9*, 1647–1658.

Reddy, P.H. (2009). Amyloid beta, mitochondrial structural and functional dynamics in Alzheimer's disease. Exp. Neurol. *218*, 286–292.

Reddy, P.H. (2013). Amyloid beta-induced glycogen synthase kinase 3β phosphorylated VDAC1 in Alzheimer's disease: Implications for synaptic dysfunction and neuronal damage. Biochim. Biophys. Acta *1832*, 1913–1921.

Robey, R.B., and Hay, N. (2006). Mitochondrial hexokinases, novel mediators of the antiapoptotic effects of growth factors and Akt. Oncogene *25*, 4683–4696.

Ross, C. a, and Poirier, M. a (2005). Opinion: What is the role of protein aggregation in neurodegeneration? Nat. Rev. Mol. Cell Biol. *6*, 891–898.

Rosso, S.B., and Inestrosa, N.C. (2013). WNT signaling in neuronal maturation and synaptogenesis. Front Cell Neurosci. *7*, 103.

Rosso, S.B., Sussman, D., Wynshaw-Boris, A., and Salinas, P.C. (2005). Wnt signaling through Dishevelled, Rac and JNK regulates dendritic development. Nat. Neurosci. *8*, 34–42.

Sakono, M., and Zako, T. (2010). Amyloid oligomers: formation and toxicity of Abeta oligomers. FEBS J. *277*, 1348–1358.

Salinas, P.C., and Zou, Y. (2008). Wnt signaling in neural circuit assembly. Annu Rev Neurosci. *31*, 339–358.

Saraiva, L.M., Seixas da Silva, G.S., Galina, A., Da-Silva, W.S., Klein, W.L., Ferreira, S.T., and De Felice, F.G. (2010). Amyloid-β triggers the release of neuronal hexokinase 1 from mitochondria. PLoS One *5*, e15230.

Schinzel, A.C., Takeuchi, O., Huang, Z., Fisher, J.K., Zhou, Z., Rubens, J., Hetz, C., Danial, N.N., Moskowitz, M. a, and Korsmeyer, S.J. (2005). Cyclophilin D is a component of mitochondrial permeability transition and mediates neuronal cell death after focal cerebral ischemia. Proc Natl Acad Sci U S A. *102*, 12005–12010.

Selkoe, D.J. (2002). Alzheimer's disease is a synaptic failure. Science *298*, 789–791.

Serrano-Pozo, A., Frosch, M.P., Masliah, E., and Hyman, B.T. (2011). Neuropathological alterations in Alzheimer disease. Cold Spring Harb. Perspect. Med. *1*, a006189.

Shankar, G.M., Li, S., Mehta, T.H., Garcia-Munoz, A., Shepardson, N.E., Smith, I., Brett, F.M., Farrell, M.A., Rowan, M.J., Lemere, C.A., et al. (2008). Amyloid-beta protein dimers isolated directly from Alzheimer's brains impair synaptic plasticity and memory. Nat. Med. *14*, 837–842.

Shevtzova, E.F., Kireeva, E.G., and Bachurin, S.O. (2001). Effect of beta-amyloid peptide fragment 25-35 on nonselective permeability of mitochondria. Bull. Exp. Biol. Med. *132*, 1173–1176.

Singh, P., Suman, S., Chandna, S., and Das, T.K. (2009). Possible role of amyloid-beta, adenine nucleotide translocase and cyclophilin-D interaction in mitochondrial dysfunction of Alzheimer's disease. Bioinformation *3*, 440–445.

Spät, A., Szanda, G., Csordás, G., and Hajnóczky, G. (2008). High- and low-calcium-dependent mechanisms of mitochondrial calcium signalling. Cell Calcium *44*, 51–63.

Stambolic, V., and Woodgett, J.R. (1994). Mitogen inactivation of glycogen synthase kinase-3 beta in intact cells via serine 9 phosphorylation. Biochem J. *303 (Pt 3*, 701–704.

Stutzmann, G.E., Smith, I., Caccamo, A., Oddo, S., Parker, I., and Laferla, F. (2007). Enhanced ryanodine-mediated calcium release in mutant PS1-expressing Alzheimer's mouse models. Ann. N. Y. Acad. Sci. *1097*, 265–277.

Sun, M.G., Williams, J., Munoz-Pinedo, C., Perkins, G. a, Brown, J.M., Ellisman, M.H., Green, D.R., and Frey, T.G. (2007). Correlated three-dimensional light and electron microscopy reveals transformation of mitochondria during apoptosis. Nat. Cell Biol. *9*, 1057–1065.

Supnet, C., and Bezprozvanny, I. (2010). Neuronal calcium signaling, mitochondrial dysfunction, and Alzheimer's disease. J Alzheimers Dis *20 Suppl 2*, S487–98.

Supnet, C., Grant, J., Kong, H., Westaway, D., and Mayne, M. (2006). Amyloid-beta-(1-42) increases ryanodine receptor-3 expression and function in neurons of TgCRND8 mice. J. Biol. Chem. *281*, 38440–38447.

Swerdlow, R.H., Burns, J.M., and Khan, S.M. (2010). The Alzheimer's disease mitochondrial cascade hypothesis. J. Alzheimers. Dis. *20 Suppl 2*, S265–79.

Szalai, G., Krishnamurthy, R., and Hajnóczky, G. (1999). Apoptosis driven by IP(3)-linked mitochondrial calcium signals. EMBO J. *18*, 6349–6361.

Takuma, K., Yan, S.S., Stern, D.M., and Yamada, K. (2005). Mitochondrial dysfunction, endoplasmic reticulum stress, and apoptosis in Alzheimer's disease. J. Pharmacol. Sci. *97*, 312–316.

Toledo, E.M., and Inestrosa, N.C. (2010). Activation of Wnt signaling by lithium and rosiglitazone reduced spatial memory impairment and neurodegeneration in brains of an APPswe/PSEN1DeltaE9 mouse model of Alzheimer's disease. Mol. Psychiatry *15*, 272–285, 228.

Varela-Nallar, L., and Inestrosa, N.C. (2013). Wnt signaling in the regulation of adult hippocampal neurogenesis. Front Cell Neurosci. *7*, 100.

Vargas, J.Y., Fuenzalida, M., and Inestrosa, N.C. (2014). In vivo Activation of Wnt Signaling Pathway Enhances Cognitive Function of Adult Mice and Reverses Cognitive Deficits in an Alzheimer's Disease Model. J Neurosci. *34*, 2191–2202.

Walsh, D.M., Tseng, B.P., Rydel, R.E., Podlisny, M.B., and Selkoe, D.J. (2000). The oligomerization of amyloid beta-protein begins intracellularly in cells derived from human brain. Biochemistry *39*, 10831–10839.

Walsh, D.M., Klyubin, I., Fadeeva, J. V, Cullen, W.K., Anwyl, R., Wolfe, M.S., Rowan, M.J., and Selkoe, D.J. (2002). Naturally secreted oligomers of amyloid beta protein potently inhibit hippocampal long-term potentiation in vivo. Nature *416*, 535–539.

Wang, H.-W., Pasternak, J.F., Kuo, H., Ristic, H., Lambert, M.P., Chromy, B., Viola, K.L., Klein, W.L., Stine, W.B., Krafft, G.A., et al. (2002). Soluble oligomers of beta amyloid (1-42) inhibit long-term potentiation but not long-term depression in rat dentate gyrus. Brain Res. *924*, 133–140.

Wang, J.-Z., Xia, Y.-Y., Grundke-Iqbal, I., and Iqbal, K. (2013). Abnormal hyperphosphorylation of tau: sites, regulation, and molecular mechanism of neurofibrillary degeneration. J. Alzheimers. Dis. *33 Suppl 1*, S123–39.

Willert, K., and Nusse, R. (2012). Wnt proteins. Cold Spring Harb. Perspect. Biol. *4*, a007864.

Wirths, O., Multhaup, G., Czech, C., Blanchard, V., Moussaoui, S., Tremp, G., Pradier, L., Beyreuther, K., and Bayer, T. a (2001). Intraneuronal Abeta accumulation precedes plaque formation in beta-amyloid precursor protein and presenilin-1 double-transgenic mice. Neurosci. Lett. *306*, 116–120.

Yao, J., Irwin, R.W., Zhao, L., Nilsen, J., Hamilton, R.T., and Brinton, R.D. (2009). Mitochondrial bioenergetic deficit precedes Alzheimer's pathology in female mouse model of Alzheimer's disease. Proc. Natl. Acad. Sci. U. S. A. *106*, 14670–14675.

Ying, W.L., Emerson, J., Clarke, M.J., and Sanadi, D.R. (1991). Inhibition of mitochondrial calcium ion transport by an oxo-bridged dinuclear ruthenium ammine complex. Biochemistry *30*, 4949–4952.

Yu, C., Nwabuisi-Heath, E., Laxton, K., and Ladu, M.J. (2010). Endocytic pathways mediating oligomeric Abeta42 neurotoxicity. Mol. Neurodegener. *5*, 19.

Zorov, D.B., Juhaszova, M., Yaniv, Y., Nuss, H.B., Wang, S., and Sollott, S.J. (2009). Regulation and pharmacology of the mitochondrial permeability transition pore. Cardiovasc. Res. *83*, 213–225.

Zou, Y., and Salinas, P. (2014). Signaling mechanisms mediating diverse Wnt functions in neural development and disease. Dev. Neurobiol.